NBS PUBLICATIONS

NBS SPECIAL PUBLICATION 634

U.S. DEPARTMENT OF COMMERCE/National Bureau of Standards

Proceedings of the Waveform Recorder Seminar

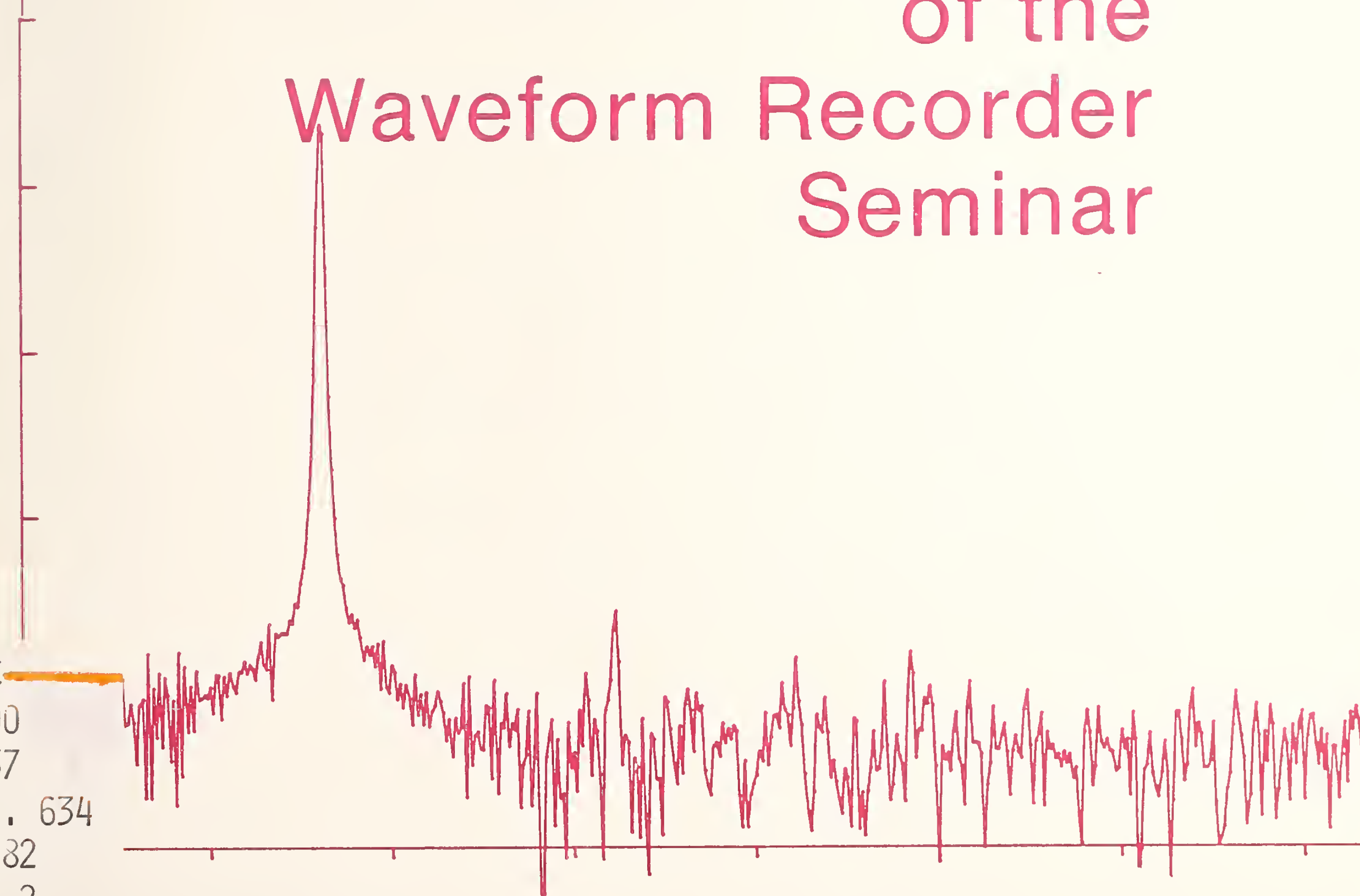

NATIONAL BUREAU OF STANDARDS

The National Bureau of Standards[1] was established by an act of Congress on March 3, 1901. The Bureau's overall goal is to strengthen and advance the Nation's science and technology and facilitate their effective application for public benefit. To this end, the Bureau conducts research and provides: (1) a basis for the Nation's physical measurement system, (2) scientific and technological services for industry and government, (3) a technical basis for equity in trade, and (4) technical services to promote public safety. The Bureau's technical work is performed by the National Measurement Laboratory, the National Engineering Laboratory, and the Institute for Computer Sciences and Technology.

THE NATIONAL MEASUREMENT LABORATORY provides the national system of physical and chemical and materials measurement; coordinates the system with measurement systems of other nations and furnishes essential services leading to accurate and uniform physical and chemical measurement throughout the Nation's scientific community, industry, and commerce; conducts materials research leading to improved methods of measurement, standards, and data on the properties of materials needed by industry, commerce, educational institutions, and Government; provides advisory and research services to other Government agencies; develops, produces, and distributes Standard Reference Materials; and provides calibration services. The Laboratory consists of the following centers:

Absolute Physical Quantities[2] — Radiation Research — Chemical Physics — Analytical Chemistry — Materials Science

THE NATIONAL ENGINEERING LABORATORY provides technology and technical services to the public and private sectors to address national needs and to solve national problems; conducts research in engineering and applied science in support of these efforts; builds and maintains competence in the necessary disciplines required to carry out this research and technical service; develops engineering data and measurement capabilities; provides engineering measurement traceability services; develops test methods and proposes engineering standards and code changes; develops and proposes new engineering practices; and develops and improves mechanisms to transfer results of its research to the ultimate user. The Laboratory consists of the following centers:

Applied Mathematics — Electronics and Electrical Engineering[2] — Manufacturing Engineering — Building Technology — Fire Research — Chemical Engineering[2]

THE INSTITUTE FOR COMPUTER SCIENCES AND TECHNOLOGY conducts research and provides scientific and technical services to aid Federal agencies in the selection, acquisition, application, and use of computer technology to improve effectiveness and economy in Government operations in accordance with Public Law 89-306 (40 U.S.C. 759), relevant Executive Orders, and other directives; carries out this mission by managing the Federal Information Processing Standards Program, developing Federal ADP standards guidelines, and managing Federal participation in ADP voluntary standardization activities; provides scientific and technological advisory services and assistance to Federal agencies; and provides the technical foundation for computer-related policies of the Federal Government. The Institute consists of the following centers:

Programming Science and Technology — Computer Systems Engineering.

[1]Headquarters and Laboratories at Gaithersburg, MD, unless otherwise noted; mailing address Washington, DC 20234.
[2]Some divisions within the center are located at Boulder, CO 80303.

N bs special publication

Proceedings of the Waveform Recorder Seminar

Proceedings of the Seminar on Waveform Recorder Measurement Needs and Techniques for Evaluation/Calibration, held in Boulder, CO, Oct. 15, 1981.

Edited by
Robert A. Lawton

Electromagnetic Technology Division
National Bureau of Standards
Boulder, CO 80303

U.S. DEPARTMENT OF COMMERCE, Malcolm Baldrige, Secretary

NATIONAL BUREAU OF STANDARDS, Ernest Ambler, Director

Issued June 1982

Library of Congress Catalog Card Number: 82-600552

National Bureau of Standards Special Publication 634
Nat. Bur. Stand. (U.S.), Spec. Publ. 634, 97 pages (June 1982)
CODEN: XNBSAV

U.S. GOVERNMENT PRINTING OFFICE
WASHINGTON: 1982

CONTENTS

BACKGROUND AND OBJECTIVE OF SEMINAR

Robert A. Lawton

In the past, for the most part, precision electromagnetic measurements were concerned with the measurement of parameters for sinusoidal (or steady state) excitation and response, e.g., magnitude, phase, and power. One reason for the popularity of frequency domain measurement was that in this domain only one complete data point need be recorded to constitute a useful measurement. Recording a thousand data points as required for precision time domain waveform measurements simply was not feasible. Today such frequency domain measurements are still important but now share their importance with transient pulse time domain measurements. With the emergence of integrated circuit components for (1) sampling or analog to digital conversion, (2) storage, and (3) control, real time digital waveform recording is now practical and widespread in usage. Furthermore, by coupling waveform recording components to minicomputers and microprocessors integrated circuitry it is now possible to record single events using compact systems (instruments) which acquire, record, process, and analyze transient signals. In fact, the incorporation of digital computation integrated circuitry appears to be a major driving force in expanding the role of waveform measurements in the academic, industrial and scientific communities.

We at the National Bureau of Standards are charged with the responsibility of encouraging the orderly development of consistent standards and measurement techniques. We have been actively engaged in waveform standards development for some time now and the papers in these proceedings will give a sample of what NBS and others in the waveform community have done already. The afternoon session consisted of a workshop which addressed the questions: Where do we go from here? and Why?, culminating in the selection of a steering committee for the development of standards for waveform recorders.

Key words: converters; electromagnetics; encoders; pulse; waveform generation; waveform measurements; waveform recorder; standards.

Papers by non-NBS authors have not been reviewed or edited by NBS. Therefore, the National Bureau of Standards accepts no responsibility for comments or recommendations contained therein.

SEMINAR ON WAVEFORM RECORDER MEASUREMENT NEEDS AND TECHNIQUES
FOR EVALUATION/CALIBRATION
October 15, 1981

PROGRAM

I. Morning Session: N. S. Nahman, Session Chairman

8:30 A.M.	Welcoming Remarks. R. A. Kamper, Chief, Electromagnetic Technology Division, NBS, 724.00, Boulder, CO
8:35 A.M.	Background and Objective of the Seminar, R. A. Lawton, Group Leader, Electromagnetic Waveform Metrology Group, NBS, 724.04, Boulder, CO
8:45 A.M.	"Some generic waveform recorder problems," N. S. Nahman, Senior Scientist, Electromagnetic Waveform Metrology Group, NBS, 724.04, Boulder, CO
8:55 A.M.	"Steady-state tests of waveform recorders," D. R. Flach, Physicist, Electrosystems Division, 722, NBS, Washington, DC
9:20 A.M.	"Characterizing dynamic performance of waveform digitizers," Phil Crosby, TV Products Engineering, Tektronix, Inc., Beaverton, OR
9:45 A.M.	"Measurement of transient versus steady state response of waveform recorders," T. M. Souders, Physicist, Division 722, NBS, Washington, DC
10:10 A.M.	Coffee Break
10:30 A.M.	"Calibration techniques for a large computerized waveform recording system," W. A. Boyer, Pulsed Power Engineering Division -4251, Sandia National Laboratories, Albuquerque, NM
10:55 A.M.	"Sampling-rate drift problems in transfer function analysis of electrical power cables," J. D. Ramboz, Electrosystems Division, NBS, Washington, DC, A. R. Ondrejka, Electromagnetic Technology Division, NBS, Boulder, CO, and W. E. Anderson, also of the NBS Electrosystems Division.
11:20 A.M.	"Automatic pulse parameter determination with the computer augmented oscilloscope system," A. A. Guido, L. Fulkerson, and P. E. Stuckert, Technical Staff, IBM Watson Research Center, Yorktown Heights, NY

11:45 A.M. "Status of reference waveform standards development at NBS," J. R. Andrews, N. S. Nahman, and B. A. Bell. J. R. Andrews, Picosecond Pulse Labs., Lafayette, CO formerly with NBS 724.04; N. S. Nahman, 724.04; B. A. Bell, NBS, 722 on assignment to NBS 724.04

12:10 P.M. Lunch

II. Afternoon Session: Workshop Leader, B. A. Bell

1:30-3:00 P.M. Workshop on measurement techniques for characterizing waveform recorder parameters and properties, and waveform recorder standards development.

3:00 P.M. Coffee Break

3:30-5:00 P.M. Workshop continues

5:00 P.M. Adjournment

Workshop on Measurement Techniques for Characterizing Waveform Recorder Parameters, Etc.

The following are official notes recorded at the workshop and consist of lists of problems presently encountered in waveform recorder evaluation and why proper evaluation of these recorders is important as suggested by the workshop attendees.

Don Flach, NBS	Difficulty in obtaining effective number of bits (every time). Need stable answers. Instruments are hard to use.
Mike Souders, NBS	Difficulty in specifying a few significant figures of merit for dynamic range (converters).
Bill Boyer, Sandia	Serial correlation in samples.
John Ramboz, NBS	Time base or sample time interval drift (change in waveform shape) for real-time and equivalent time.
Paul Stuckert, IBM	Terminology and definiton of terms for waveform recorders.
J. R. Andrews, Picosecond Pulse Labs.	Characterizing the leading edge (H.F.) properties of waveform recorders.
Gordon DeWitte, EG&G Los Alamos	Terms and Definitions Reliable, readily available, inexpensive pulse standards.
David Hutton, EG&G Los Alamos	A major problem is the lack of methods and tools for <u>accuracy</u> measurements that can be translated into overall performance specs., i.e., one has to be able to predict performance for any input from a small (presumably) number of test measurements.
Bob Billings, LeCroy Research Systems	Separation of stimulus/measurement artifacts from the device under test. Availability of measurement standards (hardware) at rational cost.
Nelson Cochrane, EG&G, Las Vegas	There is a real need to develop various methods of characterization that will allow someone to make measurements on his waveform recorder and know the methods are valid. Example: Is sinewave response calibration valid for making pulse measurements?
Chuck McConaghy Lawrence Livermore National Lab.	Comparison of analog (scopes) and waveform digitizers. Is there some standard that will characterize both so that they can be compared? Figure of merit for transient recorders to compare one against another. Bits vs. frequency for example.

Sedki M. Riad, Virginia Polytech. & State University

I believe that the time base drift problem is the most important one. One can deal to a certain extent with almost all of the others on the list except the time drift one.

Second in priority in my opinion is characterizing the leading edge HF properties of the recorder. Characterizing the recorders distortion to the waveform is more or less the same kind of thing.

Serial correlation in samples.

Terminology and definitions.

Pete Schuller, Tektronix

Real time and equivalent time samplers give rise to both amplitude and time time base distortion. Amplitude distortion is particularly severe for real time scopes since they are usually used with large amplitude signals which result in more serious thermal effects. Resonances due to more complicated triggering arrangements also cause problems. Equivalent time samplers also generate amplitude distortion. This is particularly true for random samplers with large voltage excursions between adjacent sample points.

Lee Sandoval, EG&G, Las Vegas

Environmental Specifications - our diagnostic instrumentation systems are housed in mobile trailers. Instrumentation real estate is very valuable and we try to put as many recording instruments as we can into a trailer. We have limited power and air conditioning available. We need specifications on environmental specs which are meaningful and valid. We also need these specs in determining what we need to do to operate these instruments in a field environment.

Repeatability
Accuracy
Reliability

We are recording diagnostic data from underground nuclear tests. Since we cannot rep-rate a nuclear test, repeatability, accuracy and reliability are very important to us. We have but one chance to record this data.

M. D. Carlisle, EG&G, Las Vegas

In addition to standardizing many of the common characteristics of waveform recorders, a need exists for a formal definition of the environmental conditions relative to device performance. Associated with this is a need for standardizing a procedure for the determination of MTBF under REAL conditions.

As an end-user of various waveform recorders, and responsible for the commitment of a large amount of Government capital dollars, these are factors of great importance in large systems. NBS could provide a valuable service in helping to establish these standards.

A major factor in the ultimate cost of a data acquisition system is the maintenance of the equipment and the peripheral equipment required to

M. C. Carlisle, Cont.	provide proper temperature, airflow, etc.
Fernando Herrera, Kelly AFB, San Antonio, Texas	Repeatability! My most current needs are in the area of ATE calibration. Presently, I am working closely with AGMC Newark AFS, Ohio in developing a PATEC (Portable Automatic Test Equipment Calibrator) package for 3 systems (consisting of 5 testers).
Tommy Thompson, EG&G.Las Vegas	In order of importance: o Difficulty in repeatility o Environmental affects to the specifications o Identifying errors that can be corrected o Drift time and amplitude o Absolute accuracy
Tommy Thompson, EG&G, Las Vegas	In my particular application, data collection at Nevada Test Site, reliability is of major importance. Some means of anticipating failure modes would be of great help. Another thought - calibration of the digital system (7912 AD's) consumes about $100K of equipment and 90% of our software time. System calibration is expensive and time consuming, anything that would decrease the cost and time would be helpful.
Jim Sorden, HP Santa Clara, CA.	Objective measures are needed that will help skilled and nonskilled (users, workers) in comparing instruments.
Bill Boyer, Sandia	People will come and say the scope is broken and one has to prove that it is O.K. and to do that I want reliable information about the measurements.
Mike Carlisle, EG&G	A device doesn't exist which can evaluate high speed diagnostic equipment.
Tommy Thompson, EG&G	Applying the same source waveform to digital (such as 7912's) and analog instruments (such as oscilloscopes) gives different results. The average difference is 5 to 7%. We calibrate to a system accuracy of 3%. The discrepancy is probably not due to the plugin.
Mike Souders, NBS	What is really required is bits per speed·(conversion time).
Dave Hutton, EG&G	Need to be able to evaluate recorders with 1 Gigasample per second, 200 MHz analog band width capability. The characterization must be inexpensive and capable of 8 bits absolute accuracy. Seven bits of absolute accuracy can be shown to yield useful physical data related to weapon yield. Other experiments require 10 gigasamples per second with less absolute accuracy.
Jim Sorden, HP	The spectrum should be extended to D.C. There are medical diagnostic sonar, electromechanical and other applications on this end of the spectrum.

Jim Sorden, Cont.	Measurement evaluation techniques should be designed with not only skilled, but also nonskilled operators in mind.
Bruce Peetz, HP	One needs to have some idea how much worse than ideal any given instrument is and how polluted the measured waveform is. These requirements are specifically different than simply determining whether the instrument is in the failure mode. .

Some Specific Tests and Other Developments Needed.

Dave Hutton, EG&G	o Differential linearity, ramp function, random trigger, histograph of values.
	o Asynchronous techniques can be used to generate statistics. The result should be flat. If it is not, look for a malfunction.
	o Use a video A/D and record a sine wave. Perform the FFT and look at the power outside the fundamental. This can be used to throw away bad A/D recorders.
Steve Hessel, HP	o Look at the time evolution of error after transition. The current need is -80 dB after 4 nanoseconds. The projected need is -80 dB after 500 picoseconds.
Barry Bell, NBS	o As with waveform recorders, sampling techniques are used in the measurement channels of modern ATE. Therefore, valid methods and standards are required for characterizing/calibrating multichannel ATE systems.
John Ramboz, NBS	o A better time base.
	o A vigorous theoretical analysis with a variety of analytic functions to relate time base drift to the resulting error in the frequency domain and determine the feasibility of applying corrections.

1. Is the timing right? Consensus = "yes".

2. What should be the charter? Consensus = "Develop standard way of characterizing both analog and digital waveform recorders for both real and equivalent time sampling.

3. Where and how often should the committee meet? Consensus = hold committee meetings and continue the seminars in connection with other conferences such as the Fast A/D converter conference and the Conference on Precision Electromagnetic Measurements (CPEM). The first steering committee meeting will be held in conjunction with the next Fast A/D Converter meeting February 15, 1982 in Santa Clara, California. The next Seminar will be held in conjunction with the next CPEM meeting June 28-July 1, 1982 in Boulder, Colorado.

4. Suggested sponsors? Instrumentation and Measurement Society of IEEE; Power Engineering Society Subcommittee on Digital Techniques; and International Electrotechnical Commission.

5. Who will be on the committee?

    1. William B. Boyer
       Sandia National Laboratories
       Division 4251
       Albuquerque, NM 87185

    2. Mr. Don Campbell
       Lawrence Livermore National Laboratory, L-473
       P. O. Box 5508
       Livermore, CA 94550

    3. Gordon DeWitte, Eng. Spec.
       EG&G, Inc.
       P. O. Box 809
       Los Alamos, NM 87544

    4. David George
       Naval Research Lab.
       Orlando, FL

    5. Fernando Herrera, Jr.
       Electronics Engineer
       SA-ALC MATTE
       Kelly Air Force Base, TX 78241

6. J. David Hutton
Scientific Specialist
EG & G, Inc.
P. O. Box 809
Los Alamos, NM 87544

7. Roydn Jones
Tektronix Mail Station 50-383
P. O. Box 500
Beaverton, OR 97077

8. Mr. Louis Navarro
Tektronix Mail Station 39-133
P. O. Box 500
Beaverton, OR 97077

9. Bruce Peetz
Hewlett Packard Co.
5301 Stevens Creek Blvd.
Santa Clara, CA 95050

10. R. Clayton Smith
Electronics Reaction History Group
Los Alamos Scientific Laboratory
University of California MS 410
Los Alamos, NM 87545

11. Christian E. Somers
Product Manager
Gould, Inc.
4600 Old Ironsides Drive
Santa Clara, CA 95050

12. James L. Sorden
R&D Section Manager
Hewlett Packard
5301 Stevens Creek Blvd.
Santa Clara, CA 95050

12. Mike Souders
National Bureau of Standards
Division 722
Metrology A-165
Washington, DC 20234

13. Paul E. Stuckert
Research Staff Member
IBM Research Center
Box 218
Yorktown Heights, NY 10598

Recommendations on Direction of Emphasis for the Standards Committee

Bill Boyer

- I think standards should be oriented towards defining figures of merit and test methods as independent as possible of the recording technique.

Sedki Riad

- I would like to see both real time and equivalent time devices included and I feel that the problem of analog vs. digital outputs is not a very critical issue. However, I am leaning to support the digital output since there is not much you can do with an analog one.

Comments on Seminar

Bill Boyer — I would like to see more talks on new recording techniques and specific test methods.

Fernando Herrera — This seminar was very well presented. Overall, I have learned some aspects which are applicable in my area of concern.

Lee Sandoval — The seminar was useful. I would like to see more papers presented.

Tommy Thompson — In general I felt the seminar was useful and informative.

Some Generic Waveform Recorder Problems

N. S. Nahman
Electromagnetic Technology Division
National Bureau of Standards
Boulder, Colorado 80303

Because of physical limitations the waveform displayed by a waveform recorder is not an exact replica of the signal or pulse applied to its input. The term physical limitations pertains to the network and electronic-device effects which can slow down and/or otherwise distort the shape of an applied pulse or transient signal. The limiting factors can be roughly grouped into two categories (1) bandwidth or signal distortion limitation and (2) analog to digital conversion limitations. A brief discussion of these limitations is given to provide some insight into the technical topics to be discussed by the remaining seminar speakers.

Key Words: Errors; pulse measurements; time domain measurements; waveform measurements; waveform recorders.

The basic reason for having this seminar is that the term pulse is not synonomous with the term waveform. The IEEE and IEC Pulse Standards, "Glossary of Pulse Terms and Definitions" defines Pulse as the physical modifications of state, and Waveform is the observed or measured shape of the pulse [1-4]. Clearly, the physical entity, the pulse, always does differ to some degree from the observable entity, the waveform.

The question that this seminar inherently poses is "How do we characterize the ability of a waveform recorder to provide an output that is a replica of a single-shot (or single-occurrance) time varying signal applied to its input?" The term single shot specifies that the recorder acquires the signal in real time as opposed to equivalent-time as encountered in sampling oscilloscopes.

There are many factors that must be considered in order to answer this question in any given case. The speakers following me will present various aspects and methods for characterizing such recorders - of course, what is presented here today will not be all inclusive, but will present some of the techniques that have proved to be useful in specific cases.

The purpose of the present paper is to provide a perspective or framework for relating the various ideas discussed by the other speakers. First of all, here is my definition of a waveform recorder:

> A WAVEFORM RECORDER is a time domain measurement instrument that is capable of recording in real-time a physical <u>Pulse</u> or <u>Transient</u> and <u>steady-state</u> signals, and provides a <u>Stored</u> (Digital) <u>Electronic</u> output.

Notice that the word digital appears in parentheses; from my perspective, the stored electronic output could be an analog one even though today's fashion requires a digital output. Furthermore, my guess is that most of you think in terms of a stored digital electronic output.

To emphasize the fact that the recorded information is never exactly identical to the input signal, the term PULSE is used for the input analog signal while WAVEFORM is used for the stored electronic output, Figure 1. These definitions are those required by the IEEE/IEC Standards [1-4].

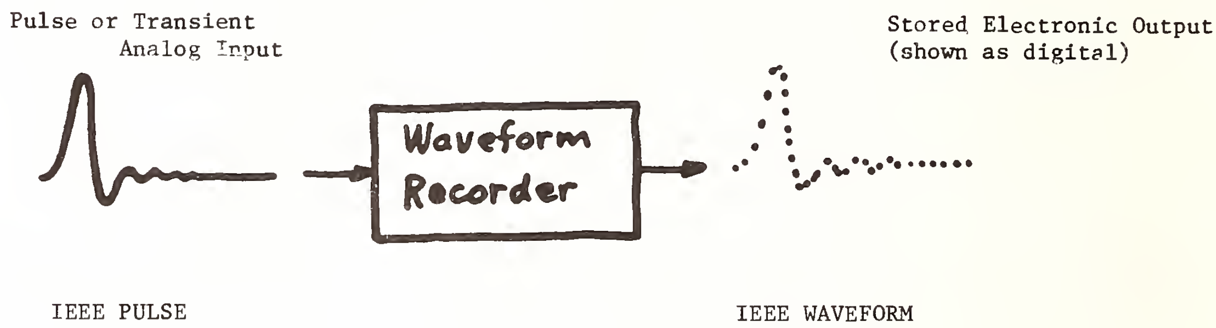

Figure 1. The physical PULSE and its observed WAVEFORM

The output WAVEFORM is not identical to the input PULSE because:

1. a finite set of discrete points can not exactly represent an analog transient signal.

2. the set of WAVEFORM discrete points overlays a distorted version of the input PULSE.

At best we could have the discrete points exactly overlayed on the PULSE, Figure 2.

Figure 2. The discrete waveform points are exactly overlayed on the pulse.

However, in an actual case we always have error, Figure 3. To some degree, the discrete waveform points are approximately overlayed on a distorted version of the PULSE.

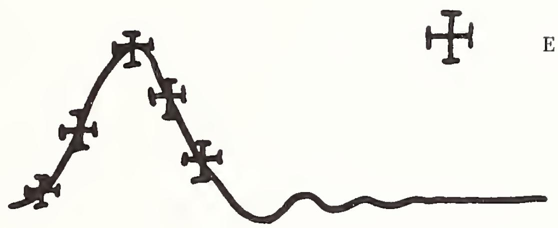

Figure 3. To some degree, the discrete waveform points are approximately overlayed on a distorted version of the pulse.

Consequently, it is possible to say at least in a qualitative sense that there are two generic problems or categories underlying waveform recorder errors:

1. Distortion

2. Digitizing Errors

Distortion has its roots in analog processes and their time and frequency domain properties. On the other hand, digitizing errors, i.e., incorrect output digital value for a given sample, result from a mixture of digital and analog circuit errors. Note that here the term digitizing-errors includes more effects than the usual definition based upon digital round-off errors. At first glance, the cause appears to be an analog one in the sample and hold circuitry, but a little thought brings one to the conclusion that that digital errors due to digital conversion speed are also limited by analog processes in the digital circuitry. Figure 4 is an attempt to diagram where DISTORTION and DIGITIZING ERRORS occur in a waveform recorder, and to catalog the processes and symptoms relevant to distortion and digitizing errors. In Figure 4, the notation T and/or F in parentheses following each item under distortion denotes that time-domain distortion and/or frequency-domain distortion results from the specified effects. In the case of sampling rate effects, only the frequency domain properties are affected when the time domain samples exactly lie upon the PULSE, Figure 2. With all samples exactly overlayed on the PULSE, the time domain distortion is zero; however, the number or density of points affects the Fourier transform or frequency domain properties as compared to the frequency domain properties of the analog PULSE.

In summary, a waveform recorder definition has been presented along with the IEEE Standard terms PULSE and WAVEFORM which specify the input and output signals, respectively, of the waveform recorder. The output WAVEFORM is not an exact replica of the input PULSE due to physical

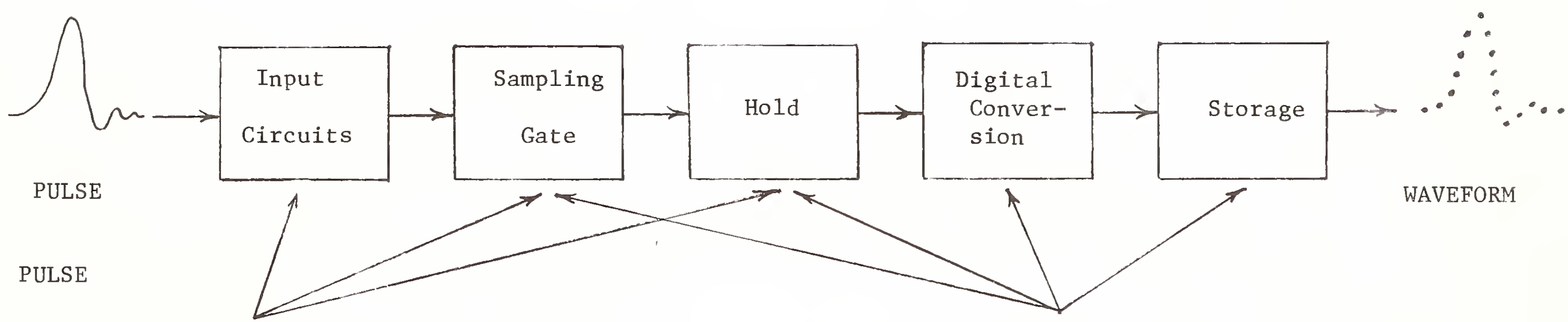

DISTORTION includes:

- Passive linear circuit effects (T,F)
- Sampling rate effects (F)
- Nonlinear effects (T, F)
- Sampling-gate effects (T, F)
- ⋮

and so on.

DIGITIZING ERROR includes:

- Sampling and hold nonlinearity
- Inadequate digital conversion speed
- Repetition rate dependence
- Quantizing Errors
- ⋮

and so on.

T - time domain distortion

F - frequency domain distortion

Figure 4. The sources of distortion and digitizing errors in a waveform recorder.

limitations in the waveform recorder passive and active circuitry. The errors or circuit problems have been divided into two generic classifications: (1) DISTORTION and (2) DIGITIZING ERRORS. A waveform recorder block diagram was given to provide a structure for illustrating the areas where distortion and digitizing errors occur.

REFERENCES

1. "IEEE Pulse Measurement and Analysis, General Considerations", IEEE Standard 181-1977, The Institute of Electrical and Electronic Engineers, N.Y., N.Y. July 22, 1977.

2. "IEEE Glossary of Pulse Terms and Definitions", IEEE Standard 194-1977, The Institute of Electrical and Electronics Engineers, N.Y., N.Y., July 26, 1977.

3. "IEC, Pulse Techniques and Apparatus, Part I: Pulse Terms and Definitions, Publication No. 469-1, First Ed., International Electro-technical Commission, Geneva, Switzerland, 1974.

4. "IEC, Pulse Techniques and Apparatus, Part II: Pulse Measurement and Analysis General Considerations", Publication No. 469-2, First Ed., 1974, International Electro-technical Commission, Geneva, Switzerland, 1974.

Steady State Tests of Waveform Recorders

D. R. Flach
National Bureau of Standards
Washington, D.C. 20234

Sinusoidal stimuli are often used for the dynamic testing of waveform recorders and fast analog-to-digital converters. This approach has the advantages that sinewaves are well-defined signals, and are easily generated over a wide frequency range with parameters that are readily measureable. Two methods are presented for analyzing the data from such tests, and two resulting figures of merit, the rms signal-to-noise ratio (S/N ratio) and the effective number of bits, are discussed. In the frequency domain, the S/N ratio is obtained from the magnitude spectrum, which is calculated by performing a Fast Fourier Transform on a set of m code words weighted with a Hanning window. In the time domain, a sinewave is fitted to the set of data words, using a nonlinear least squares computation. The fitted curve is then compared with the original digitized data to calculate the S/N ratio. The results of sinewave tests on different types of waveform recorders are presented, along with a comparison of time domain and frequency domain analysis of the data. The influence of two specific types of analog-to-digital errors on the resulting S/N ratio are computed and presented as examples.

Key words: analog-to-digital converter; digitizer; dynamic testing; effective number of bits; frequency domain; quantizing error; signal-to-noise ratio; time domain; transient recorder.

1. Introduction

One method for the dynamic testing of waveform recorders and fast analog-to-digital converters is to apply a periodic waveform to the input and analyze the performance of the test unit by using digital signal processing on the output data [1-4]. Sinusoidal stimuli of high purity that are uncorrelated with the sampling frequency are often used for this purpose since they are well-defined signals easily generated and characterized over a wide frequency range. Figure 1 shows a test system with a sinusoidal input as the stimulus. The final output from this test is the rms signal-to-noise ratio (S/N ratio) or a related number, the effective number of bits of the instrument. As will be shown later, the quantizing error of an ideal n-bit waveform recorder results in a S/N ratio of 6.02n + 1.76 decibels. Deviations from this ideal value are an indication that there are errors in the test instrument in addition to the inherent quantizing errors associated with an ideal digitizer. Using the measurement approach indicated in figure 1, the S/N ratio can be calculated from the digital output code using either frequency or time domain analysis.

In the frequency domain, the S/N ratio is calculated from a set of m output code words, where m is a power-of-two from 16 to 1024, by weighting the data with a Hanning window, and performing a Fast Fourier Transform to obtain the magnitude spectrum needed for the calculation. In the time domain, where the power-of-two restriction does not apply, a sinewave of the form $y = A + B \sin (CX+D)$ is fitted via a nonlinear least squares computer program to the digital output data, and this fitted curve is compared with the original digitized data to calculate the S/N ratio. Finally, the concept of the "effective number of bits" of the test instrument can be employed. If a waveform recorder behaves like a perfect digitizer, then its only error is the quantizing noise. If the S/N ratio is measured, the effective number of bits n_1 can be calculated from

$$(S/N)\ \text{measured} = 6.02n_1 + 1.76.$$

2. Quantizing Error

In figure 2 the transfer function of an ideal 3-bit analog-to-digital converter is shown along with the quantizing error or noise of the converter. Let Q = the voltage corresponding to one least significant bit (LSB) of the converter, FSR = full-scale range of the converter, then $Q = FSR/2^n$ for an n-bit converter. For each digital output code word there is a continuum of analog input voltages that range from $-Q/2$ to $+Q/2$. The quantizing error is the difference between the analog input and the analog value computed from the digital output code. As shown in figure 2, the quantizing error can be represented as a sawtooth waveform with amplitudes from $+Q/2$ to $-Q/2$ in each quantizing interval. As illustrated in figure 3, the rms value of this waveform is calculated to be $Q/\sqrt{12}$.

3. RMS Signal-to-Noise Ratio

Let $S = V/\sqrt{2}$ be the rms value of a sinewave input signal of peak value V. If V is a full-scale input signal applied to a bipolar range digitizer, then

$$S = \frac{FSR}{2\sqrt{2}} = \frac{Q2^n}{2\sqrt{2}} .$$

Let N be the rms quantizing error or noise of the digitizer, which has been shown to be equal to $Q/\sqrt{12}$, then the S/N ratio of this ideal n bit digitizer is

$$S/N = \frac{Q(2^{n-1})/\sqrt{2}}{Q/\sqrt{12}}$$

and in decibels, $20 \log(S/N) = 6.02n + 1.76$.

For a signal V less than full scale,

$$S/N = 2^{n-1} \sqrt{6} \; \frac{2V}{FSR}$$

or, in decibels

$$20 \log (S/N) = 6.02n + 1.76 + 20 \log \frac{2V}{FSR}.$$

4. Computation of S/N Ratio in Frequency Domain

The S/N ratio was computed using the Fast Fourier Transform by taking the rms value of the largest signal spectral line and dividing it by the rms value of the remaining lines. The magnitude of the Kth spectral line is given by

$$M_K = \sqrt{(\text{Kth real coefficient})^2 + (\text{Kth imaginary coefficient})^2}$$

and the S/N ratio by

$$S/N = \frac{\text{rms value of largest signal spectral line.}}{\text{rms value of remaining lines}}$$

The K = 1 line corresponds to the dc component and is omitted. Separate static tests can be used to examine and identify the effects of dc offset errors.

It was also found necessary to introduce other correction factors to compensate for errors caused by the use of a window function. Since there are generally not an integral number of periods of the input waveform in the data window due to the power-of-two restriction, a tapering or window function [5] is applied to the data set to reduce the leakage phenomena. Even when using a Hanning window function of the form y = 0.5 (1-cosx), spectral leakage into adjacent frequencies is not completely eliminated. This is illustrated in figure 4 for the worst case where the number of periods in the data window is an integer plus one-half. A number of spectral lines on each side of the fundamental are deleted from the noise computation because they are contaminated with leakage from the fundamental. The noise is computed from the equation

$$N = \sqrt{\frac{1}{2} \sum_{1}^{m/2} M_k^2}$$

To establish an average value or "noise floor" of M_k in the ideal case, consider all M_k's = M, and let $N = Q/\sqrt{12}$.

Then

$$Q/\sqrt{12} = \sqrt{\frac{1}{2} \frac{m}{2} M^2}$$

and

$$M = 2Q/\sqrt{12m}.$$

In figures 10 and 12, the data is scaled to a range of ±1 volt to allow comparison of different test ranges; M = -89.1 dB for these figures. Thus, based on results obtained from the graph shown in figure 4, spectral lines with amplitudes greater than $2Q/\sqrt{12m}$ were not included in the noise computation.

Also associated with the window function is the processing loss, which is a fixed value as depicted in figure 5. This figure shows the spectrum of the function y = sin 4X + sin 32X where there is an integral number of periods in the data set, and no tapering function is applied, which is equivalent to using a rectangular window. If sin 4X is considered to be the signal, and sin 32X the noise, then the S/N ratio is zero dB. After a Hanning window function is applied to the same data set, and the identical set of computations are performed, the resulting S/N ratio is -1.76 dB. If the number of periods in the data set is not an integral number, an additional error is incurred which varies with the remaining fractional period and is a maximum at 0.5 period. This pickett fence or scallop effect is depicted in figure 6 when a Hanning window function is used, and has a maximum value of -1.42 dB. For an integral number of periods in the data set, the measured value of the fundamental (and other periodic functions) will be one-half (-6.02 dB) of the actual value. As the remaining fractional period in the data set increases from zero to one-half, this attenuation increases from -6.02 to -7.44 dB. If the fractional number of periods in the data set is known, a correction can be applied for this effect.

Another result of using the Hanning window is that if a dc offset exists in the data, this introduces a low frequency component into the first line (K = 2) of the spectrum. Therefore, this line was also deleted from the noise in these calculations. Finally, a factor was used that multiplied the measured noise by a number proportional to the number of spectral lines deleted around the fundamental to compensate for the lost lines. This factor was

$$H = \sqrt{m/(m - 2(\text{number of deleted lines}))}.$$

H can cause an error in the noise computation if, for instance, one spectral line contributes the majority of the noise. This line then gets weighted by the factor H, and the resulting noise computation is too high.

5. Computation of S/N Ratio in Time Domain

An alternative to the frequency domain method is to analyze the data in the time domain [6]. This approach involves fitting a sinewave of the form $y = A + B \sin(CX + D)$ to the digital output code from the waveform recorder using a nonlinear least squares fit program [7]. This fitted curve is then assumed to represent the original input waveform. A fit of a sinewave to a set of digital output codes is shown in figure 7. For the ideal digitizer, the residuals (fitted curve - output code) should fall within the range of ±0.5 LSB. The S/N ratio is then calculated from

$$20 \log(S/N) - 20 \log = \frac{\text{rms (amplitude fitted sinewave)}}{\text{rms (sum of residuals)}}$$

and the effective number of bits can be calculated as previously shown, or from the equation

$$n_1 = n - \log_2 \frac{\text{rms(sum of residuals)}}{Q/\sqrt{12}}.$$

Nonlinear curve fitting requires preliminary estimates of the parameters A, B, C, and D; the closer the initial guess the faster the program converges to a final value. A pre-fit program estimates these parameters (offset, amplitude, frequency, and phase) from the maximum data point, minimum data point, and the zero crossings. A commercial software regression analysis package based on Marquardt's nonlinear least squares method then performs a fit of the data to the sinewave function.

The residuals from an ideal 4-bit simulation are also shown in figure 7. Figure 8 is a computer printout of results based on a 10-bit simulation, with the errors expressed in LSB's. This printout gives the ideal value of the S/N ratio for a full-scale input (61.96 dB) and also the ideal value computed from the 90 percent of full-scale amplitude (61.05 dB), as determined by the equations given in section 3. The measured value of S/N ratio (60.95 dB) was determined using the curve fit routine and for a perfect digitizer, should be equal to the ideal 90 percent of full-scale value. The maximum error is 0.525, and the rms error is 0.292, which is close to the theoretical value of $Q/\sqrt{12} = 0.289$.

6. Effect of Errors On S/N Ratio

The effects that some types of errors have on the S/N ratio have been analyzed by modeling with a computer an n-bit successive approximation, offset binary coded analog-to-digital converter. The first type of error studied involves a one LSB quadratic nonlinearity, shown in figure 9. The error function $Q-QX^2$ is the deviation from the ideal transfer characteristic caused by a nonlinearity in the converter. The input variable X is normalized and has the range -1 to +1. For an input of the form $X = A \sin \omega t$, this error could be expected to produce a second harmonic spectral line in the output spectrum which has an rms value of $Q/2\sqrt{2}$ for a full-scale input voltage. The value of the noise can then be computed as being approximately equal to

$$N \approx \sqrt{Q^2/12 + (Q/2\sqrt{2})^2} = 0.46Q$$

and the S/N ratio should be

$$20 \log(S/N) = 6.02n - 2.3 \text{ dB}.$$

For the simulation results given in figure 10, the internal digital-to-analog converter of the model was assumed to have a one LSB quadratic nonlinearity. For a 10-bit digitizer, a value of 57.9 dB is calculated compared with ~58.0 dB obtained with the simulation.

The second type of error studied involves bit errors, an example of which is a one LSB error in the second bit as shown in figure 11. As in the previous example, N is the rms total of the quantizing noise and other errors, given by

$$N \approx \sqrt{Q^2/12 + (Q/2)^2} = 0.58Q.$$

While this computation gives the correct value for the noise produced by an error in bit 2, a S/N ratio test will give a lower value. Such tests fail to take into account that the spectra associated with the cyclic occurrence of the second bit contains a fundamental frequency component of the applied sinusoidal input. Therefore, this fundamental component is necessarily measured as signal rather than noise, producing an overestimate of true S/N ratio. This situation exists for other bit adjustment errors also, for instance, the cycling of bit one (most significant bit) follows a square wave of the same frequency as the applied sinusoidal input. If this bit has an adjustment error of 1.0Q, then the rms contribution to the fundamental spectral line caused by this error is 0.45Q, and the rms sum of the contributions of all remaining spectral lines is 0.22Q. As an example, a simulation with a 10-bit converter having a one LSB error in the second bit produced a S/N ratio of 57.1 dB which compares with 55.9 dB, calculated using N = 0.58Q. Numerous other errors can also be expected to affect the S/N ratio.

7. Test Results

Three waveform recorders were tested with both time domain and frequency domain analysis of the data. Due to computer memory limitations, a maximum of 256 data points were fitted by the time domain method. Fast Fourier Transforms were performed on 1024 data points, and subsets of these were used in the time domain solutions. Runs were made at various test frequencies, and in many cases amplitudes of both 50 and 90 percent of full scale were used.

Figure 12 shows the results of a frequency domain test on a 10-bit recorder which had a maximum sampling rate of 500 kHz. Figure 13 is a plot of the residuals from the curve fit for this test; a four LSB outlier is easily seen. A printout from the time domain analysis at a different frequency is shown in figure 14. Note that the maximum outlier has become slightly smaller, as reflected by the larger number of effective bits.

Plots of the effective number of bits vs frequency are shown in figures 15 through 17. Data from the 500 kHz 10-bit recorder plotted in figure 15 shows the 90 percent of full-scale values gave better results than the 50 percent of full-scale values. Data from a medium speed 10-bit recorder with a maximum sampling rate of 10 MHz is plotted in figure 16. Finally, data from an 8-bit 100 MHz recorder is shown in figure 17. Glitches observed in the output data at the faster sampling rates probably account for the deterioration in the effective number of bits at higher frequencies. These instruments were not tested at frequencies greater than one-fifth of the maximum sampling rate.

8. Conclusions

The above tests show that the time domain and frequency domain methods of calculating the effective number of bits give similar results. The frequency domain approach is computationally faster by virtue of Fast Fourier Transform routines, but restricts the number of data points to a power-of-two. The time domain method has no restriction on the number of data points, does not require a window function to control leakage, but does require subjective decisions by the operator in estimating a preliminary fit of the data, and is susceptible to a poor fit if not monitored. Harmonics of the fundamental input frequency are easily identifiable in the frequency domain method, but are difficult to detect from a time domain curve fit. Outliers in the data set are difficult to detect in the magnitude spectrum resulting from the frequency domain method, while a simple examination of the residuals computed from the time domain curve fit will easily point these out. Both methods obscure errors that result in fundamental frequency components as described in section 6.

9. References

[1] Pretzel, G., Dynamic testing of high-speed A/D converters. J. Solid-State Physics. SC-13(3): 368-370; June 1978.

[2] Burton, P. B., Checking A/D converter linearity analog dialogue. 13(2): 10; 1979.

[3] Pratt, B., Test A/D converters digitally. Electronic Design. 25: 86-88; December 6, 1975.

[4] Ramirez, R. W., Digitizer specifications and their applications to waveforms. Electronics Test. 4(9): 74-80, September 1981.

[5] Harris, F. J., On the use of windows for harmonic analysis with the discrete Fourier Transform. Proc. IEEE. 66(1): 51-83; January 1978.

[6] DeWitt, L., Dynamic testing reveals overall digitizer performance. Handshake, Tektronix Publication: 9-12; 1981, Spring/Summer.

[7] Daniel, C.; Wood, F. S., Fitting equations to data. New York: John Wiley and Sons; 1980, 458 p.

LIST OF FIGURES

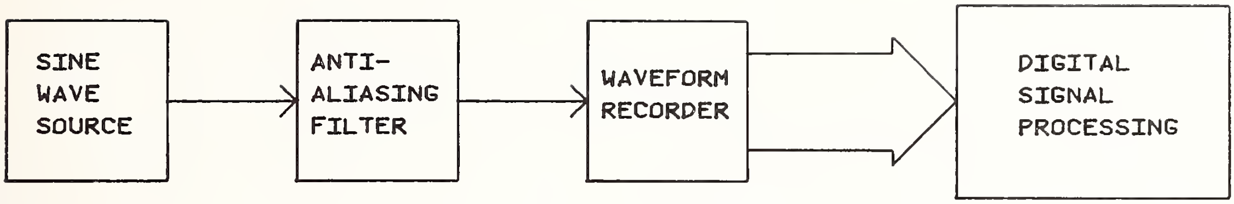

Figure 1. General measurement approach

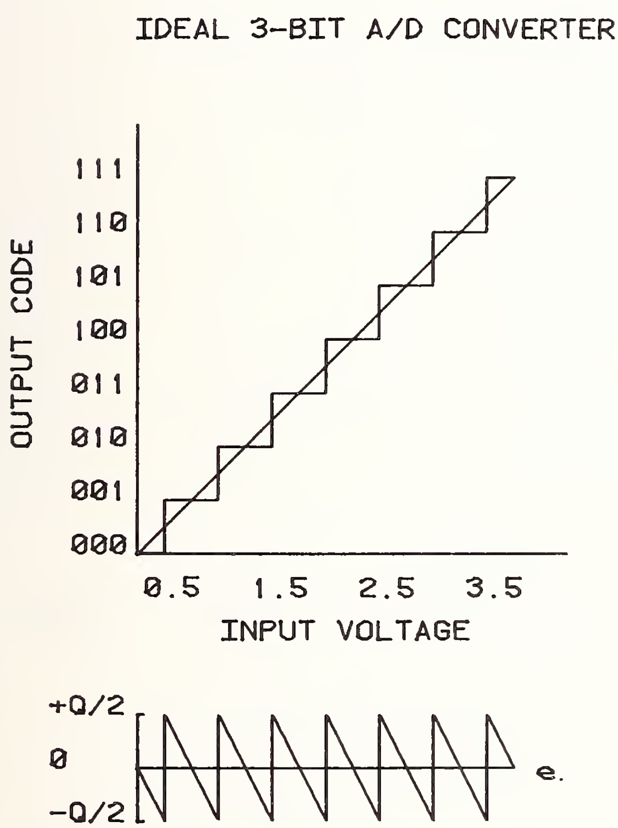

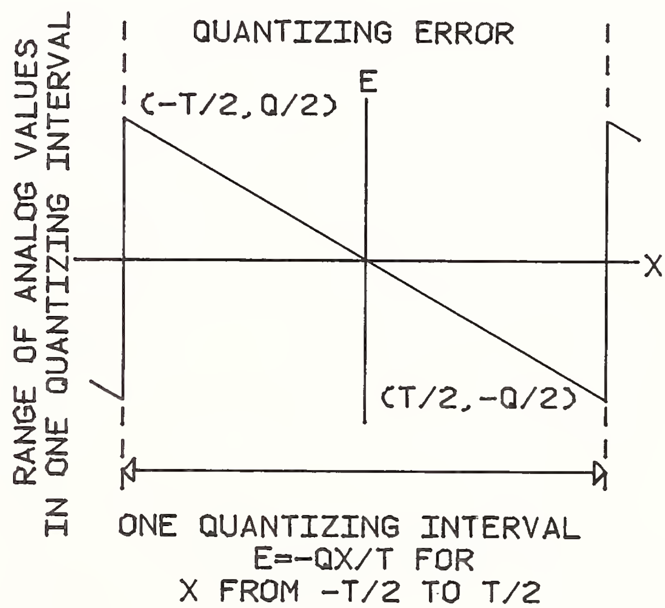

$$E_{rms}^2 = (1/T)\int_{-T/2}^{T/2} E^2 dX = Q^2/12$$

Figure 3. Quantizing error calculation

Figure 2. Quantizing error of ideal converter

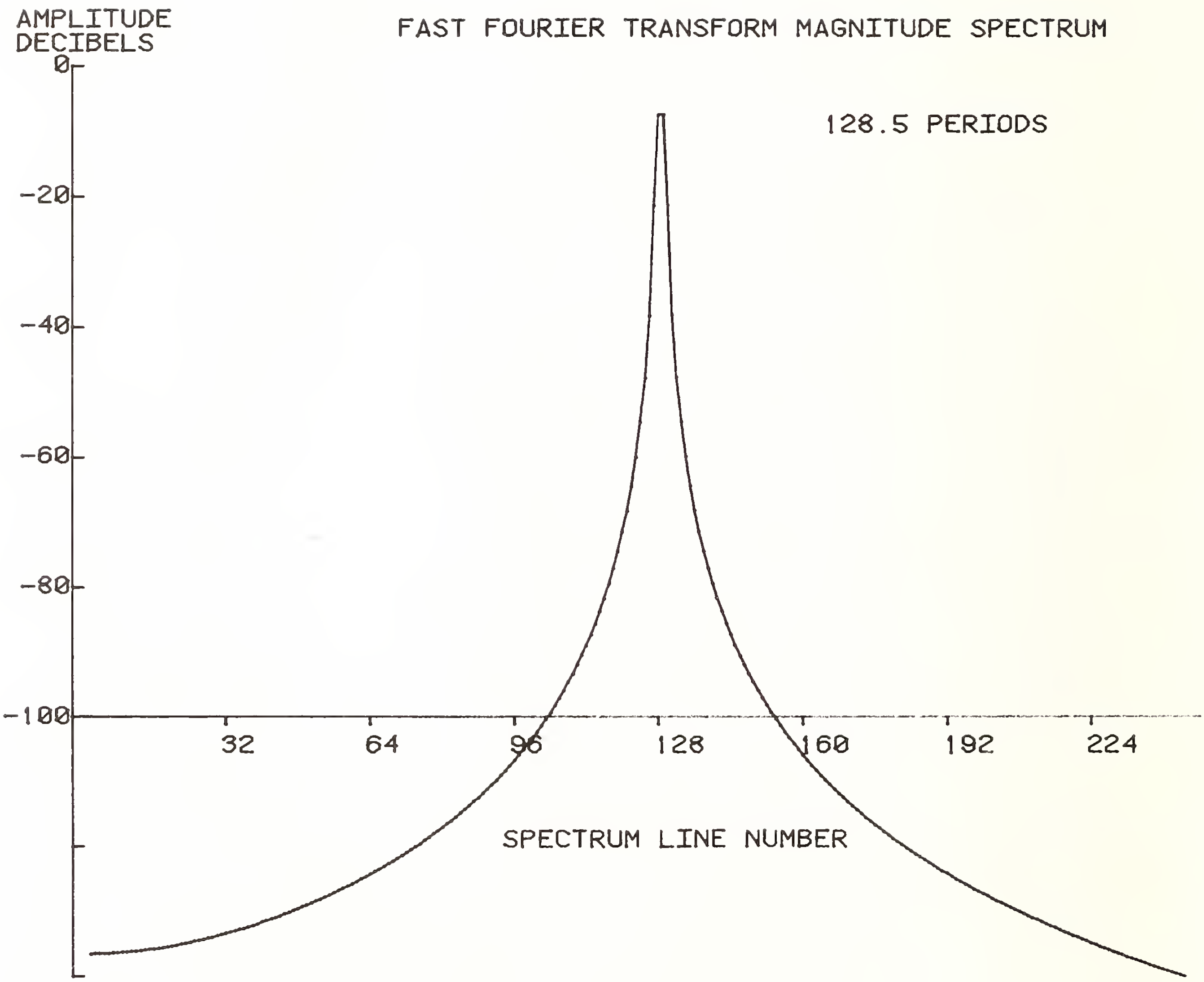

Figure 4. Leakage effect from Hanning window

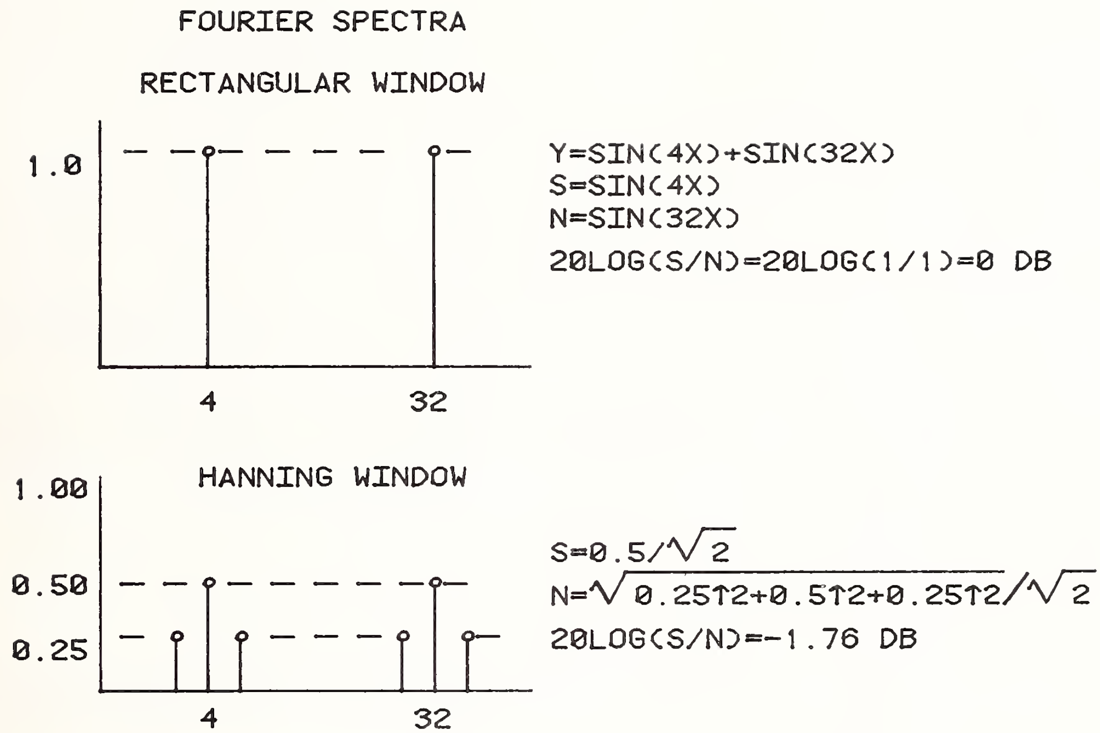

Figure 5. Hanning window processing loss

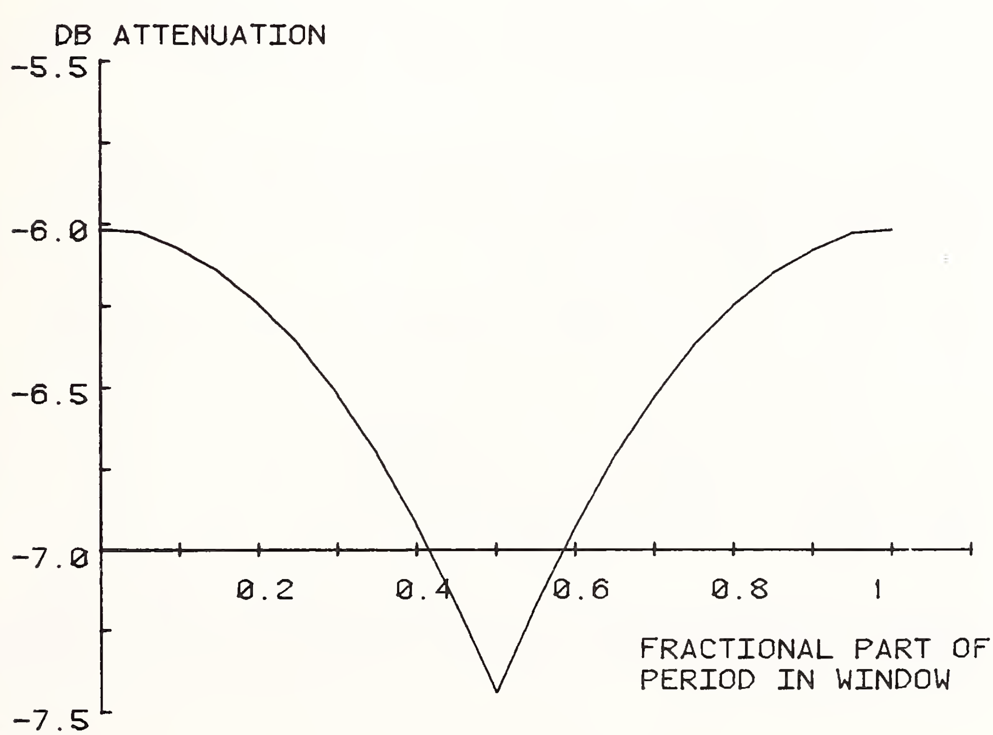

Figure 6. Hanning window - pickett fence effect

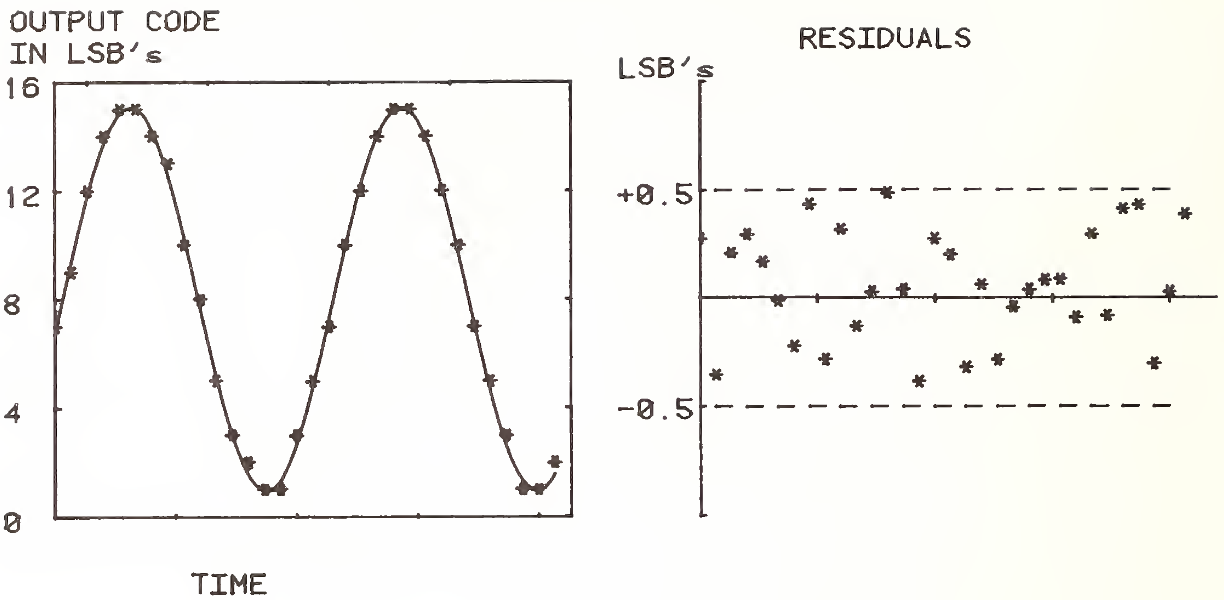

Figure 7. Time domain approach: sinewave fit to output data, and determination of residuals

```
************* TIME DOMAIN ANALYSIS ****************

      OF A SINE WAVE INPUT TO A DIGITIZER

IDEAL rms S/N RATIO FOR A 10 BIT CONVERTER WITH
A FULL SCALE SINE WAVE INPUT IS  61.96 DECIBELS
MEASURED rms S/N RATIO IS   60.95 DECIBELS
EFFECTIVE BITS ARE   9.984

FOR THE   90.00 PERCENT OF FULL SCALE SINE WAVE
USED IN THIS TEST, THE THEORETICAL rms S/N RATIO
IS   61.05 DECIBELS

MAX POSITIVE ERROR IS   0.498659
MAX POSITIVE ERROR LOCATION IS   185
MAX NEGATIVE ERROR IS  -0.524760
MAX NEGATIVE ERROR LOCATION IS  165
RMS ERROR IS   0.291913

10 BIT SIMULATION
256 DATA POINTS
8.274 PERIODS
```

Figure 8. Results of time domain analysis of an ideal simulated, 10-bit recorder

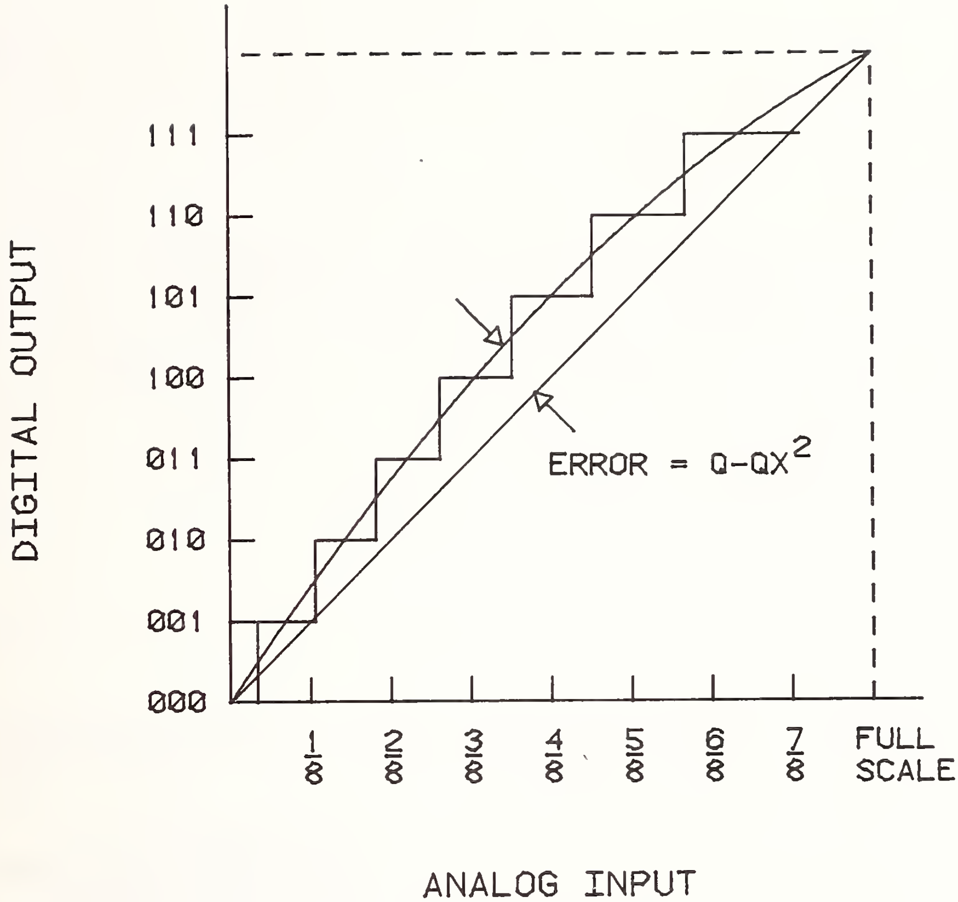

Figure 9. Quadratic nonlinearity error

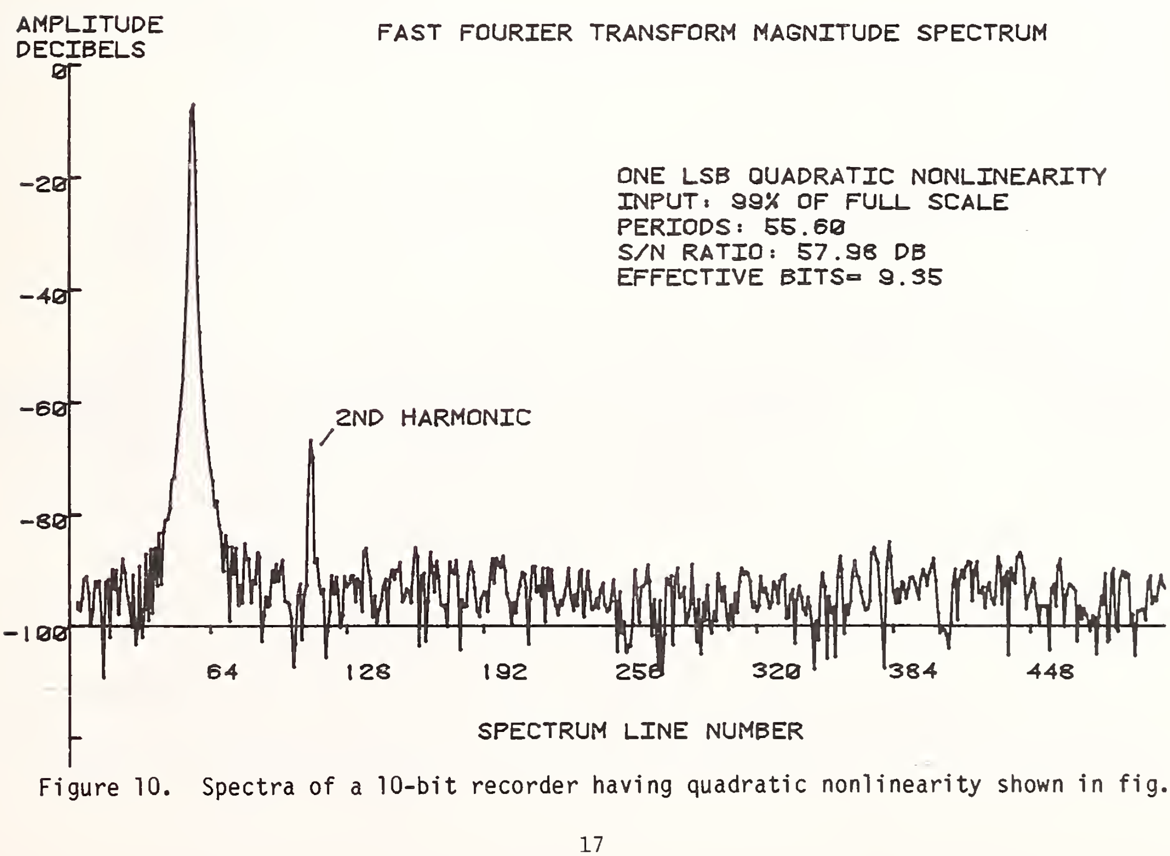

Figure 10. Spectra of a 10-bit recorder having quadratic nonlinearity shown in fig. 9.

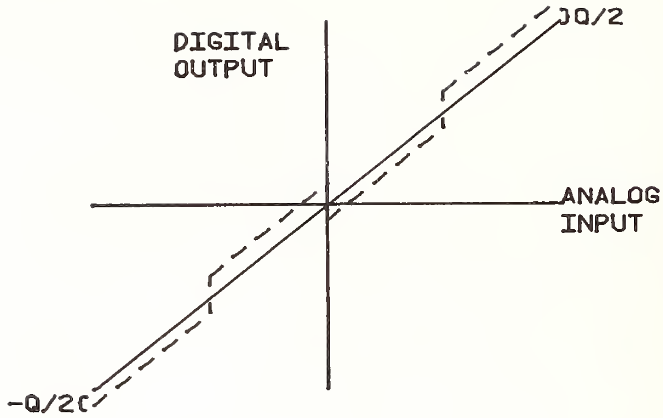

Figure 11. Second bit error

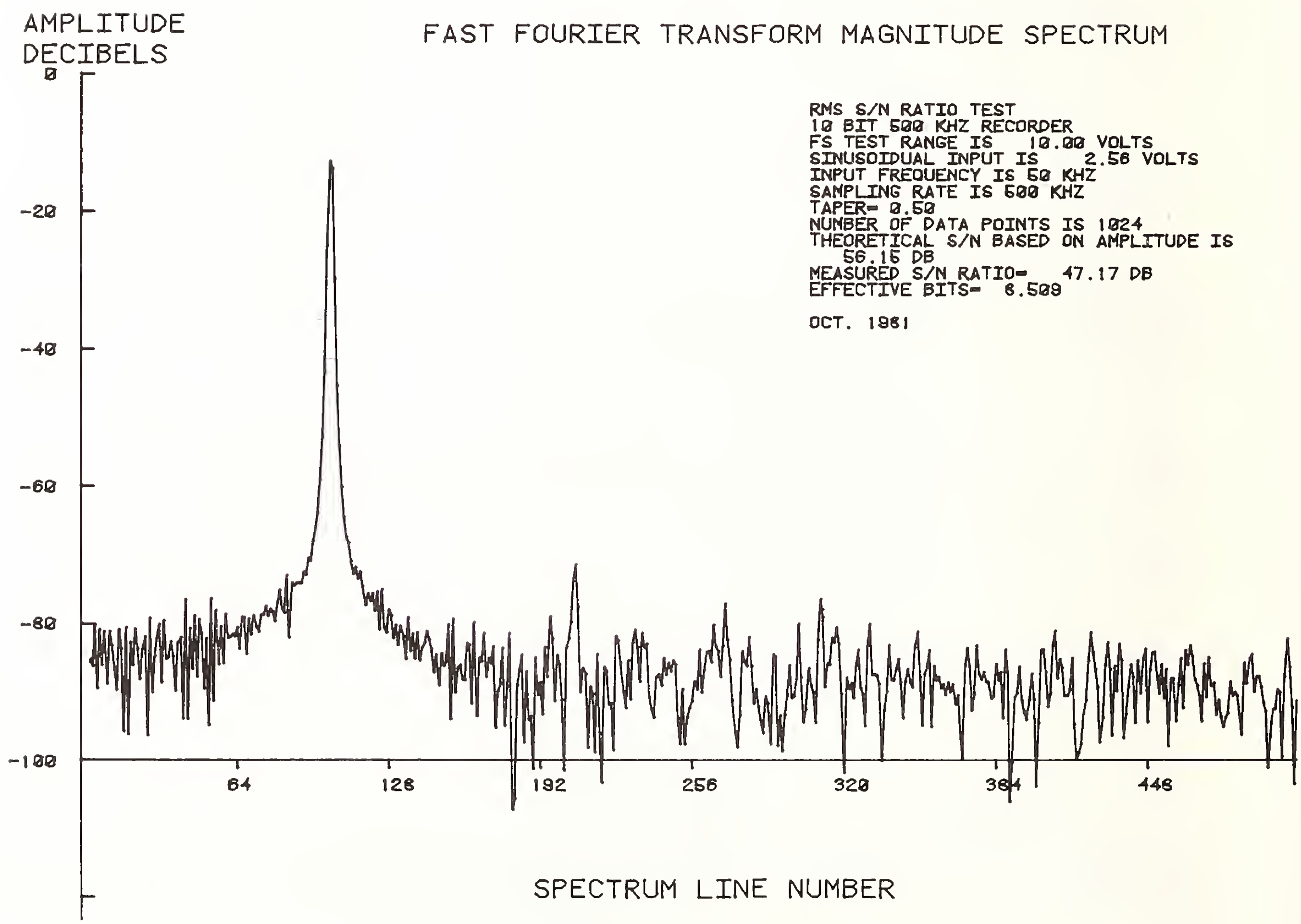

Figure 12. Frequency domain test results: 10-bit recorder with maximum sampling rate of 500 kHz

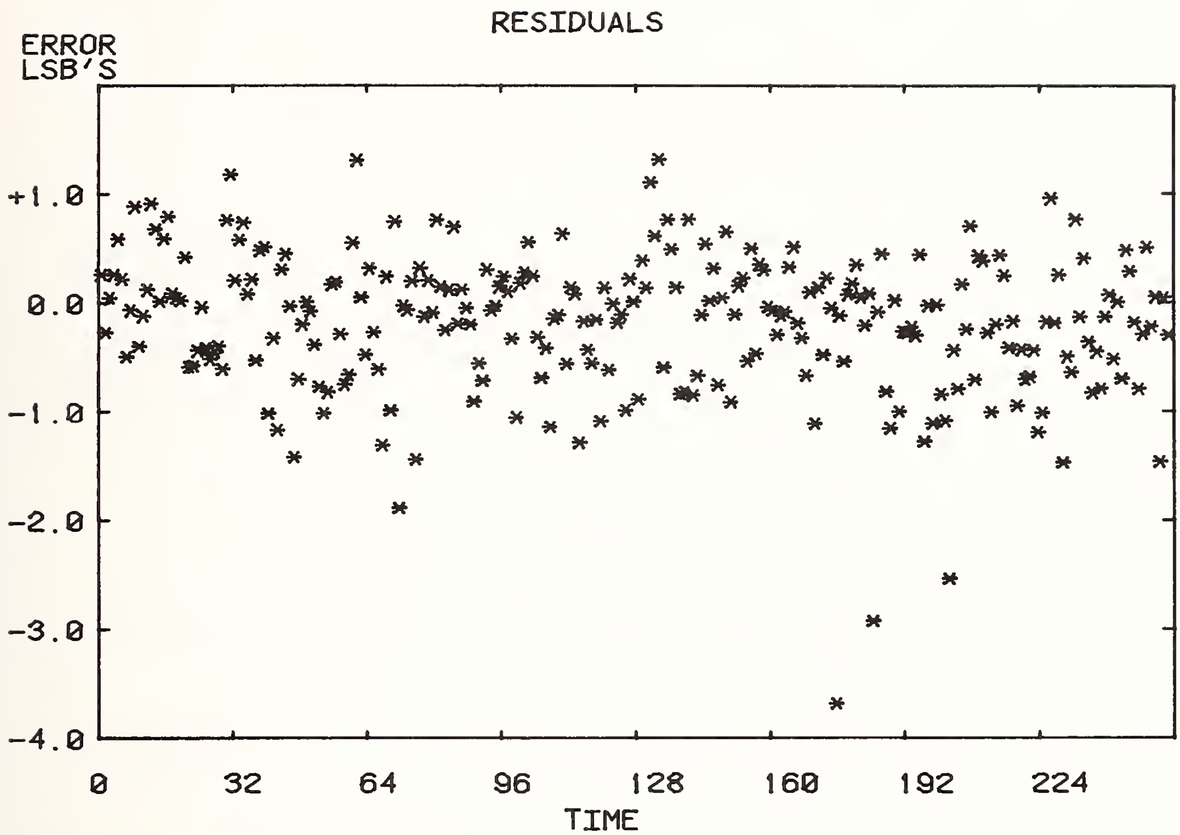

Figure 13. Residuals from time domain test: 10-bit recorder with 500 kHz sampling rate, 1 kHz test frequency

```
************ TIME DOMAIN ANALYSIS ***************

      OF A SINE WAVE INPUT TO A DIGITIZER

IDEAL rms S/N RATIO FOR A 10 BIT CONVERTER WITH
A FULL SCALE SINE WAVE INPUT IS  61.96 DECIBELS
MEASURED rms S/N RATIO IS   49.78 DECIBELS
EFFECTIVE BITS ARE   8.957

FOR THE   50.64 PERCENT OF FULL SCALE SINE WAVE
USED IN THIS TEST, THE THEORETICAL rms S/N RATIO
IS   56.06 DECIBELS

MAX POSITIVE ERROR IS   1.386669
MAX POSITIVE ERROR LOCATION IS   134
MAX NEGATIVE ERROR IS  -3.230074
MAX NEGATIVE ERROR LOCATION IS  176
RMS ERROR IS   0.594861

10 BIT RECORDER MAXIMUM SAMPLING RATE 500 KHZ
INPUT 10 KHZ, SAMPLING RATE 50 KHZ
FSR 10 VOLTS, 256 DATA POINTS
```

Figure 14. Results of time domain analysis of 10-bit recorder with maximum sampling rate of 500 kHz

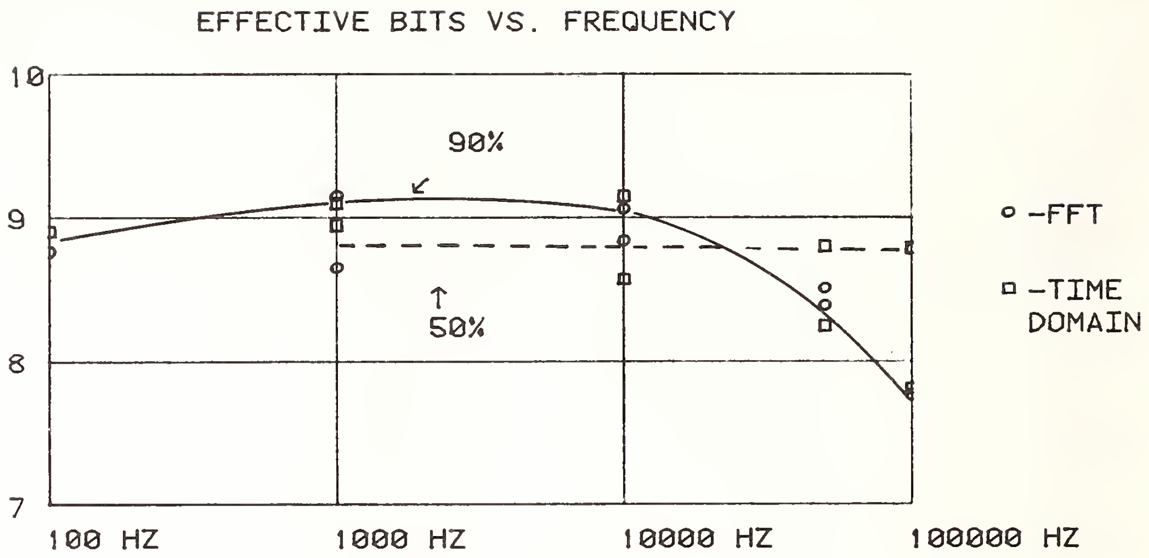

Figure 15. Results from both time and frequency domain tests: 10-bit recorder with 500 kHz sampling rate

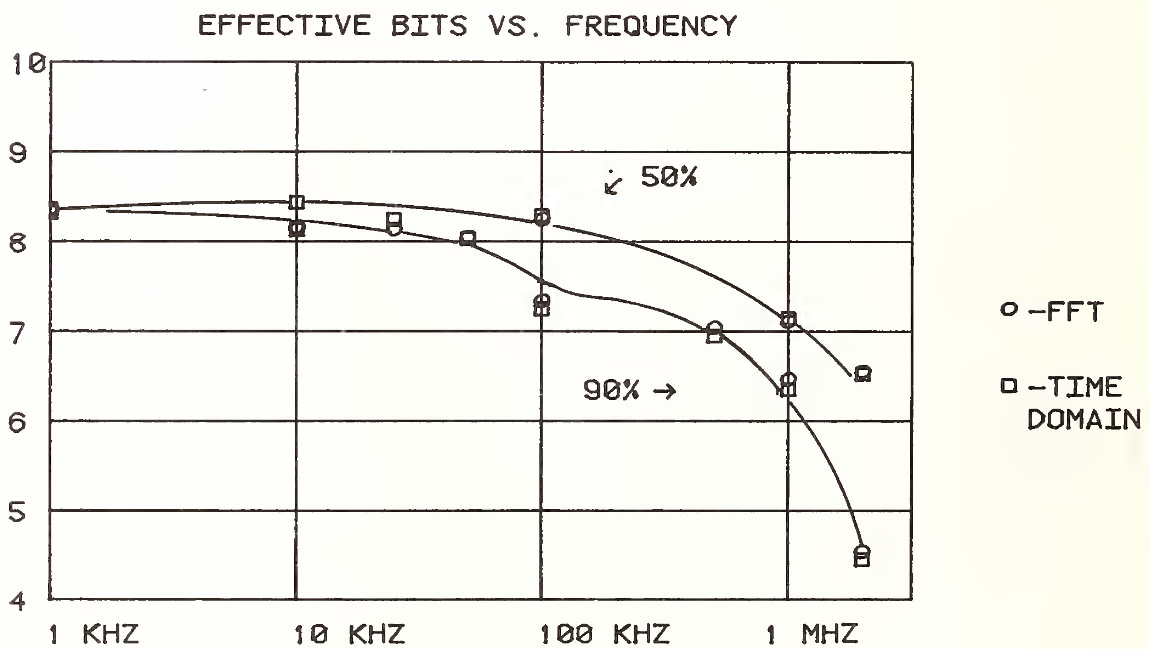

Figure 16. Results from both time and frequency domain tests: 10-bit recorder with 10 MHz sampling rate

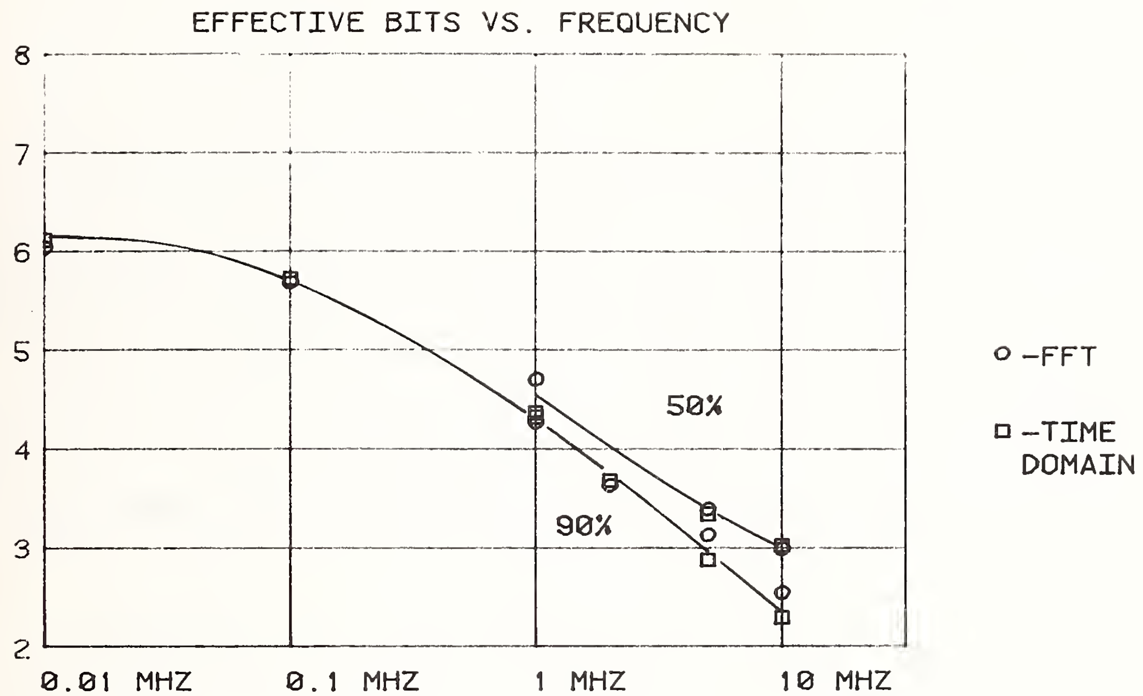

Figure 17. Results from both time and frequency domain tests: 8-bit recorder with 100 MHz sampling rate

CHARACTERIZING THE DYNAMIC PERFORMANCE OF WAVEFORM DIGITIZERS

Philip S. Crosby
Tektronix, Inc.

The obvious question that comes to mind when one considers using a waveform digitizer for a specific application is: "Is it good enough?". The answer to that question has two states; yes or no. However, the number of states that the code sequence of a digitizer can occupy can become astronomical in a pretty short time. Thus, the characterization of a digitizer must become an exercise in data reduction, coupled with careful consideration and selection of allowable test stimuli. The test stimulus should have low entropy, that is, the number of coefficients needed to describe it fully should be small in number.

There is very little that can be said about a sinewave; this will be shown to be of considerable advantage for our purpose. In an absolute sense, the only two properties that a sinewave has are amplitude and frequency. However, a sinewave applied to a digitizer must be represented by two additional properties, phase and D.C. offset. Therefore, we can perhaps envision a process downstream from the digitizer where the operator might push a button marked "sinewave" and out come the four numbers:

Amplitude	- A	Phase	- Ø
Frequency	- F	D.C. Offest	- D

These values having been computed from a sample sequence:

$\{s\}$

It is obvious that sequence $\{s\}$ must contain at least four terms, but the upper limit on the number of terms is unbounded.

Now, if we distrusted magic buttons and wanted to see if the sequence, $\{s\}$, really produced those values, we could work backwards.

$$\{s\}_{test} = D + A\cdot \mathrm{Sin}(\{i\}\cdot F + \emptyset)$$

Where

$$\{i\} = 0,\ \frac{1\cdot 2\pi}{F_s N},\ \frac{2\cdot 2\pi}{F_s N},\ \ldots\ ,\ \frac{(N-1)\cdot 2\pi}{F_s\ N}$$

And

F_s = sampling frequency

N = number of samples in sequence $\{s\}$

This enables us to produce an error sequence, $\{e\}$

$$\{e\} = \mathrm{ROUND}(\{s\}_{test}) - \{s\}$$

Where the function, ROUND, is a rounding function.

It can be shown that the function tied to the button marked "sinewave" can be recursively optimized by recycling $\{s\} - \{s\}_{test}$ through the function and updating the coefficients A , F , Ø , and D until the R.M.S. value of $\{s\} - \{s\}_{test}$ has sensibly reached a minimum value. At this point, the R.M.S. value of $\{e\}$ should express the sample-by-sample difference between the digitizer being used and an ideal digitizer, providing the errors in the digitizer do not cause the measured parameters A , F , Ø , and D to systematically interact.

Comparisons between this method and more complex methods that place restrictions on frequency or phase values and/or require sample sorting have indicated that this method correlates very well with other methods. Also, the measurements of the sinewave properties agree very closely with externally measured properties (note that Ø is the only parameter that is difficult to verify externally).

Now, we might ask, "What properties of the digitizer are actually being measured ? By changing the frequency of the sinewaves, we can get a measure of effective bits vs. frequency, but what actually goes on and what relevance does it have with respect to measurements of a more complex waveform?"

That is a good question that demands an answer. Unfortunately, the answer that can be offered is not a complete one, but it is the best one we can think of, and, perhaps as good an answer as we may get with any test method.

Digitizers really have three classes of errors:

1. Quantization Error - this is customarily treated simply a rounding error, but in reality, we must include two other components:
   A. The errors due to nonlinear quantization thresholds.
   B. The errors due to sampled analog noise.

   These errors are independent of the sinewave frequency and represent a kind of baseline accuracy the sum of which can be inferred from the test method described herein.

2. Aperture Jitter

   This is the characteristic that is usually measured by sampling a rapidly rising (or falling) voltage. This would normally be expected to produce an error value that increased linearly with respect to frequency. This characteristic is inferred by measuring the variance of sample values over many repetitions of the test signal. Note that the mean value is seldom measured.

   This error component is usually associated with time jitter in the strobe pathway. It is certainly real, but is probably less significant than the next term to be described, which has received little attention.

3. Signal-Dependent Aperture Errors.

   Any digitizer must explicitly or implicitly sample the input signal. This sampling operation involves the variation of a parameter which must be a component of a low-pass filter, if the hold mode is to have any meaning. For most samplers, this parametric variation occurs most rapidly when the time derivative of the signal being sampled is zero. If the time derivative is non-zero, then the "on" resistance of a sampling bridge or the 1/Gm of a strobed comparator is usually higher than its optimum value. This produces a consistent increase in what might be called the "analog set-up time" of the digitizer. This error is nearly proportional to the square of the dV/dt of the signal. This suggests that our sine-wave test should indicate an error that is proportional to the square of the frequency-amplitude product.

Our analyses of various digitizers indicate that this third error term quickly becomes dominant as the frequency is increased. It is also easy to see how the existence of this error type could have been missed in the course of making aperture jitter measurements, since this kind of error would result in the mean sample value having been shifted.

ADVANTAGES

This test method allows the evaluation of digitizer distortion at any frequency that can be generated by a sinewave generator. No special relationship between the generator and the sample clock need be set up. Results can be plotted in a manner similar to the plots of frequency response of analog systems. Furthermore, the measurements that must be made in order to infer the effective bits measure may be sued seperately to describe the conventional frequency response and to diagnose the conversion errors more fully.

While it is true that rather involved processing of the sample data is necessary, once that analysis method has been put in place, many types of digitizers may be tested in the same manner.

POSSIBLE CONCERNS

Although the performance of the digitizer can be assessed relative to sinewave inputs, are there other, more complex waveforms that could produce unexpected errors? The answer would seem to be,"no", providing that the signal being digitized is truly reconstructable. The proposed method can be used for signal frequencies up to nearly one half of the sampling frequency. That involves sampling time derivatives that must at least be equal to the highest values that can be contained in any reconstructable signal at any portion of the dynamic range.

It is possible that the best fitted sine wave that can be computed from the sample record may differ significantly in phase, amplitude or D.C. offset (a significant frequency error is very unlikely). The amplitude and D.C. offset errors can be detected independently without too much effort, but the measurement of phase is likely to be somewhat more difficult. This area has not been investigated as completely as might be hoped, but digitizers that have performed well according to the "effective bits" measure have been used in some extremely phase-sensitive applications (group delay measurements, for example) and have acheived accuracies that were within predicted limits.

ACKNOWLEDGEMENTS

The first and most important, of course, is to Lyle Ochs, who developed the concept in the first place. The author's role in this paper has been more in the way of evaluation rather than invention. Thanks also to John Lewis, Dale Jordan and Jim Prouty, who provided me with tools to independently test Lyle's method.

Measurement of the Transient Versus Steady-State Response of Waveform Recorders

T. M. Souders and D. R. Flach
Electrosystems Division
National Bureau of Standards
Washington, DC 20234

A simple test method is proposed in which the transient and steady-state responses of waveform recorders are compared. The transient signals employed in this method are single period sinusoids accurately characterized in terms of a steady-state sine wave from which they are derived. Digital recordings of the transient and steady-state waveforms are made with the test instrument and are subsequently compared. Differences are analyzed using time-domain digital processing. A gated S/H amplifier is used to produce the single period transients from a sine-wave input. Techniques are presented for generating the appropriate gating pulses, and for accurately comparing the transient and steady-state waveforms. Test results are included for three different instruments, having up to 10 bits of resolution and conversion rates to 100 MHz.

Key words: analog-to-digital converter; digital processing; dynamic testing; sine-wave testing; transient digitizer; transient response; waveform recorder.

Introduction

Dynamic testing of waveform recorders is most commonly performed with steady-state, sinusoidal stimuli [1,2,3]. The advantages of such approaches are many: accurate sinusoidal waveforms are among the easiest to generate, they are rather easily related to other waveforms through Fourier analysis (assuming the system is linear), and applicable hardware and software analysis techniques are readily available to perform spectral analysis, time domain analysis, signal-to-noise ratio calculations, etc. However, waveform recorders are frequently employed to measure transient rather than steady-state phenomena. Therefore, it is desirable to relate the transient response to the more easily measured steady-state response.

A simple test method is proposed in which the transient and steady-state responses are compared, as illustrated in Fig. 1. The transient signals employed in this method are single period sinusoids accurately characterized in terms of a steady-state sine-wave from which they are derived. Digital recordings of the transient and steady-state waveforms are made with the test instrument and are subsequently compared. Differences are analyzed using time-domain digital processing.

Implementation

The single-period sinusoids can be accurately generated from the steady-state sine wave by using a sample/hold (S/H) amplifier placed in the track mode for a single period, as shown in Fig. 2. Digital circuitry shown in the upper part of the figure is included to generate the appropriate S/H mode control, and a resistive divider at the bottom is added to provide an accurate means of monitoring the S/H amplifier's performance. The digital mode control signal is derived from the trigger output which is a standard feature on many commercial signal generators. The timing relationships in this and subsequent trigger signal stages are shown in Fig. 3. The trigger output signal is first passed through a commercial variable digital delay circuit, which permits the trigger to be delayed with respect to the sine-wave output. In this way, the sine wave can be gated at different phase angles to provide transient wave shapes such as those illustrated in Fig. 4. Next, the delayed trigger is applied to the block labeled "÷N" (Fig. 2). The first stage of this block is a symmetrical divide-by-2, which produces a string of positive pulses, each having a duration equal to that of the reference sine-wave period. This waveform is subsequently divided by 10, producing a ripple carry output from the divider which is a rectangular pulse having a duration again equal to the sine-wave period, and occurring once every 20 periods of the sine wave. This ripple carry output signal is used to control the S/H amplifier, and to trigger the waveform recorder under test. With a mode control signal thus developed, single sinusoidal periods can be gated through the S/H amplifier, commencing (and ending) at any arbitrary phase angle, with a 5 percent duty cycle.

Since the objective is to measure the response to transient versus steady-state waveforms, it is important to accurately characterize the transient sinusoid in terms of the steady-state input waveform from which it is derived. Absolute characterization of the two waveforms is not required. An error signal proportional to the difference between the transient and steady-state signals can be obtained with the circuitry shown at the bottom of Fig. 2. This is readily accomplished by selecting a gain of -1 for the S/H amplifier, and using a matched 1/1 resistive divider connected as illustrated in the figure. An oscilloscope at the node connecting the two resistors monitors a voltage equal to one half the algebraic sum of the input and output voltages. While this voltage tracks the input during the hold mode (when the output voltage is fixed), it represents only the error signal between input and output during the track mode, when the transient signal is developed. Diode bounding at the measurement node minimizes the overdrive of the oscilloscope during the hold mode, permitting quicker recovery in the subsequent track mode. This has proved adequate for settling time measurements to be made with an uncertainty of approximately 1 mV; however, measurements to higher accuracy may require further signal limiting.

Since the steady-state as well as the transient waveforms are sampled at the output, the steady-state input waveform to the S/H amplifier serves only as a reference with which to compare the other two test waveforms. If the S/H amplifier produces negligible distortion at the test frequency, then comparisons can easily be made by first trimming the resistive divider to produce a null at the measurement node while in the track mode, under steady-state conditions. This requires matching the divider ratio to compensate for the dynamic gain error, and adding a small shunt capacitance across one resistor to balance the phase delay through the amplifier. Once the divider is thus trimmed, any subsequent error signals measured in the transient mode indicate the differences between the transient and steady-state waveforms as they appear at the waveform recorder's input.

The results of such measurements can be seen in the oscilloscope photographs reproduced in Fig. 5. Note that the error voltage (which is twice the indicated voltage) settles to within approximately 40 mV in 100 ns, and within 5 mV in 200 ns, for a 20-V peak-to-peak transient. These values represent errors of 2 LSB's and 0.25 LSB magnitude, respectively, for a 10-bit recorder having 20-V full-scale range.

Measurement of the waveform recorder response to the transient versus steady-state signals is made by first selecting the steady-state signal via the mode control switch in Fig. 2. The recorder is then armed and subsequently triggered by the next mode control signal. All encodings following this trigger signal are thereby stored. The resulting data set is then transferred to the controlling computer, the mode control switch is set to select the transient signal, and the encoding and data transfer processes are repeated. Differences between the steady-state and transient responses are then simply calculated by subtracting the second data set from the first, as illustrated in Fig. 1.

Error Sources

The success of this measurement process is dependent upon the validity of three assumptions:

1. That the differences between the transient and steady-state waveforms, measured as discussed above, are negligibly small.

2. That the signal source is sufficiently stable that no appreciable change in waveform takes place between successive applications of the steady-state and the transient inputs

3. That the two recorded sampled data sets are taken from identical segments of the two waveforms, i.e., that there is no timing skew between them.

The first assumption is tested as previously discussed. If significant errors are measured between the transient and steady-state waveforms, corrections can possibly be applied by using the recorder-under-test to digitize the error signal at the resistive divider's measurement node, and subtracting the recorded data from the final measurement. This method requires a high input impedance to the recorder so that the resistive divider is not loaded, and assumes that the error signal can be measured on a more sensitive range, to minimize the effects of errors in the test unit.

The second assumption can be tested by observing the cycle-to-cycle and longer term stability of the waveform peaks and zero crossings at high gain on a storage oscilloscope. A sensitive differential preamplifier with adjustable dc bias is useful for this measurement. Waveform instability was found to contribute negligible errors (<0.02%) in tests of 8- and 10-bit recorders.

Unfortunately, the final assumption will generally not be valid using the test method illustrated in Fig. 2. The difficulty arises because the encoding process of the recorder under test is generally controlled by an internal clock which runs asynchronously with the input and trigger signals. The result is that the first recorded encoding will be delayed with respect to the trigger signal by a random duration $\Delta t_d < \Delta t$, where Δt is the conversion time of the recorder under test. Subsequent encodings will take place at times (with respect to the trigger command) given by $\Delta t_d + n\Delta t$, where n represents the nth encoding following the trigger. Since Δt_d randomly changes with each new trigger command, subsequent data sets will be displaced in time with respect to each other by a duration given by $-\Delta t < \Delta t_d' < \Delta t$. All corresponding samples from the two data sets will be displaced by this same amount, therefore, the amplitude displacement between corresponding samples will, to a first approximation, be equal to the time derivative of the waveform at that location, multiplied by the time displacement. For a sinusoidal test waveform $Y = A \sin(\omega t)$, an error signal will be generated by this time displacement, given by $\omega A \Delta t_d' \cos(\omega t)$.

This effect can be minimized or eliminated by appropriate modifications to the basic test technique. While in principle the error source can be eliminated by phase-locking the recorder's sampling instants to the trigger signal, this may not always be feasible in practice. A simple approach is to minimize the error by averaging a number of consecutive pairs of data sets, each pair containing a steady-state and a transient sample set. Assuming the recorder's time base is independent of the test signal, then the values of Δt_d should be randomly distributed about the average value, within the limits of $-\Delta t/2$ and $+\Delta t/2$. It can be shown that the standard deviation of the mean of n such sample sets is given by $\Delta t/\sqrt{12n}$. Therefore, the standard deviation of the mean amplitude is given by $\omega A \Delta t/\sqrt{12n}$.

Results

The transient versus steady-state response of three different instruments has been measured using the techniques outlined above, and typical error plots from these tests are presented in figures 6-8. The three instruments are respectively, a 10-bit, 10-MHz sampling rate waveform recorder, a 10-bit, 500-kHz digital storage oscilloscope, and an 8-bit, 100-MHz waveform recorder. In each of the tests, some data averaging was performed to reduce the error caused by time skew. Unfortunately, since the mode control switch (Fig. 2) had not been automated, an operator was required to manually throw this switch for each new pair of waveforms, with the ensuing boredom resulting in some cases in fewer data sets than desirable. Thus, while Figs. 6(a-d) represent true errors, the remaining figures still contain strong time-skew components. Figure 6, for example, shows various offset and distortion errors as large as 2-3 LSB's. These represent true transient versus steady-state response errors, and are likely due to thermal unbalances occurring within the test instrument. Other effects which have the appearance of high frequency noise bursts are also present in this figure. These appear randomly in both the steady-state and transient representations, and therefore are not due to differences in response to the two signals. On the other hand, it is readily apparent that the errors plotted in Figs. 7(a-b) are 90° out of phase with the input signal (see inset), and are therefore predominantly due to time-skew rather than being true errors, and, in figure 8, a combination of time-skew errors and an offset are present. In these figures, therefore, further averaging is required.

References

1. "Test A/D Converters Digitally," Bill Pratt, Electronic Design, No. 25, Dec. 6, 1975.

2. "Dynamic Testing Reveals Overall Digitizer Performance," Handshake Spring/Summer 1981, pp. 9-12, Tektronix, Inc.

3. "Digitizer Specifications and Their Applications to Waveforms," R. W. Ramirez, Electronics Test, Sept. 1981.

Figure 1. Basic test method.

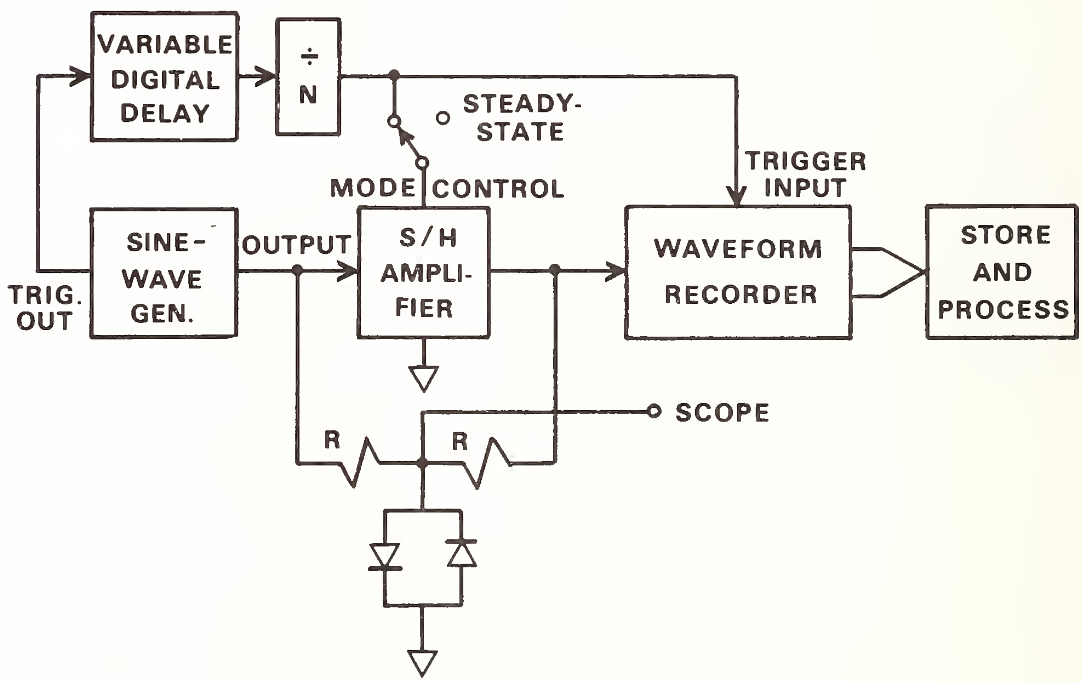

Figure 2. Test circuitry for generating and comparing transient and steady-state waveforms.

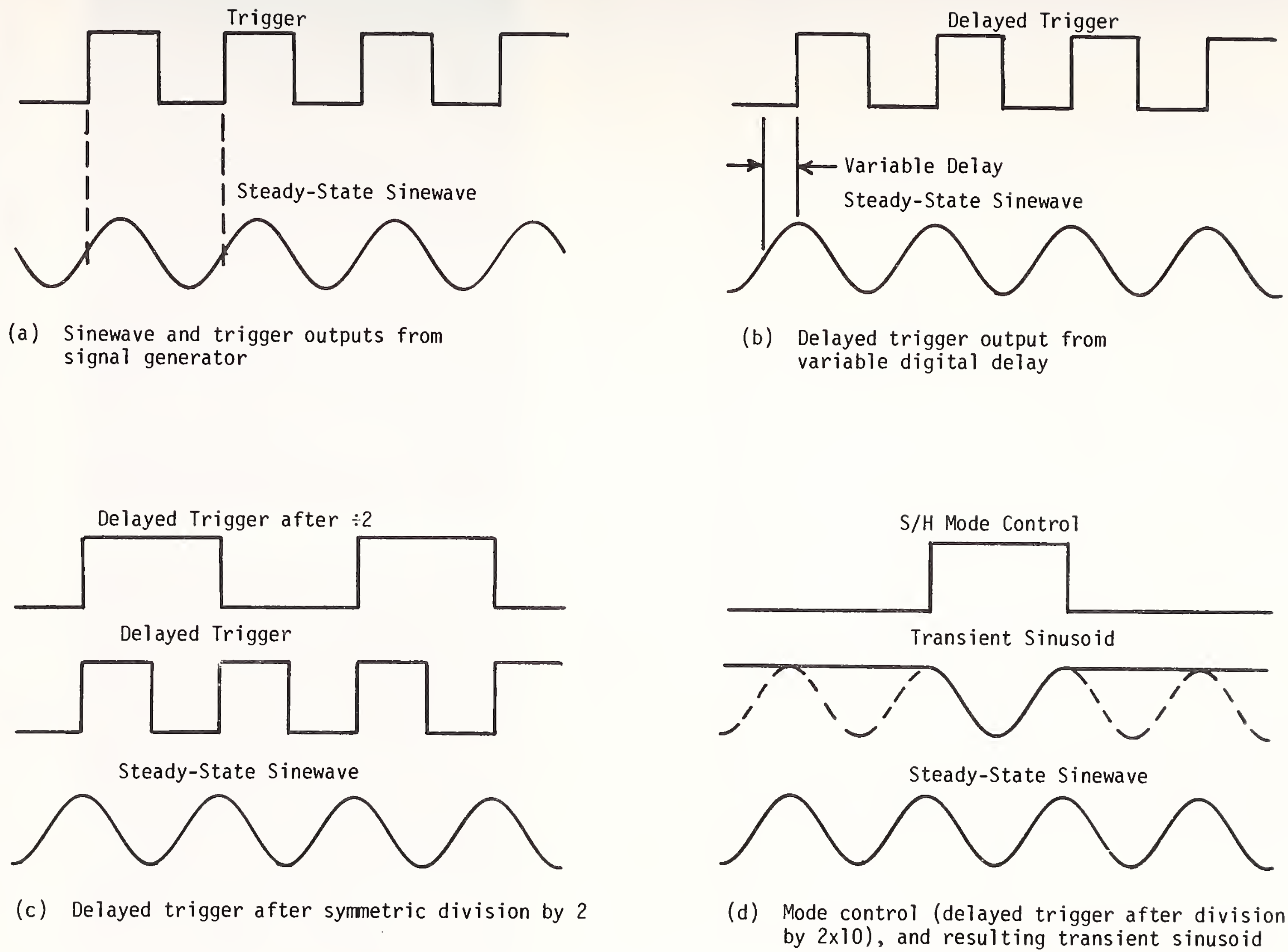

(a) Sinewave and trigger outputs from signal generator

(b) Delayed trigger output from variable digital delay

(c) Delayed trigger after symmetric division by 2

(d) Mode control (delayed trigger after division by 2x10), and resulting transient sinusoid

Figure 3. Timing relationships at subsequent trigger signal stages.

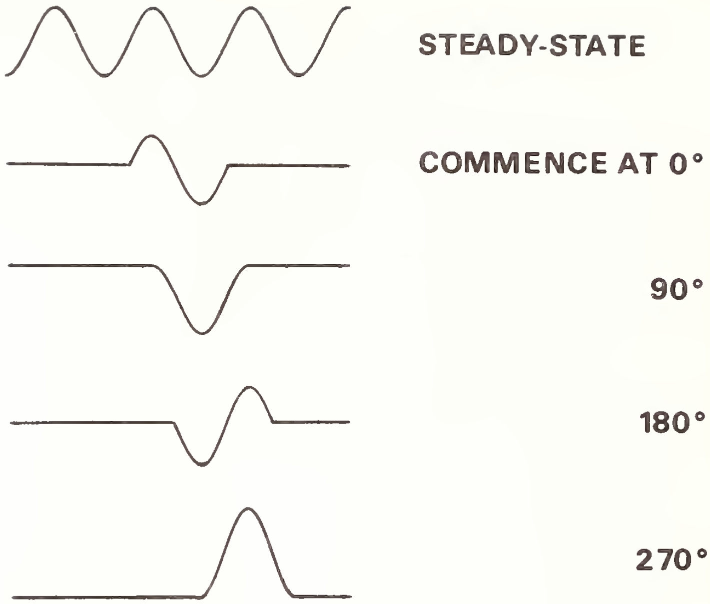

Figure 4. Transient waveforms produced by gating sinewave at various phase angles.

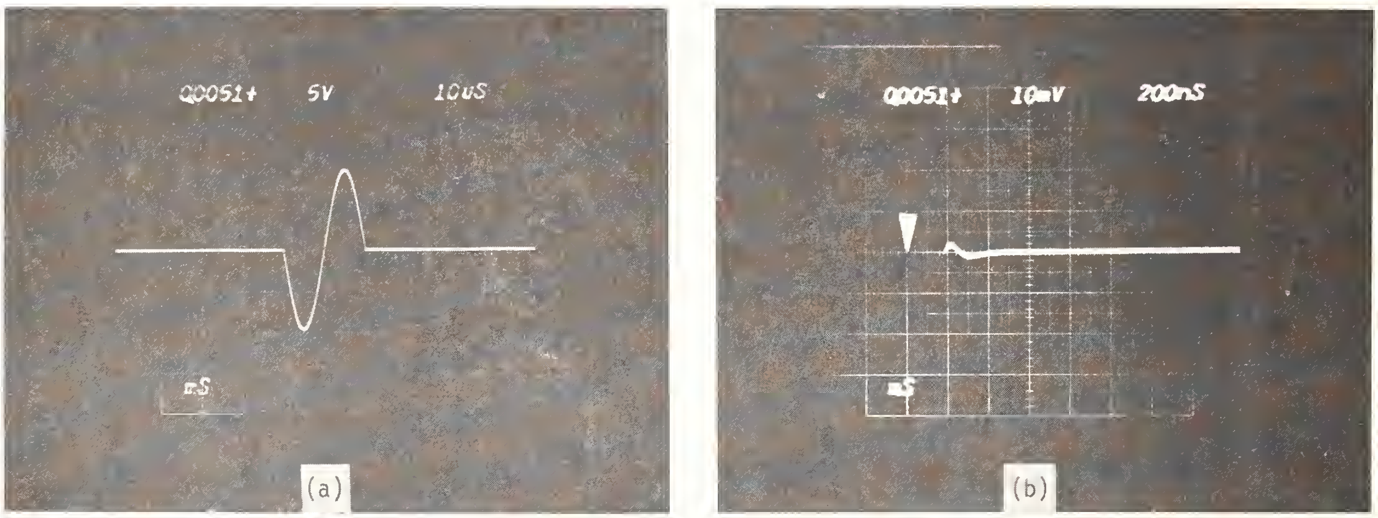

Figure 5. Oscilloscope photographs showing

a) Transient waveform at output of S/H amplifier (20 V peak-peak, 20 μs duration).

b) Error signal observed at "scope" terminal in Fig. 2, while transient waveform shown in a) is produced at S/H amplifier output. Marker indicates commencement of track mode control level. (Vertical scale is 10 mV/div.; horizontal scale is 200 ns/div.).

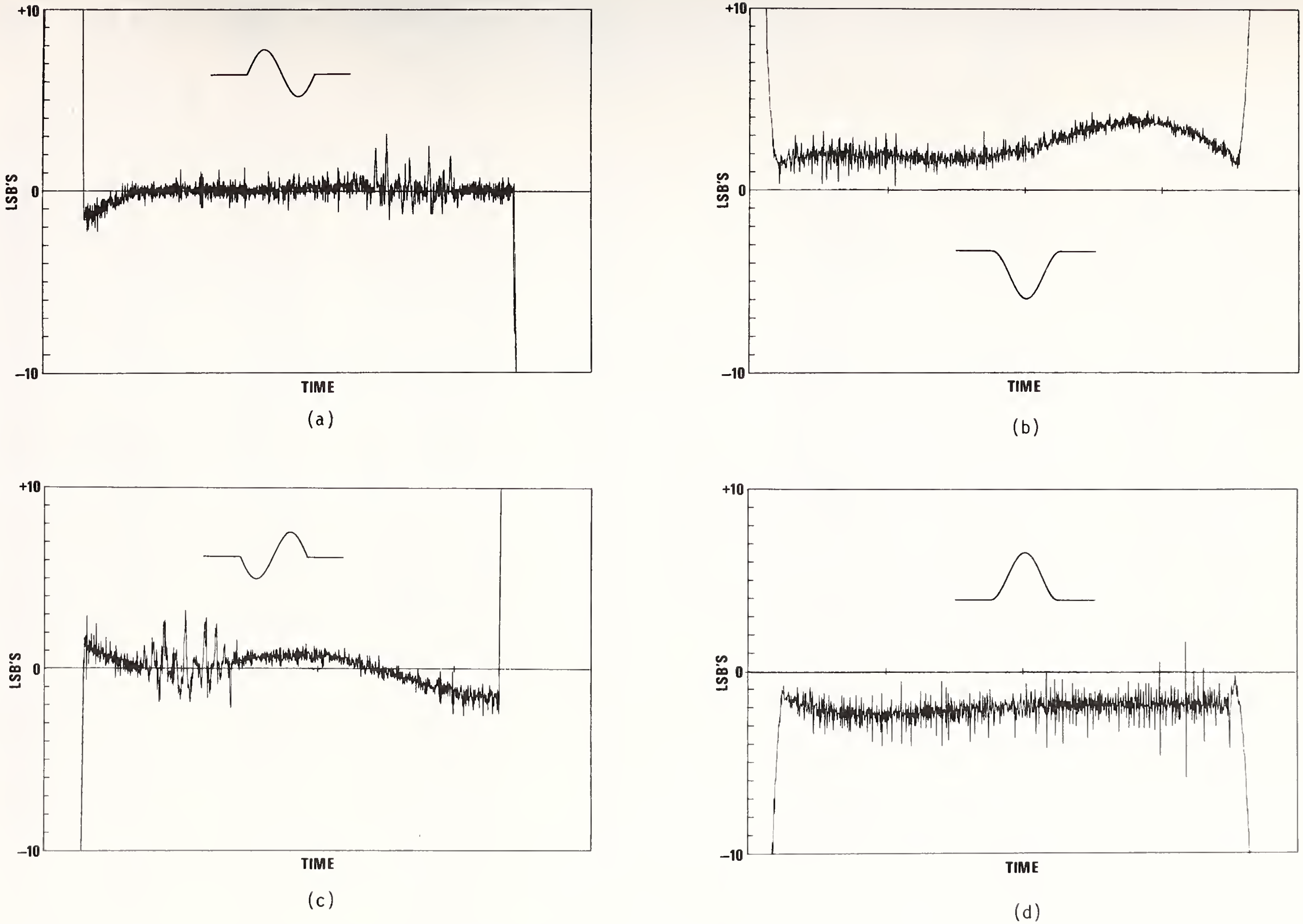

Figure 6. Transient minus steady-state response of a 10-bit, 10 MHz recorder on ±10 V range, for various (full scale, 100 μs) waveforms as depicted in the insets. Time skew errors are negligible as the result of sufficient averaging.

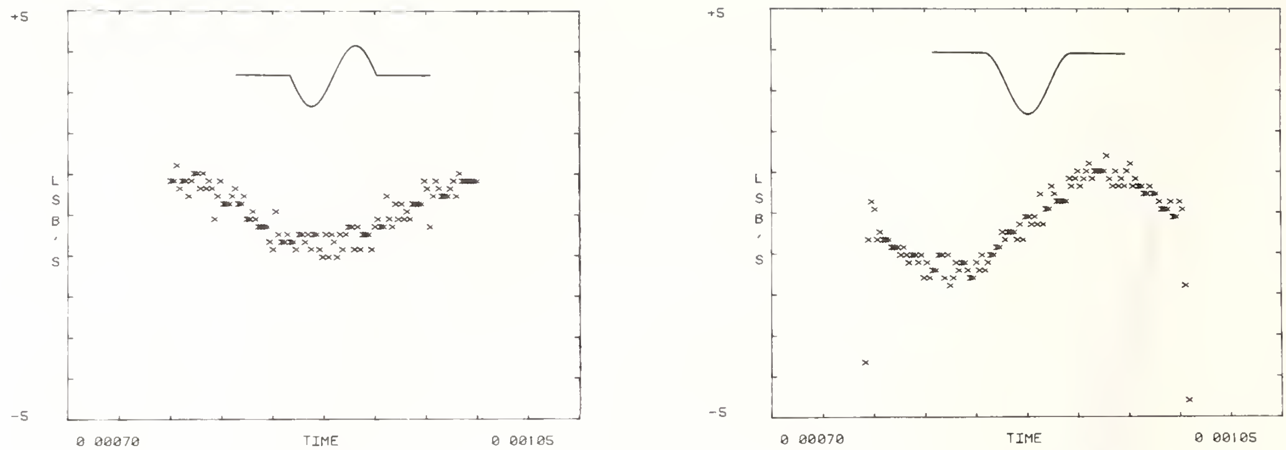

(a) (b)

Figure 7. Transient minus steady-state response of a 10-bit, 500 kHz digital storage oscilloscope on ±5 V range. Input waveforms are full-scale amplitude, 200 μs signals as depicted in the insets. Significant time skew errors are present as a result of inadequate averaging.

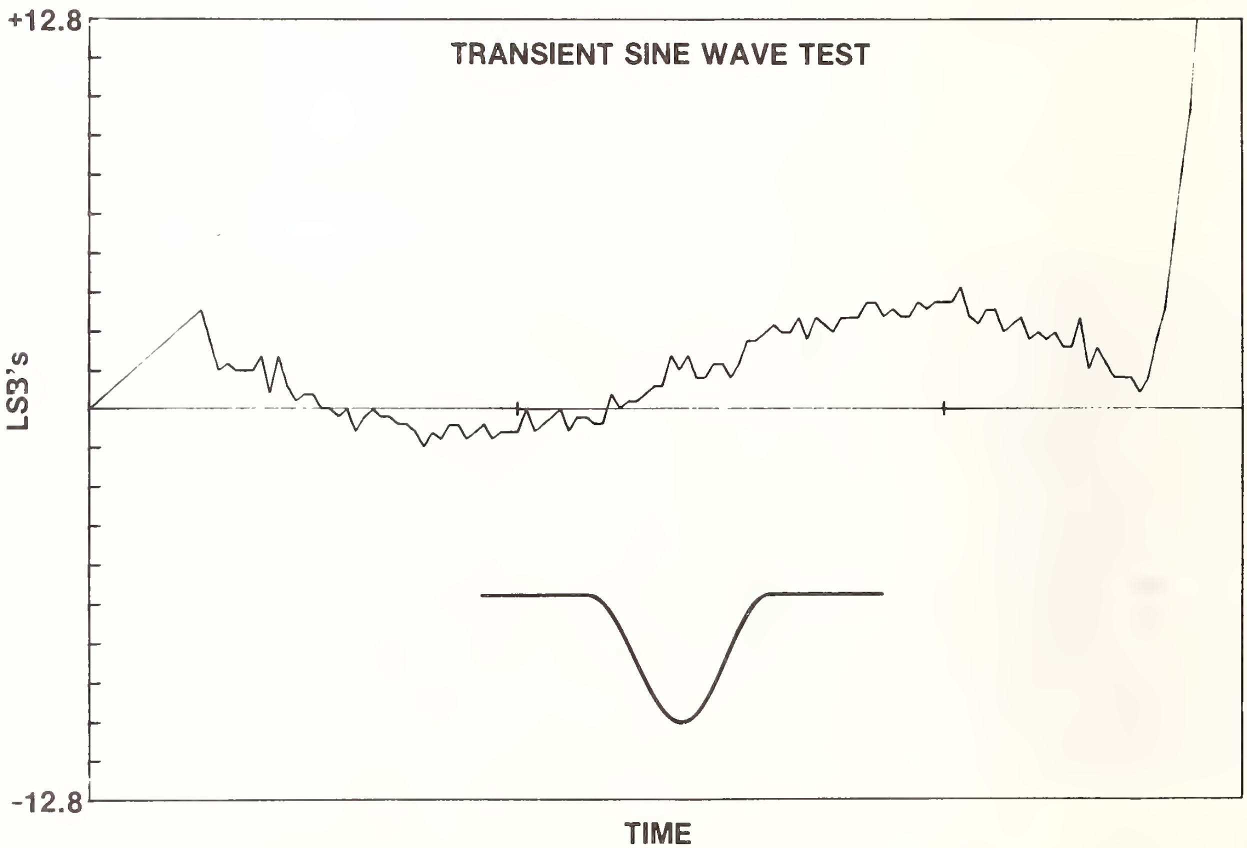

Figure 8. Transient minus steady-state response of an 8-bit, 100 MHz waveform recorder, on ±0.5 V range, with 100 ns sampling intervals. Input waveform is 10 μs, full-scale signal as shown. Time skew and offset errors are present.

CALIBRATION TECHNIQUES FOR A LARGE COMPUTERIZED WAVEFORM RECORDING SYSTEM

W. B. Boyer

Sandia National Laboratories
Albuquerque, New Mexico 87185

A transient waveform recording and processing facility has been developed for the Sandia Particle Beam Fusion Accelerator, PBFA I. Signals from diagnostic monitors on the accelerator and associated experiments consist of transient pulses of 10-1000 ns duration and 1 to 5000 volts peak amplitude. The waveform recording system consists of 44 Tektronix 7912AD Transient Digitizers interfaced to a HP-1000/45 minicomputer. The facility also contains computer-controlled calibration, switching, and attenuation devices. The calibration and switching hardware can route either precision dc voltages or precision frequency frequency periodic signals to the attenuators and digitizers. Software has been developed to automatically calibrate the attenuators and digitizers and store the curves in disc files. These data are used to calibrate waveforms recorded from accelerator experiments. The facility cable system is also calibrated for frequency response using the 7912AD's in a semiautomatic mode. Waveform calibration consists of averaging to center of trace, linear amplitude adjustment, nonlinear sweep speed processing, and cable frequency response compensation. System tests indicate that waveforms can be calibrated to an amplitude accuracy of $\pm$ 3 percent. Signals recorded from different monitors can be aligned in time to within $\pm$ .4 ns.

1. Introduction

A computerized, on-line data acquisition and processing facility has been developed to support Sandia's Particle Beam Fusion Accelerator, PBFA I. [1] A transient waveform recording system constitutes a major part of this facility. This paper describes methods used to calibrate and verify the performance of the waveform recording system.

2. Accelerators

PBFA I has 36 independent beam lines and is capable of delivering 30 terawatts and 1 megajoule in a 2 or 4 megavolt, 35 ns pulse into a target chamber. [2] The accelerator can be configured to generate either electrons or ions. The objective is to deliver sufficient beam energy to demonstrate the scientific feasibility of inertial confinement fusion. A cutaway drawing of PBFA I is shown in Figure 1. The data acquisition facility also supports the SuperMITE accelerator which is used for testing advanced pulsed power components for PBFA II. A third machine, MABE, is currently being brought on-line. MABE is a prototype for advanced weapons effects simulation accelerators.

3. Data Signals

The waveform recorders digitize signals produced by voltage, current, and radiation monitors on both the accelerators and associated experiments. These signals are fast transient pulses of 10 to 1000 ns duration and 1 to 5000 volt peak amplitude. These waveforms must be recorded in the presence of EMP levels generated by di/dt and dv/dt of 10^{15} amps and volts per second.

4. Waveform Recording System

A block diagram of a typical waveform recording channel is shown in Figure 2. The cable run from the monitor to the waveform recorders consists of 120 feet of RG-214 and 150 feet of RG-331 coaxial cable. This is about the minimum length which will reach all portions of the accelerator with equal length cable runs and also provide flexibility in jumpering between monitors and waveform recorders.

The facility has 44 Tektronix 7912AD Transient Digitizers with 7A16P programmable vertical amplifiers and 7B90P programmable time bases. The vertical amplifier has a specified minimum bandwidth of 200 MHz. This is adequate for recording virtually all accelerator and experiment diagnostic signals.

Data signals from up to three different experiments are cabled to the input ports of a computer-controlled, four-position coax rotary switch module. Signals with amplitude greater than 500 volts are first attentuated by specially designed high power 5X attenuators.

The output signal from the coax switch is fed into a programmable attenuator. A fiducial timing marker pulse can then be added to the data signal via a wideband isolating power adder. In some cases, the fiducial signal is routed to the 7912AD vertical amplifier B channel, and timing information is only recorded during the preshot baseline check.

Both the 7912AD's and the fiducial pulse generator are triggered by a special trigger pulse generator. The trigger generator is triggered by some event in the accelerator.

An HP-1000/45 minicomputer controls the coax switches, programmable attenuators, 7912AD transient recorders, and the trigger generator.

5. Calibration System

The computer controlled calibration system is shown in Figure 3. A Tektronix 1340 Data Coupler contains vertical and horizontal reference signal generator cards as well as digital output cards for controlling the coax switch matrices.

The vertical reference card can generate sensed dc voltages of 0, .01, .025, .050, . . . , 1.0, and 2.5 volts. Actual outputs have been measured to $\pm$ .1 percent. These values are used to compute vertical calibration factors. The vertical reference generator is used to automatically calibrate the 7A16P vertical amplifiers, wideband couplers, and programmable attentuators.

The 7A16P vertical amplifiers are computer calibrated by injecting a single known dc voltage into the input and measuring the deflection. This process is averaged over four tries. Linear deflection is assumed. Each of the six sections in the programmable attenuators is also computer calibrated by injecting known dc voltages into the unit and measuring output with the associated transient recorder. Fixed attenuators are manually calibrated using dc power supplies and voltmeters. All dc equipment is corrected to $\pm$ .1 percent using a calibrated Fluke 382A dc voltage reference source.

The horizontal reference card can generate periodic signals with frequencies in the range 0.25 Hz to 125.0 MHz in a .25 , .625, 1.25 sequence. Period accuracy is specified at .02%. The horizontal reference signal is used to compute time base sweep curves. The calibration software locates zero crossings on the waveform and generates a calibration curve of time vs. zero crossing addresses. The data acquisition program uses this curve to process recorded signals. The curve is assumed to be nonlinear. The time at which each signal sample point occurs is computed by a double sliding parabolic interpolation. [3] The signal data points are transformed into an array of data points occurring at a fixed sample rate by linear interpolation.

Cable runs are calibrated by a hybrid computer/manual technique. A fast rise step pulse is injected directly into a digitizer and recorded. The same pulse is then injected into the cable run to be calibrated and recorded by the transient recorder. A constrained deconvolution process is used to compute a compensating impulse response function for the cable run. The recorded data signal is convolved with this impulse response to compensate for cable losses.

The automatic data acquisition program uses the calibration factors described above to process each recorded waveform. The overall accuracy of this system was checked as follows. A 150 V, 50 ns rectangular pulse was recorded by a transient digitizer. This signal was then manually calibrated using deflection factors determined by the Fluke 382A reference source. The same pulse was injected into the input of a cable run. It was recorded and processed by the data acquisition program. A least squares comparison was made of the two waveforms. The overall scale error was .4 percent and the standard deviation normalized to the peak level was 2.8 percent. The undegraded signal, recorded degraded signal, and calibrated signal are shown in Figure 4. An overlay plot is shown in the fourth quadrant.

Time measurement accuracy of calibrated waveforms has also been measured. The 62.5 MHz periodic waveform from the horizontal reference signal generator card was digitized on a 7912AD. The waveform was calibrated using the time base calibration information. The resulting signal is shown in Figure 5. The period of each cycle of this signal was measured by locating alternate zero crossing times. Linear interpolation was used when no sample actually equalled zero. Cumulative zero crossing times were also computed. The resulting data and errors are shown in Table 1. All individual cycle errors are less than 2.5 percent and the total cumulative error is .259 percent.

Accurate alignment in time of signals recorded on different digitizers is critical for analyzing accelerator and experiment performance. Alignment information is recorded by placing a narrow fiducial

timing marker on each trace when a baseline is taken. The data acquisition software locates the peak of the fiducial pulse.

After each signal is time calibrated, the leading edge is truncated at a time equal to the distance to the fidu peak plus one-half of a division. This truncation aligns all signals in time.

Tests have been made to determine the accuracy of the data recording system in aligning signals. A pulse generator with ten 20 ns wide outputs simultaneous to within .1 ns was used. The pulses were injected into the input of the cable run and recorded by the 7912AD's at 10 ns/div. The waveforms were processed by the data acquisition software. This process was repeated five times to separate fixed time delays from shot-to-shot jitters. Fixed time delays are caused by unequal cable lengths.

Least squares comparison fits were made of different signals over the same shot to measure differences in arrival times. These arrival times were averaged over all shots to get fixed time delays. The fixed time delays were removed and the arrival times were analyzed for different signals over the same shot and for the same signal over different shots. The results are that the expected alignment error for different signals on a given shot was .26 ns with a worst case spread of .96 ns. The expected shot-to-shot alignment error was .33 ns with a worst case spread of 1.04 ns.

The most significant source of timing error is the software process of locating the peak of the fiducial timing marker pulse. Digitization noise results in an expected error of about $\pm$ 1.5 sample. At 10 ns/div (.2 ns/sample), this is $\pm$ .3 ns.

6. Uncorrected Errors

There are two prime sources of amplitude error inherent in the 7912AD transient digitizer. The first is nonreproducible wideband noise. This noise is illustrated in Figure 6. This signal is the result of acquiring two baselines from a digitizer and subtracting them. The vertical axis is in units of 7912AD digitization levels. There are 512 possible levels.

The second source of error is reproducible, low frequency, sweep geometry error. This problem is illustrated in Figure 7.

Baseline traces were averaged 21 times at three different vertical positions. Note the position dependent low frequency oscillations. This error may be removed by performing a geometry distortion correction on the digitized data. This is a difficult process and is not done in the PBFA I system since the predominant error is caused by the wideband noise.

The PBFA I system also does not compensate for nonlinear vertical amplifier deflections. This effect was measured by manually injecting dc voltages and digitizing the traces. The average value was computed for each trace. This procedure was performed with the trace initially positioned at the top, middle, and bottom of the screen. The results in all three cases were essentially identical.

The curve of deflection vs. voltage for the trace initially in the middle of the screen is shown in Figure 8. A least squares fitted straight line is also shown. The deviations of the measured data points from the fitted line are shown in Table 2. The table shows that nonlinearity errors in the vertical deflection system are insignificant compared to low and high frequency noise.

7. Conclusion

The waveform recording system described above has been operational on PBFA I and SuperMITE since January 1980. Automated calibration techniques have been developed for linear amplitude attenuations, nonlinear time base sweeps, and frequency-dependent cable losses. Applying these correction factors to digitized waveforms results in signals accurate to within 3 percent in both amplitude and time. Additional error corrections cannot substantially increase performance on single shot pulses due to the inherent digitization errors.

This work was supported by the U. S. Department of Energy under contract DE-AC04-76-DP00789.

8. References

[1] W. B. Boyer, "Data Recording Techniques for the Sandia Particle Beam Fusion Accelerator," Workshop on Measurement of Electrical Quantities in Pulse Power Systems, National Bureau of Standards, Boulder, Colorado, March 1981.

[2] G. Yonas, "Pulsed Power Particle Beam Fusion Research," IAEA Technical Committee on Inertial Confinement Fusion, Osaka, Japan, November 1979.

[3] M. E. Bauder, Operations and Maintenance Documentation for Program PLBRD, Sandia National Laboratories Report No. TC-TM-70-114, 1970.

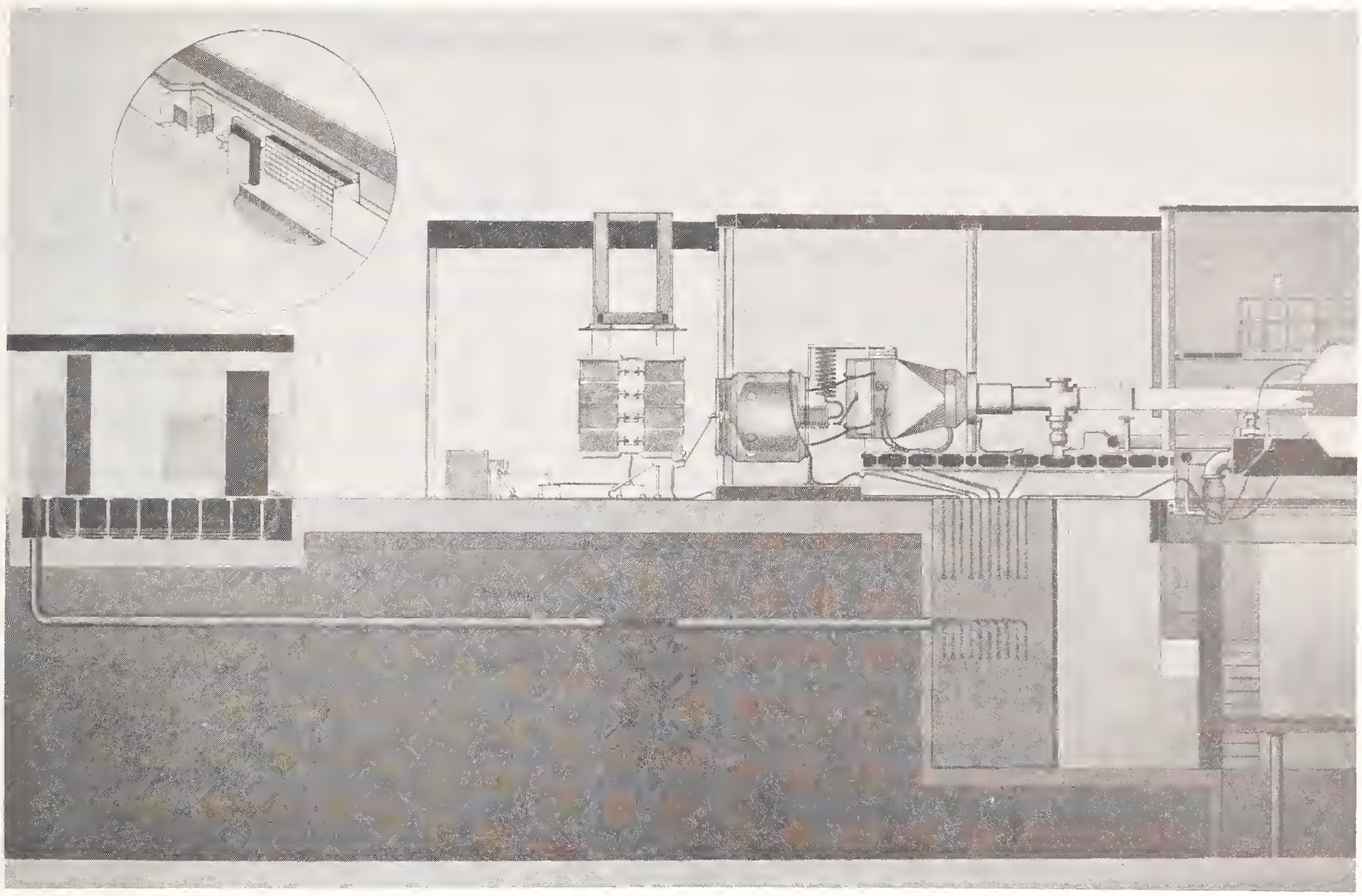

Figure I. Cutaway artist's conception of PBFA I.

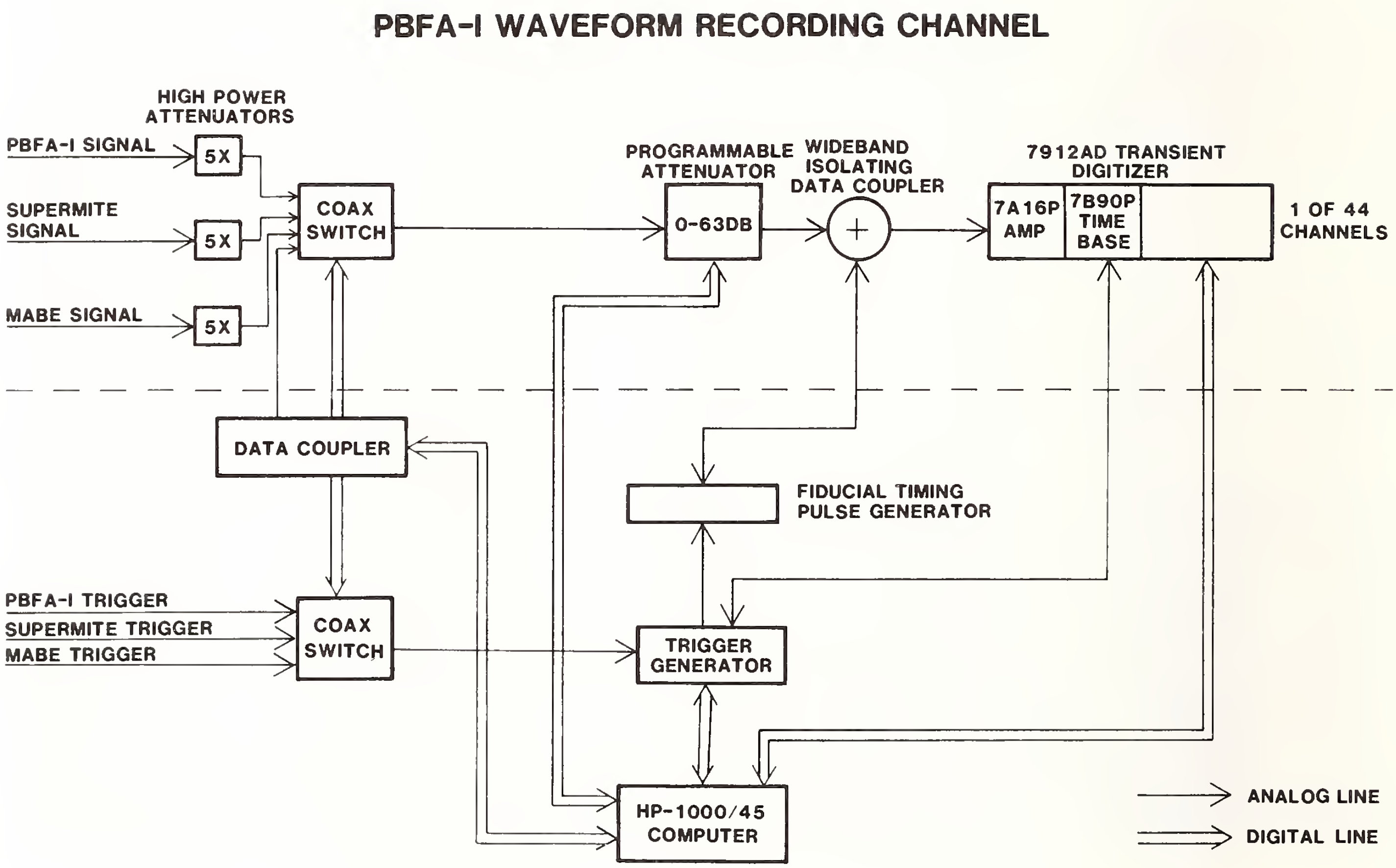

Figure 2. Block diagram of a typical waveform recording channel.

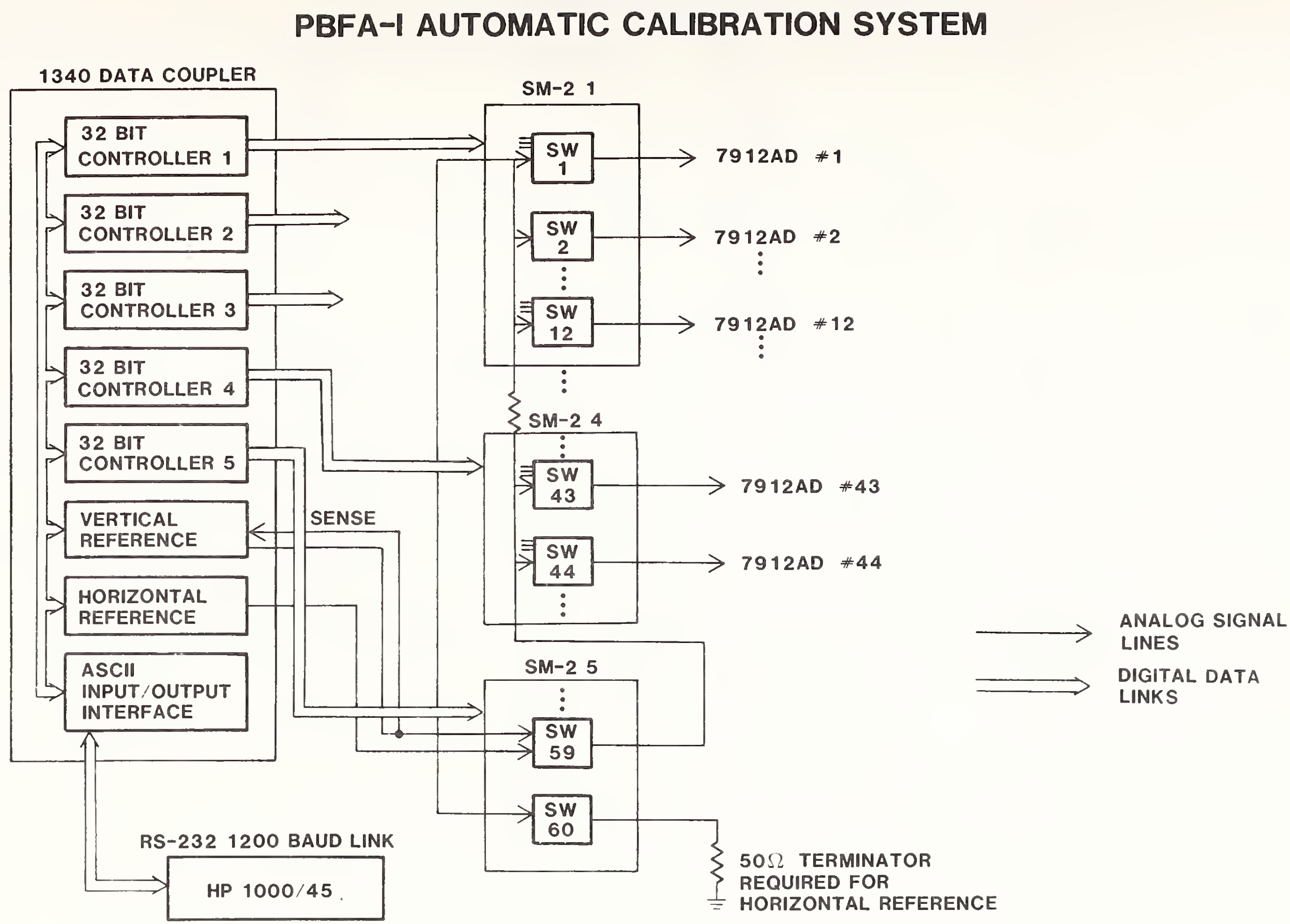

Figure 3. Block diagram of the computer-controlled calibration system.

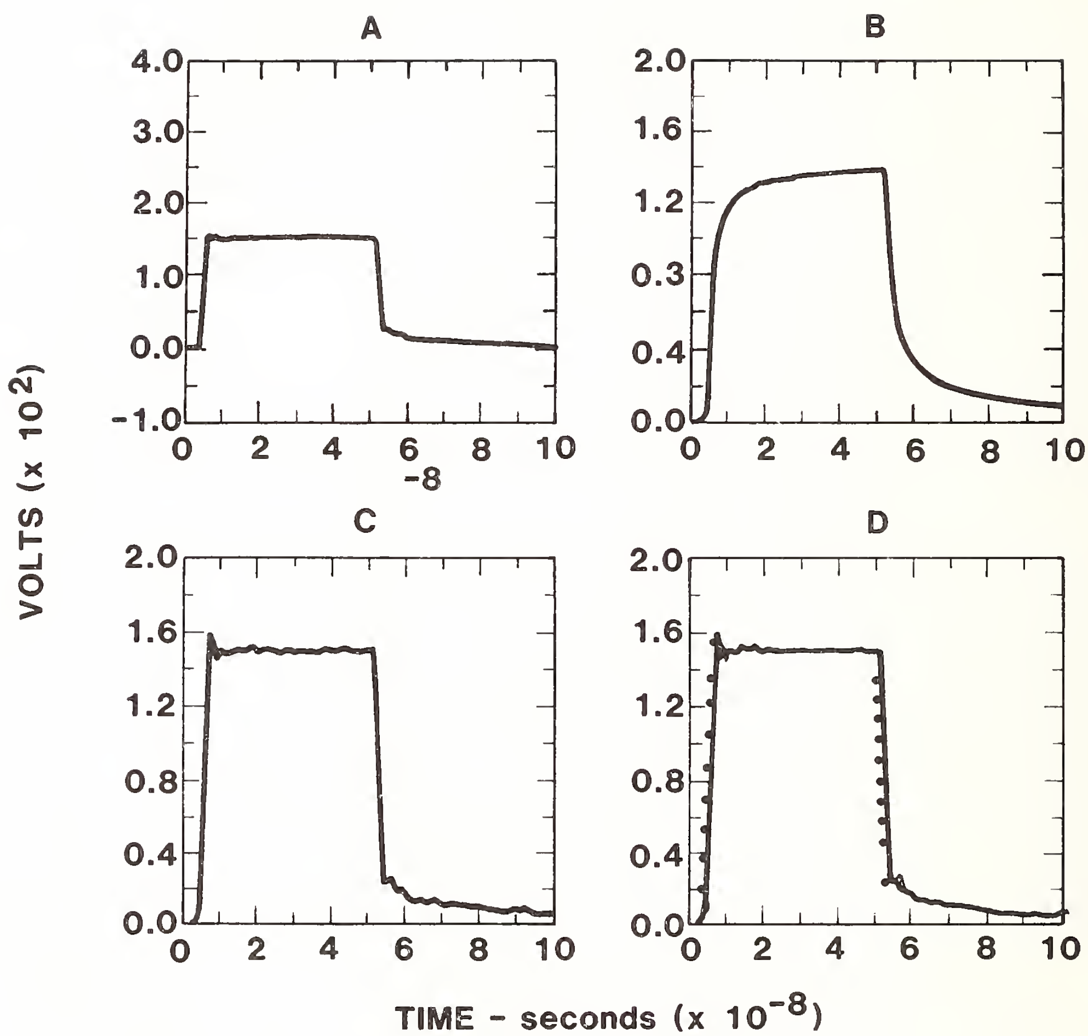

Figure 4. Waveforms used to test overall system calibration performance: (a) undegraded pulse recorded at digitizer and manually calibrated; (b) pulse recorded through cables; (c) calibrated, cable compensated, signal; and (d) overlay of (a) and (c).

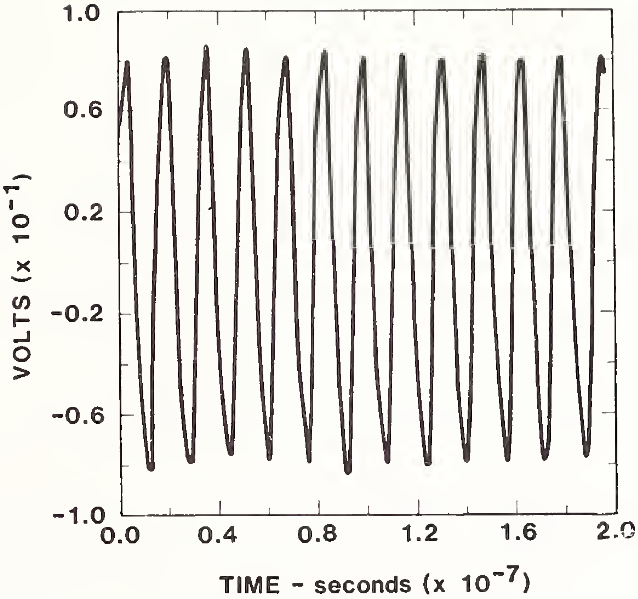

Figure 5. Digitized periodic signal from horizontal reference signal generator for time base sweep accuracy sweep.

Table I. Time period measurement accuracy For 62.5 MHz (+ .02 percent) periodic signal.

Cycle	Actual Period ns	Measured Period ns	% Error	Cumulative Cycle Time ns	Measured Cumulative Time ns	% Error
1	16.000	16.115	.721	16.000	16.115	.721
2	16.000	16.208	1.299	32.000	32.323	1.010
3	16.000	16.203	1.266	48.000	48.526	1.096
4	16.000	15.963	.231	64.000	64.489	.764
5	16.000	15.615	2.407	80.000	80.104	.130
6	16.000	16.084	.525	96.000	96.188	.196
7	16.000	15.947	.329	112.000	112.135	.121
8	16.000	16.145	.905	128.000	128.280	.219
9	16.000	16.299	1.871	144.000	144.579	.402
10	16.000	15.835	1.030	160.000	160.415	.259

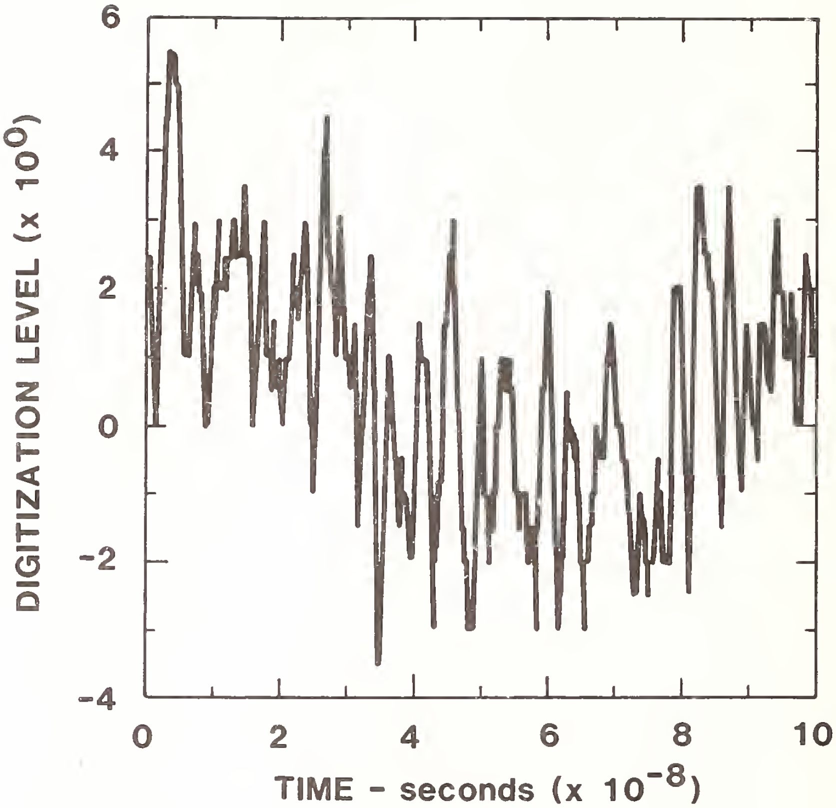

Figure 6. Wideband noise left over after subtracting two 7912AD baselines.

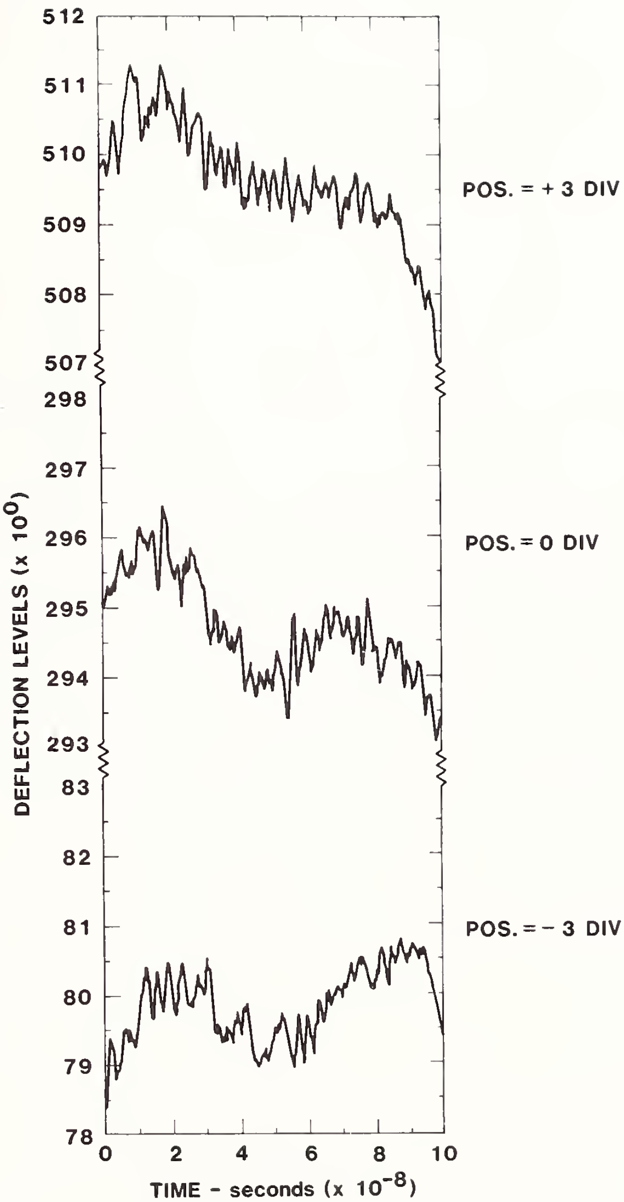

Figure 7. Vertical position dependent, low frequency 7912AD noise. Each signal is averaged over 21 traces.

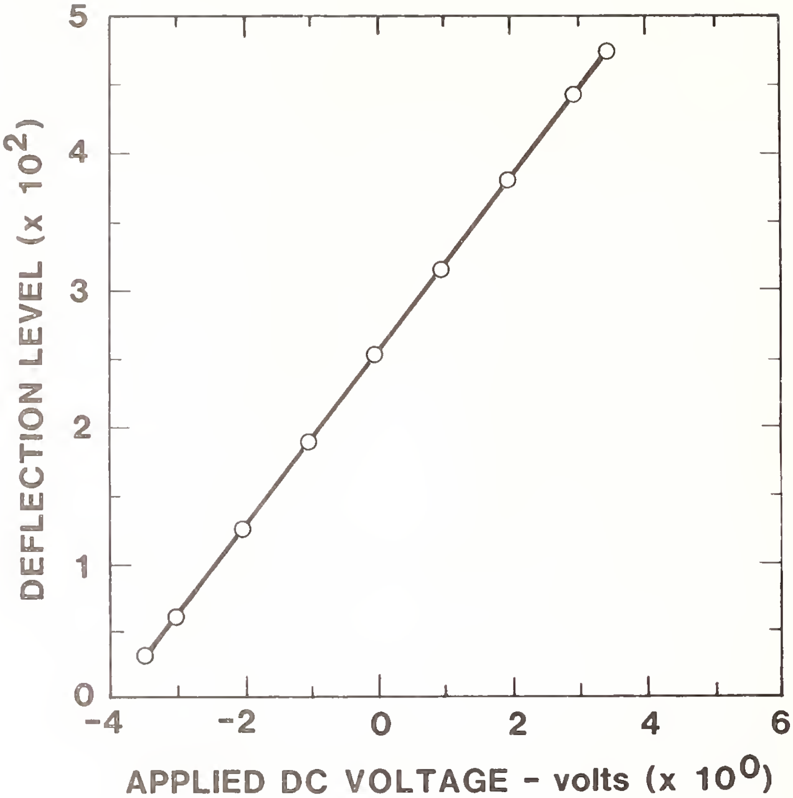

Figure 8. Vertical amplifier deflection data. Both the actual measured points (*) and least squares straightline fit are shown.

Table 2. Vertical amplifier nonlinearity test data for trace positioned in the middle of the screen.

Voltage	Measured Deflection	Fitted Deflection	Difference
-3.50V	30.53	31.05	-.48
-3.00V	62.16	62.72	-.56
-2.00V	126.5	126.0	+.5
-1.00V	189.9	189.4	+.5
0.00V	253.5	252.8	+.7
1.00V	316.3	316.1	+.2
2.00V	379.3	379.4	-.1
3.00V	442.4	442.8	-.4
3.50V	474.2	474.4	-.2

SAMPLING-RATE DRIFT PROBLEMS IN TRANSFER FUNCTION ANALYSIS OF ELECTRICAL POWER CABLES

J. D. Ramboz,* A. R. Ondrejka,** W. E. Anderson*
National Bureau of Standards
Washington, D.C. 20234

An examination of measurement problems caused by sampling-rate drift has been initiated at the National Bureau of Standards. This work arose from the study of degradation in underground power distribution and transmission cables, where precise measurements of radio-frequency dispersion characteristics (i.e., attenuation and phase delay as a function of frequency) are necessary. Cable dispersion results are obtained using time-domain-reflectometry and fast Fourier transform methods and spectra obtained from different data sets are compared. But because the data are necessarily taken at different times, drifts in sampling rate can occur and cause erroneous results in the frequency domain. Measurement methods for the detection of sampling rate drifts and computation methods for correcting the data are discussed and illustrated.

Key words: sampling-rate drift; digital sampling; deconvolution; fast Fourier transforms;

1. Introduction

There is an increasing interest in underground electric power transmission and distribution which is growing from environmental and economic concerns. Fault location in buried power cables can present technically challenging problems, especially when it is required that the fault site be located accurately at some great distance from the measuring location. There is an additional interest by the utilities in being able to use the same buried cables for communication purposes. Both of these needs require a knowledge of the rf propogation characteristics of the cable.

An experimental program had been initiated at the National Bureau of Standards to determine the rf characteristics of power cables using time-domain reflectometry (TDR). A thorough examination of the systematic sources of error using TDR techniques revealed the problem of sampling-rate drift and the effects such drift can have on the measured transfer function of the cable.

In the time domain, the effects of sampling-rate drift are readily apparent. Basically, in experiments of this sort, two different time-domain waveforms are acquired. One, for example, would correspond to the pulse response of a known length of cable and the second would correspond to a longer length of the same cable. The parts of the pulse-response waveforms corresponding to the output impedance of the pulse generator, the connection between the pulse generator and the cable, and the response of the shorter length of cable should be identical. If they are not, sampling-rate drift has occurred. If the two waveforms are then transformed to the frequency domain and divided to obtain the transfer function of the extra length of cable, errors will result. Based on the expected behavior of the cable, the transfer function can be corrected to minimize the effects of sampling-rate drift.

Sampling-rate drifts are discussed, along with their effects, and a method to correct this type of error is given. Analytical generation of typical TDR-type waveforms is used in the discussion to aid in the understanding of the problem and to show the effects of the correction process. Real data is then examined before and after corrections are applied.

2. Power Cable RF Attenuation Measurement Process

One method to measure the radio-frequency (rf) attenuation of underground power cables over a wide band of frequencies is to employ time-domain-reflectometry (TDR) techniques in conjunction with Fourier analysis. A method used by the authors requires that a length of cable be pulsed and the TDR response be recorded. A known change then is made in the length of the cable being measured and a second TDR response recorded. The data collection and analysis process are diagrammed in figure 1. The change of measured response between the two recorded waveforms can be related to the change of length and, thus, attenuation per unit length can be calculated. Specific details of the measurement process relating to coupling the cables and other miscellany are the subject of a forthcoming paper. This discussion is aimed more directly to the data analysis and, specifically, the effects of a sampling-rate drift.

---

* Electrosystems Division, NBS, Washington, DC 20234
** Electromagnetic Technology Division, NBS, Boulder, CO 80303

Referring to figure 1, the recorded waveforms are each amplitude shifted in a software process so that the two recorded waveforms, shown by figure 2, begin at zero amplitude, rise through a step-like function, and then continue at some positive amplitude. The data originally began at a non-zero value because of offsets in the measuring instrumentation, some of which were intentionally introduced to improve amplitude resolution. However, the particular fast Fourier transform (FFT)

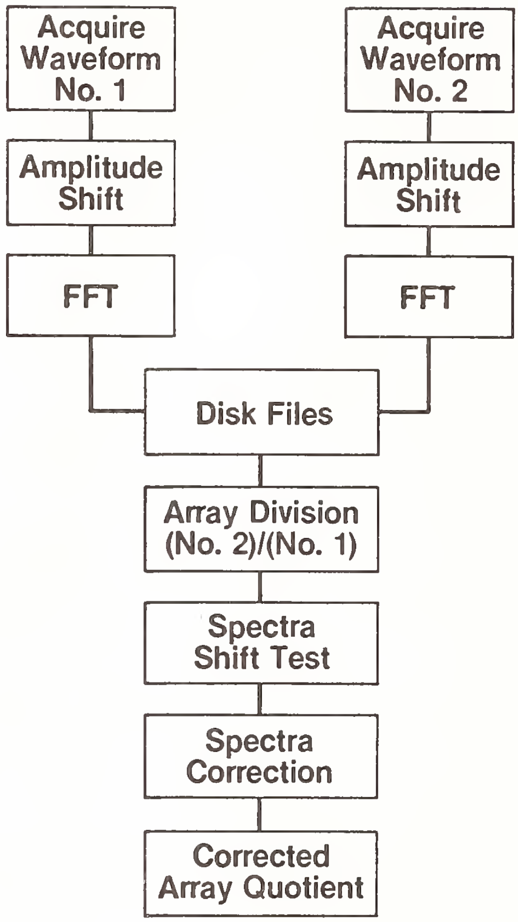

Fig. 1. The data collection and analysis process steps.

algorithm used in this analysis requires that the beginning points of the waveform be made zero. After the amplitude shift, an FFT result is obtained for each of the two waveforms and these results are stored on computer disk files. An array division corresponding to the deconvolution in the time domain is then done. The logarithm of the magnitude of this quotient is scaled to place the results in normalized attenuation units of dB per unit length of cable.

Figure 2 shows two recorded TDR response waveforms (already amplitude shifted) which were obtained from the cable measurement setup. No changes were made in the setup arrangement and, therefore, the two waveforms should be the same. The second waveform was taken 44 minutes after the first. Processing these two waveforms yielded the results shown in figure 3. Attenuation is given over a ±1 dB range and the frequency is shown over a range from 0 to 128 GHz, which results from a time interval between samples of about 2 ps and a total of 512 sample points. It is not expected that useful data can be obtained for frequencies beyond 10 to 20% of the Nyquist frequency because of noise and, in this instance, band limited frequency content of the TDR pulses. The pulse responses shown in figure 2 have rise times of the order of 35 ps, which should contain measurable frequency components up to the 15 to 20 GHz range.

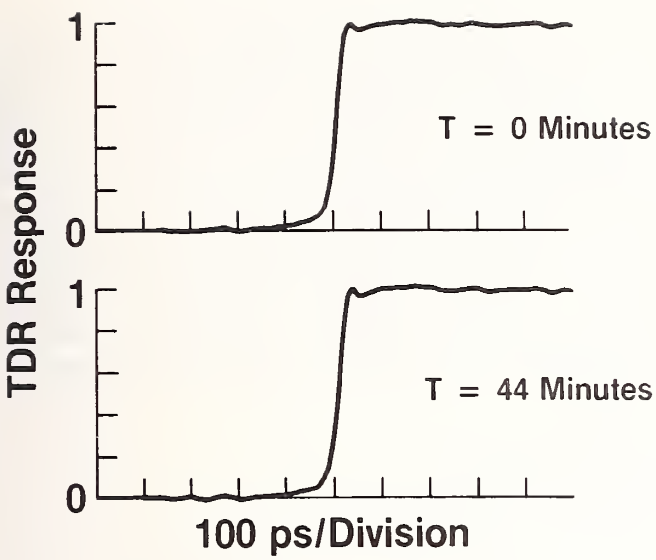

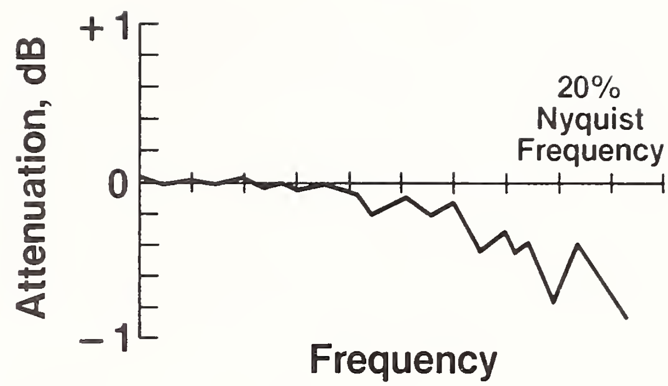

Fig. 3. Erroneous cable attenuation results due to sample-time drift.

Fig. 2. Typical TDR response waveforms for two collection cycles.

If the recorded waveforms as shown in figure 2 were identical, the array division would yield a straight line of 0 dB over the entire frequency range up to the Nyquist frequency (and, indeed, if one uses this technique, the identical data can be analyzed in the two analysis "channels" to verify that the software is functioning correctly). Note, however, in figure 3 that the attenuation as computed shows a value more than -1 dB at a frequency less than 10% of the Nyquist where, in fact, a straight line of 0 dB over the range would be expected. If interpreted literally, a negative attenuation represents a system gain which, for these experiments, is not possible. This result led the authors to examine sampling-rate drift.

3. Sampling-Rate Shifted Data

Electronic sampling devices, such as the TDR equipment, sample a waveform at periodic intervals, either as a function of linear ramp sweep circuits or by some system "clock." In either instance, if the sweep-speed or clock rate changes from one set of measurements to a second set, then the "true" waveform is "time distorted" by this sampling-rate drift. It is assumed for purposes of this discussion that the time interval, or period between each individual sample of one "sweep" or data-gathering cycle, is constant and that for a second cycle, the period is also constant but not necessarily the same as the first. This is illustrated in figure 4. An arbitrary rising waveshape is shown as an "unshifted" waveform with the sampling occurring at times indicated by the solid dots. The time

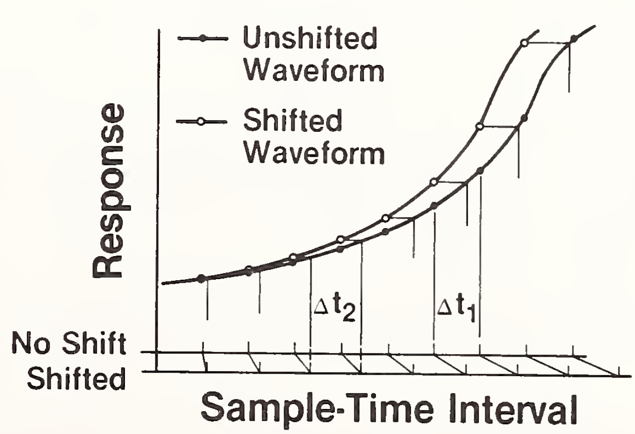

Fig. 4. An arbitrary rising waveform with and without sampling-time drift.

interval between individual samples is shown as Δt_1 on the time scale identified as "no shift." Here each Δt_1 is equal for the entire data collection cycle. If, at some later time, a second data set is collected where a change has occurred in the sampling rate, as shown by figure 4 as Δt_2, time distortion occurs. Bear in mind that it is exactly the same waveform that is being measured but because of the change in sampling rate, the apparent waveshape as shown by the "shifted" waveform results. Any particular sample is made at time $N\Delta t_2$, where N is the Nth sample, on the unshifted waveform as indicated by the vertical line from the "shifted" time axis. It is assumed, however, that the measurement was made at a time $N\Delta t_1$, as indicated by the open dots. For example, for an increase in the sampling period from Δt_1 to Δt_2, an apparent faster rising waveshape results. The same phenomenon occurs on an ordinary oscilloscope if a constant and repetitive waveform is being observed and the horizontal sweep speed is decreased a small amount; the waveshape appears to have a faster rise time to the observer. Figure 5 shows an exaggerated example on a typical TDR response for two different sampling times. One rise time appears faster than the other; however, this was due purely to a change made in the sample-time interval between the time sweeps.

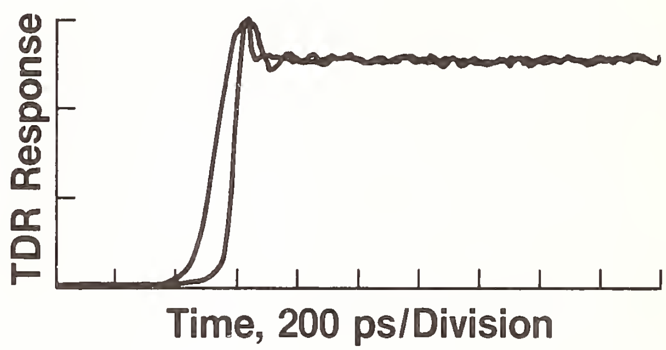

Fig. 5. An exaggerated example of a typical TDR response waveform sampled at two different rates.

When the subsequent data processing occurs, it is assumed that the sampling-time intervals were the same for the two recorded waveforms. However, because of a sampling-rate drift, one waveform appears to be "steeper" than the other. This waveform, in turn, when processed through Fourier analysis, contains more high frequency components than the "slower" (or unshifted) waveform. When the array quotient is obtained from two "apparently" different spectra, erroneous results such as those shown in figure 3 are obtained.

For measurements of cable attenuation, precision of the order a few tenths of one dB are often required. It has been observed that a sampling-rate drift of only a few tenths of 1% can cause results such as shown in figure 3; these are considered unusable.

To characterize the process, an analytically-generated waveform was used. The expression is shown by eq. (1).

$$W(I) = [M/(M^2 + 100)^{1/2}] + C \tag{1}$$

where M = I - 256.5.

The function is generated for an array of 512 points and is symmetrically centered in and around the center point of 256.5. The expression W(I) is in an array notation where I varies from 1 to 512 in steps of 1. The constant, C, is chosen to force the first point to zero amplitude so that it may be operated on by the subsequent FFT computations.

Figure 6 shows two computed waveforms having step-like transitions similar to those of actual TDR responses. The waveforms were generated using eq. (1). The lower waveform has been time-shifted by an amount 1% with respect to the upper waveform. This simulates a typical sampling-rate drift situation.

Figure 7 is the result of the array division process as discussed previously. The ordinate is plotted for a range of ±1 dB and the abscissa is given for a frequency range from 0 Hz to 20% of the Nyquist frequency. The "droop" is clearly present and is entirely the result of the 1% shift in sampling rate.

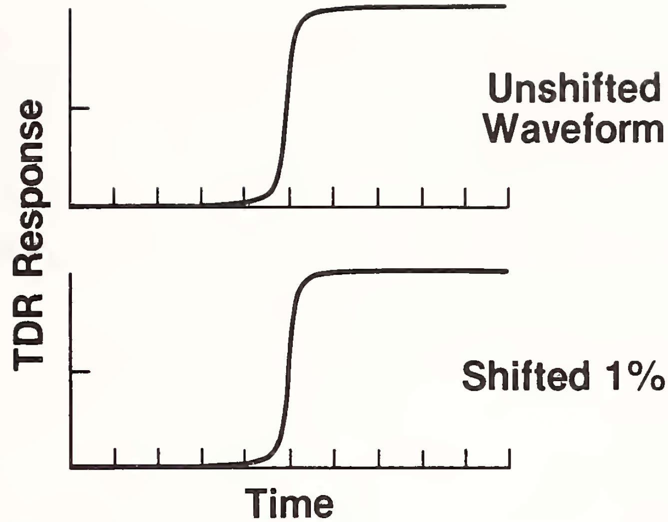

Fig. 6. Analytically-generated wave forms having similar characteristics to typical TDR responses, the lower waveform being time-shifted by 1%.

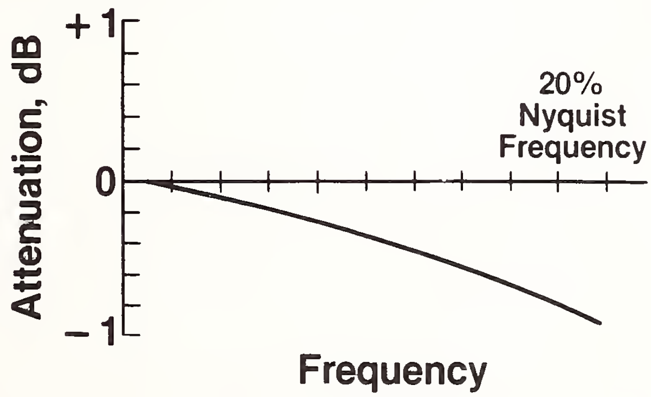

Fig. 7. Attenuation versus frequency from the waveforms shown in fig. 6; erroneous due to sampling-time drift.

The response droops when the second of the two time-domain waveforms is shifted to appear as a slower rising pulse (i.e., sampling rate is faster), and conversely, the attenuation plot would rise when the sampling rate for the second wave form is slower. Had no sampling-rate drift occurred (as in a perfect measuring system), then the attenuation plot would be a straight level line at 0 dB over the entire frequency range. For the set of measurements made by the authors, it was judged more advantageous to correct the "rate-drift" problem in software in the frequency domain rather than to try to eliminate the drift from the sampling hardware, or to correct for it in time-domain software. Because it is known that typical sampling-rate drifts result in attenuation responses such as shown in figure 7, it was predicted that expanding or compressing one of the two frequency spectra would, in effect, compensate for the rate drift and would, in turn, force the attenuation back to zero for some reference condition over the frequency range of interest. An expression shown in eq. (2) operates on an array B(M) such that the array division results in a corrected array D(I) which has the "droop" removed.

$$D(I) = \{(I*A_2-M)*[B(M+1)-B(M)] + B(M)\}*A_2^{-I/32} \qquad (2)$$

where D(I) is the Ith point in the corrected array,
I is an integer, $1 \le I \le 512$,
M is the integer part of $(I*A_2)$ for $1 \le I \le 512$,
B(M) is the Mth point in the uncorrected array, and
A_2 is a correcting factor derived from the slope.

The correcting term A_2 is derived from the slope of the uncorrected attenuation response (figure 7). A weighted mean slope is calculated from 33 points, starting with the third array point B(3) and continuing to point B(35). The weighting is such that the individual slopes received weighting factors inversely proportional to the order; thus, the lower points influence the results more heavily than do the higher points. This was done because the amount of noise increases as the order becomes higher and this weighting scheme reduces the effect of noise. The term A_2 is equal to 1 + the mean slope.

The process using eq. (2) adds a small positive shift to the process and this can be removed by using the following empirically derived relationship (shown in array notation):

$$D(I) = D(I)-[16*(1-A_2)]. \quad (3)$$

Figure 8 is the corrected attenuation plot of the uncorrected attenuation shown in figure 7. Here the response has been corrected to be within approximately ±0.05 dB over a frequency range up to 20% of the Nyquist frequency.

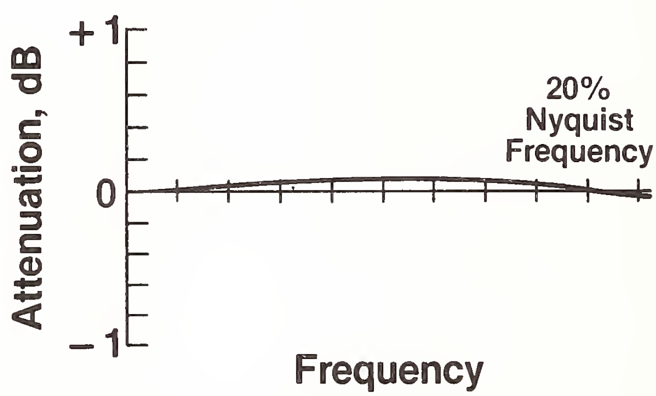

Fig. 8. Corrected attenuation of the data shown in fig. 7.

For real TDR data, a pulse such as shown in figure 9 was obtained from the laboratory. A second response was obtained which had a synthesized sampling-rate shift of 0.1%. Figure 10A shows the attenuation plot that resulted when no rate-shift correction was applied. Figure 10B shows the corrected attenuation which removed the effect of the "droop" in an attempt to improve the results.

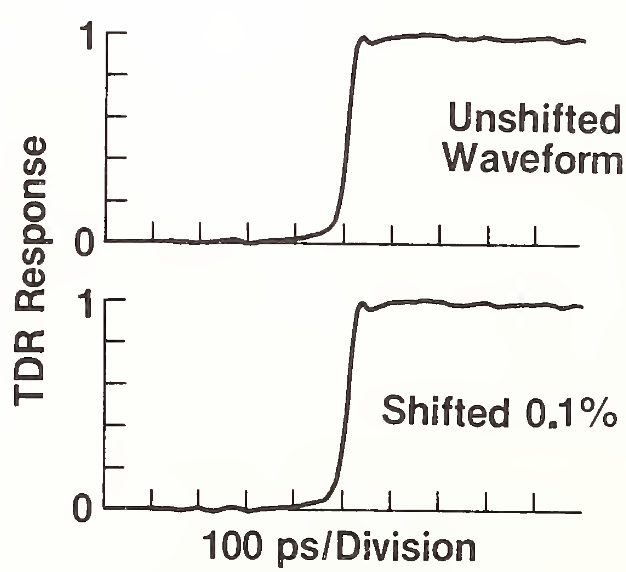

Fig. 9. Two TDR response waveforms, the second having a time shift of 0.1% with respect to the first.

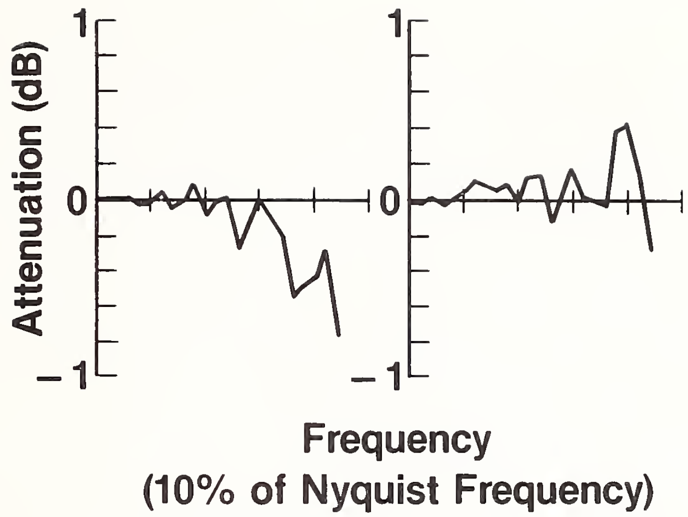

Fig. 10A. (Left) Attenuation results from waveforms shown in fig. 9 containing a sampling-time drift of 0.1%.

Fig. 10B. (Right) Corrected attenuation results using technique discussed.

The techniques discussed above analyzed a TDR response which had been "time-shifted". In practice responses are compared for two different experimental conditions (e.g., two different cable lengths). The overall TDR response for the second test condition can be markedly different from the first because of the increased cable length. The part of the time-domain response representing the impedance transitions between the TDR generator and the cable under study however should be constant for both measurements and the only change in response would be due to a sampling-rate drift. It is from the analysis of this data that sampling-rate drift can be determined and a correction factor estimated.

4. Conclusions

Errors in transfer function analysis, which result from digital techniques where the sampling-rate drifts between sets of measurements, can be minimized by applying a correction factor in the frequency domain. Analytical examples are shown that demonstrate the effect when such drifts occur. Empirically-derived equations are given which, when applied to the array quotient, correct for the effects of the time drift. In analytical examples, errors of several dB can be corrected to the order of 0.1 dB or less.

Most of the relationships given in this paper were derived empirically. Their applicability, therefore, depends on the details of the process studied and the apparatus used. They are intended only to illustrate the errors which can be produced by sampling-rate drift and to suggest an approach to the correction of these errors. It is presumed, however, that more general and more rigorous correction algorithms can be derived. The correction appears to be a direct function of TDR pulse characteristics and this complicates the possible solution. A thorough examination of the sampling-rate drift needs to be completed.

5. Acknowledgments

This work was sponsored by the Office of Electric Energy Systems of the Department of Energy.

6. References

1. W.E. Anderson, J.D. Ramboz, 1980 Annual Report. Technical Contributions to the Development of Incipient Fault Detection/Location Instrumentation, NBSIR 81-2235, Nat. Bur.Stand., March 1981.

Automatic Pulse Parameter Determination with the Computer Augmented Oscilloscope System*

A. A. Guido, L. Fulkerson, P. E. Stuckert

IBM Thomas J. Watson Research Center
P. O. Box 218
Yorktown Heights, New York 10598

The Computer Augumented Oscilloscope System (CAOS) is a special computer terminal facility intended for laboratory experiments involving waveforms and their interpretation. The system provides digital acquisition of waveform data, system control and calibration, data analysis, and graphic and alphanumeric display.

Pulse parameter determination requires the use of all system capabilities since a) hardware and software options must be chosen or controlled, b) the pulse waveform must be digitized, c) the appropriate analytical algorithms must be applied to the data and d) the results of analysis must be displayed. Specific attention is given to the algorithms required for pulse parameter determination and a new procedure for determining base and top magnitude of a pulse waveform is presented.

Key Words: automated oscilloscope; computer aided measurement; laboratory automation; pulse analysis; pulse waveform analysis; waveform analysis; waveform recording.

Introduction

A significant trend toward the automation of laboratory experiments has emerged in the past several years. This trend has origins in the realization that automation frequently improves efficiency, permits the execution of experiments that otherwise could not be performed and minimizes the amount of detail with which the experimenter must cope.

The Computer Augmented Oscilloscope System (CAOS) provides automation for the laboratory experimenter who is concerned with waveforms and their interpretation. Figure 1 shows the CAOS laboratory ensemble, which includes a modified sampling oscilloscope, the CAOS terminal and the telephone data set that couples the ensemble to a remote computer. CAOS hardware, its features and its operation have been described previously [1] and the following operational summary is adequate in this paper. By appropriate entries on the terminal's alphameric and function keyboards, an experimenter may invoke programs which:

- digitize and store in the computer a waveform displayed on the oscilloscope;
- analyze the waveform data thus stored;
- display raw waveform data;
- display calculated graphical results;

Figure 1 CAOS laboratory ensemble.

- display calculated numerical results;
- calibrate an oscilloscope sampling channel;
- display instructional or diagnostic information; and
- permit the specification of options to be used in the execution of programs.

All of the operations listed above are, in effect, self-terminating. When an operation terminates, the oscilloscope is available for use in its conventional stand-alone fashion.

CAOS has potential application in numerous experimental situations. With suitable software the system can emulate a number of conventional laboratory instruments (e.g., spectrum analyzer, distortion analyzer, phase meter, etc.). Beyond emulation, and solely as a function of the analysis and display software, the system permits the development of new techniques [2] and instruments. This paper describes one such instrument, a pulse parameter analyzer. An algorithm for determining the base and top magnitudes of a waveform is discussed and some examples of pulse parameter determination are given.

Pulse Parameter Analysis

Typically, pulse parameter analysis involves the evaluation of a waveform which is displayed on an oscilloscope or an x-y plotter. Figure 2 shows a pulse waveform and the reference lines and points which the experimenter, either literally or figuratively, superimposes on the waveform in the course of the analytical process. Using these superimposed geometrical constructs, the experimenter determines the magnitude of the parameters of interest. The entire process entails considerable subjective judgment.

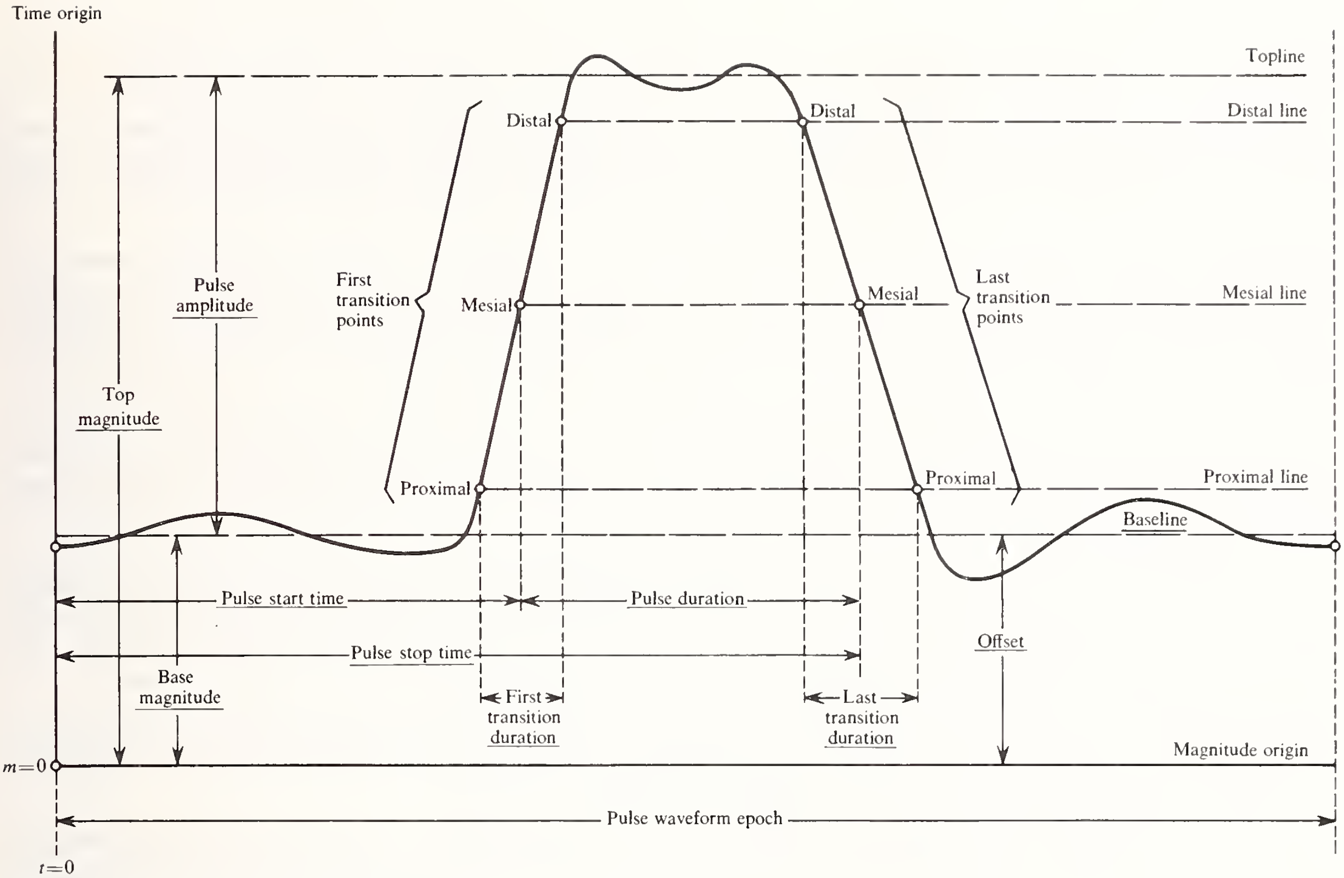

Figure 2 Pulse waveform nomenclature.

Some instruments (e.g., the Tektronix Type 567 Digital Readout Oscilloscope) provide a degree of automatic parameter determination, but no instrument, to our knowledge, provides automatic determination of the eleven major pulse parameters which are underlined in Fig. 2. More importantly, no known instrument incorporates adequate techniques for determining base magnitude and top magnitude, the two crucial parameters on which all other parameter determinations depend.

Pulse Waveform Nomenclature

Figure 2 shows the nomenclature used throughout this paper. The eleven pulse parameters to be determined are underlined and all other reference lines and points required in intermediate steps are identified. Although the nomenclature in Fig. 2 appears somewhat novel, the authors use it because it is the only available nomenclature that is complete, internally consistent and general enough to satisfy all needs.

The nomenclature of Fig. 2 does not imply any new procedure in pulse parameter analysis which, quite conventionally, involves the sequential determination of:

1) base magnitude,
2) top magnitude,
3) pulse amplitude,
4) proximal, mesial, and distal line locations either:
   a) as percentages of the pulse amplitude, or
   b) as absolute values,
5) proximal, mesial and distal point locations on the first and last transitions, and
6) the magnitudes of all other parameters from computed differences between appropriate line and/or point pairs.

Base and Top Magnitude Determination

The sequence that is outlined immediately above illustrates the importance of the base and top magnitude determinations. They are the first parameters evaluated, and their values are prerequisite to all other evaluations. Conventional methods for determining these two parameters involve either:

- estimates of their magnitudes by the experimenter from his observation of, or his graphical constructions on, the waveform, or
- location of single points on the waveform base and the waveform top by some procedure, where the magnitudes of the point so located are taken to be the base and top magnitudes.

The first technique is fraught with undesirable subjective factors, and the second can lead to bizarre results when applied to the "dirty" pulse waveforms frequently encountered in practice. Clearly, a technique which eliminates subjective judgment and which yield "reasonable" and consistent results for a wide variety of pulse waveforms is needed.

CAOS software incorporates an algorithm for the determination of base and top magnitudes that was first suggested by a former colleague, K. Maling [3]. This algorithm is based on the determination of the probability density of the waveform data within the pulse waveform epoch and is closely related to a technique independently suggested by Boatwright [4]. A graphical description of the algorithm follows:

1) Assume that a pulse waveform, such as that shown in Fig. 3(a), has a superimposed rectangular grid in which each elementary rectangle has dimensions Δt and Δm.
2) Construct the initial probability distribution histogram as follows:
    a) for each horizontal stripe (of width Δm) count the number of elementary rectangles through which the waveform passes.
    b) at the magnitude corresponding to the location of the horizontal stripe, draw a histogram element whose length is proportional to the count. (This procedure yields the truncated bimodal distribution of Fig. 3(b) in which P'_B and P'_T are identified.)

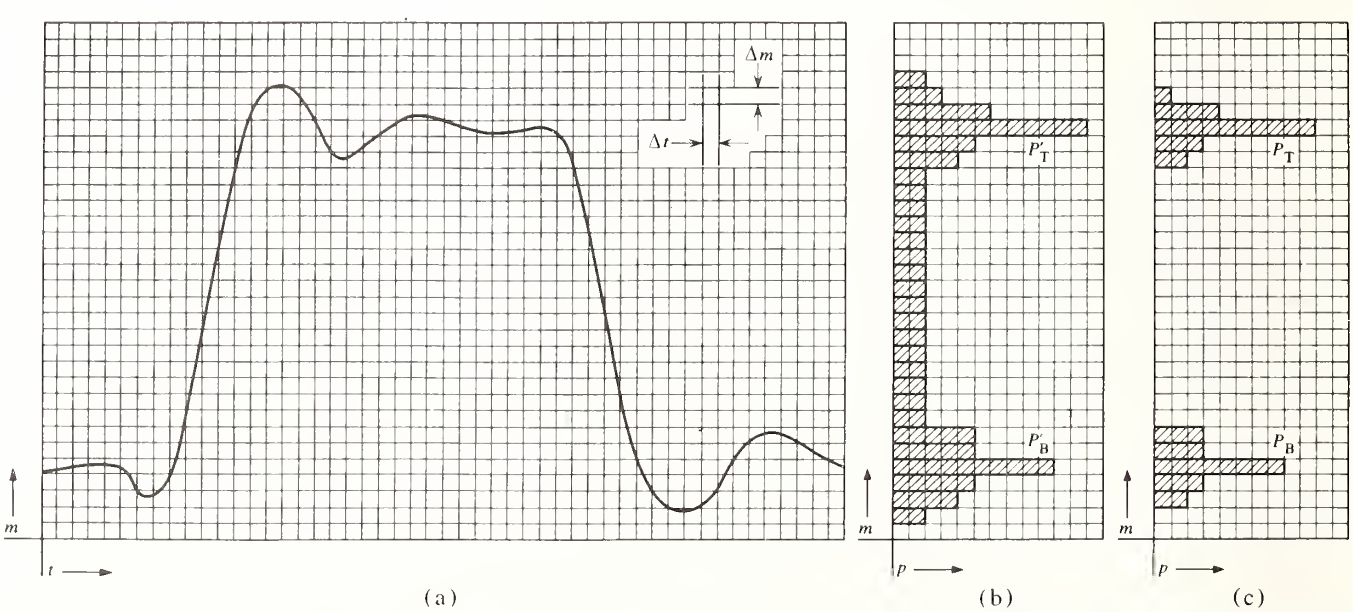

Figure 3 (a) Pulse waveform with superimposed rectangular grid, (b) initial probability distribution histogram, (c) final probability distribution histogram.

3) Count the number of transitions in the pulse waveform. (In Fig. 3(a) there are 2.)
4) Subtract the count obtained in 3, above, from each histogram element of Fig. 3(b) to produce the final probability distribution histogram, Fig. 3(c). This procedure removes contributions from the transitions and produces the two separate truncated distributions P_B and P_T.
5) Calculate the values of the means and the modes, in m, of P_B (and P_T). Either the mean or mode of P_B (or P_T) may be chosen as the base (or top) magnitude.

The previous graphical presentation yields crude results, but as Δt and Δm become smaller the magnitudes of the means (or modes) of P_T and P_B become more refined measures of the base and top magnitudes. The technique is particularly applicable in CAOS since Δt is equal to the number of waveform sample points and Δm is determined by the resolution of the A/D converter which digitizes the magnitude of each sampled point.

The algorithm given above yields two possible values for the base (or top) magnitude, and a choice must be made. However, one additional factor is pertinent. The probability density algorithm is inappropriate, and sometimes fails for pulse waveforms that have bases (or tops) of substantially zero duration (e.g., sawtooth waveforms, exponential waveforms, etc.). In these cases the peak value of the waveform is the appropriate choice. In the CAOS pulse parameter determination program, which is discussed in a later section, the authors resolve the choice between mean, mode and peak by providing independent selection for base magnitude and top magnitude wherein for each:

- the mode of the probability distribution corresponding to the pulse base (or top) is the default option. This option should be taken when results that are consistent with conventional observed results for pulse waveforms with bases (or tops) of significant duration are desired.

- the peak magnitude of the waveform base (or top) is included as a selectable option which, in general, should be taken when a base (or top) has substantially zero duration.

- the mean of the probability distribution corresponding to the pulse base (or top) is also included as a selectable option. This option should be taken when results having the highest possible precision for pulse waveforms with bases (or tops) of significant duration are desired.

CAOS Programming System

Before describing the pulse parameter determination program used with CAOS, a brief description of the CAOS Programming System (CAPS) and its interaction with an application program, the computer and the terminal is necessary. Figure 4 shows a system block diagram in which the information flow between the major constituents is indicated. As described in a previous paper [1], the CAOS terminal hardware executes a set of wired-in instructions in response to information (i.e., commands and, where applicable, data) from the computer. Typically, any useful CAOS operation entails the execution of a sequence of these wired-in instructions. Sequences for all such operations are included in the CAPS software, a library of FORTRAN routines which may be called by any application program. Typical examples are:

- DIGA (or DIGB) - digitize the waveform on Channel A (or B) of the oscilloscope.
- CALAKY (or CALBKY) - calibrate Channel A (or B).
- ERASTR - erase a specified storage screen.
- WRTLIN - write a line of EBCDIC text on a specified storage screen.
- RDLINE - read a line of EBCDIC text entered via the alphanumeric keyboard.

In addition, CAPS contains interpretive and supervisory routines which activate applications programs in response to keyboard entries.

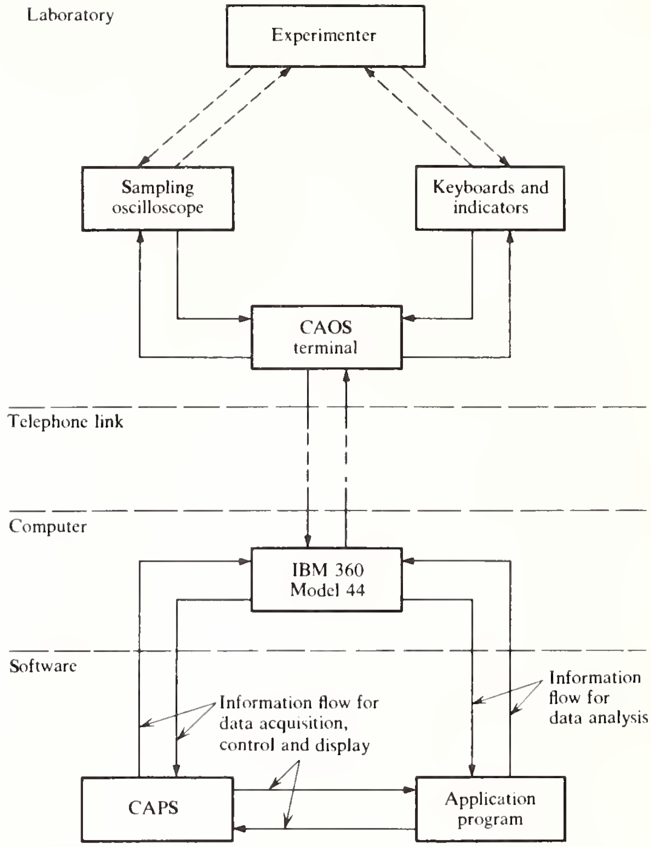

Figure 4 System block diagram.

An application program may contain up to 24 routines, each of which is associated with one of the 24 available function keys. Figure 5 shows the function keyboard overlay card for the pulse parameter determination program. With this card inserted, CAPS interprets each function key depression as a call for the execution of a specific routine in its associated application program. CAPS thus renders the CAOS terminal totally transparent to the user, who needs no knowledge of the detailed workings of the terminal or the software, both of which are completely masked. CAPS also minimizes core requirements since only it and the application routine associated with a single key must be present in the memory at any time. CAPS provides a high degree of interaction since:

- the sequence of operations is determined by the user's actuation of the function keyboard, and
- conversational features in CAPS, or in an application program, guide and prompt the user with instructional or diagnostic messages.

The CAOS library currently contains application programs for time-jitter correction, spectrum analysis, deconvolution and signal averaging in addition to the program for pulse parameter determination. New application programs, as required, may be written in FORTRAN and added to the library.

Pulse Parameter Determination Program

The program for pulse parameter determination (PPD) is invoked by inserting the overlay card shown in Fig. 5 in the terminal. PPD makes extensive use of terminal displays, for example, when the operator depresses "Choose Mode" (key 21) and enters a "1" via the alphanumeric keyboard, the display shown in Fig. 6 results. Modes 1 through 4 comprise, in effect, an interactive instruction manual for the operation of PPD and the terminal itself. Space limitations preclude the presentation here of the 8 displays which these

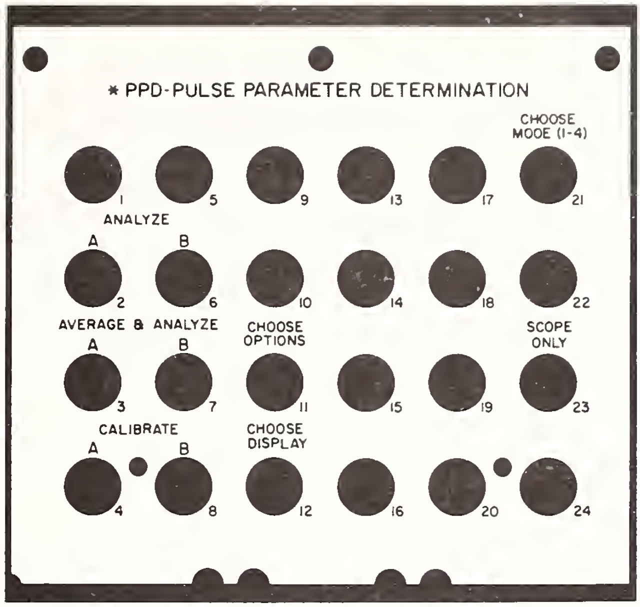

Figure 5 Function keyboard overlay card.

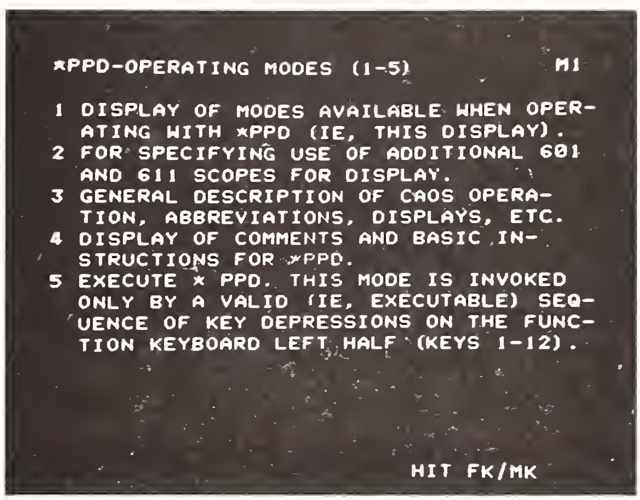

Figure 6 Mode 1 display.

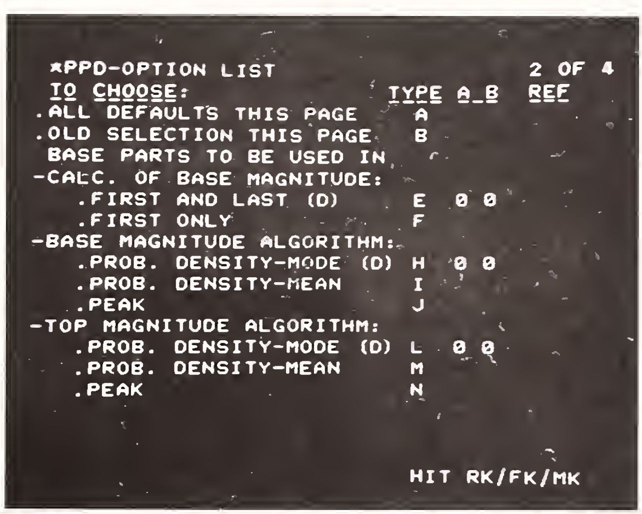

Figure 7 Typical option list display.

four modes contain. The operator, as a function of his familiarity with the PPD program and the terminal, may execute any or all of these modes or he may proceed directly to Mode 5, the PPD program proper. All displays have the following features in common with the display of Fig. 6:

- The top line always contains a page title and the mode and/or page numbers.
- The bottom line always contains abbreviated instructions for exiting from the page (i.e., in Fig. 6, "HIT FK/MK").

Mode 5, the PPD program proper, is executed with the 8 active keys on the left half of the function keyboard (see Fig. 5). Typical operation begins with:

1) execution of "Choose Display" (key 12) which provides an interactive control display through which the operator may format the display of results from the PPD program. The default (i.e., complete) display will be provided if no options are exercised.
2) execution of "Choose Options" (key 11) which provides interactive control displays through which the operator may exercise a number of data acquisition and analysis options. Again, default options are taken if the operator makes no specific choices.

Figure 7 shows a typical page of the PPD option list in which all default options are indicated by "(D)." By typing the specified alphabetic characters the operator may for either or both oscilloscope channels:

- select all default options on the page;
- retain his previous option selection;
- specify whether the determination of base magnitude shall be based on:
  a) both sections of the pulse waveform base, or
  b) that section of the base which precedes the first transition;
- specify whether the base (or top) magnitude shall be calculated as:
  a) the mode of its probability distribution,
  b) the mean of its probability distribution, or
  c) the peak magnitude of the pulse waveform.

Again, space limitations preclude showing the complete PPD option list which provides the following additional options:

- whether calibration of the sampling channel shall be
  a) continuous, or
  b) under manual control from the function keyboard;
- whether waveform averaging shall be
  a) continuous, or
  b) under manual control from the function keyboard (default);
- whether the pulse waveform analysis shall be based on:
  a) the entire waveform (default) or
  b) on a specified continuous portion of the waveform;
- whether the base magnitude shall be
  a) assumed to be zero (default);
  b) determined on an absolute basis, or
  c) assigned a specific value;
- whether the time origin shall be
  a) assumed to be zero (default), or
  b) assigned a specified value;
- whether the locations of the proximal, mesial, and distal lines shall be
  a) at 10%, 50% and 90%, respectively, of the pulse amplitude (default),
  b) at specified percentages of the pulse amplitude, or
  c) at specified magnitudes;
- whether the polarity of the pulse waveform shall be

a) automatically determined by the program (default), or
b) specified by the operator;

- whether attenuation external to the oscilloscope shall be assumed
  a) to be zero (default), or
  b) to be a specified value.

When the operator has completed executing the option list -- an operation which can take negligible to significant time, depending on the number of default options which must be overridden -- he executes the PPD program by depressing one of keys 2 through 4 or 6 through 8 (in Fig. 5) for each operation required. The operator may revert to conventional stand-alone oscilloscope operation at any time by depressing the "Scope Only" (key 23).

Examples of PPD Operation

Space limitations preclude a comprehensive description of all modes of PPD operation with the sampling oscilloscope. The authors, instead, present a limited set of examples which illustrate PPD operation in general and indicate the degree of precision which can be achieved with CAOS. Throughout this section the discussion of numerical results is solely in terms of precision, that is, "... the degree of mutual agreement characteristic of independent measurements of a single quantity yielded by repeated applications of the [measurement] process under specified conditions ..." [5].

Table 1 lists the hardware conditions and PPD software options for three types of test (A, B, and C) which were performed 9 times in a one-week period. Figures 8, 9 and 10 show the results of the first of these tests wherein:

Table 1 Test conditions and options.

Type A (Fig. 8)	
Pulse source	Hewlett Packard Model 215A Pulse Generator
Repetition frequency	60 kHz
Pulse distorting circuit	Passive RLC network
Sampling head	Tektronix S-2 (75 psec)
Oscilloscope settings	
Vertical sensitivity	100 mV/cm
Horizontal sensitivity	10 nsec/cm
Number of sampling points	800
Triggering	External from pulse source
PPD operation	
Analyze A (key 2 in Fig. 5). All default options *except* that base magnitude and top magnitude were computed as the means of the probability density histograms.	
Type B (Fig. 9)	
Same as Type A, above, except:	
Vertical sensitivity—10 mV/cm. External attenuation of 20 dB (nominal) inserted between pulse distorting circuit and sampling head.	
Type C (Fig. 10)	
Same as Type B, above, except:	
PPD operation—Average and analyze A (key 3 in Fig. 5) with 10 digitizations of the waveform specified.	

(a) (b) (c)

Figure 8 (a) Pulse waveform, (b) probability distribution histograms, (c) calculated pulse parameters.

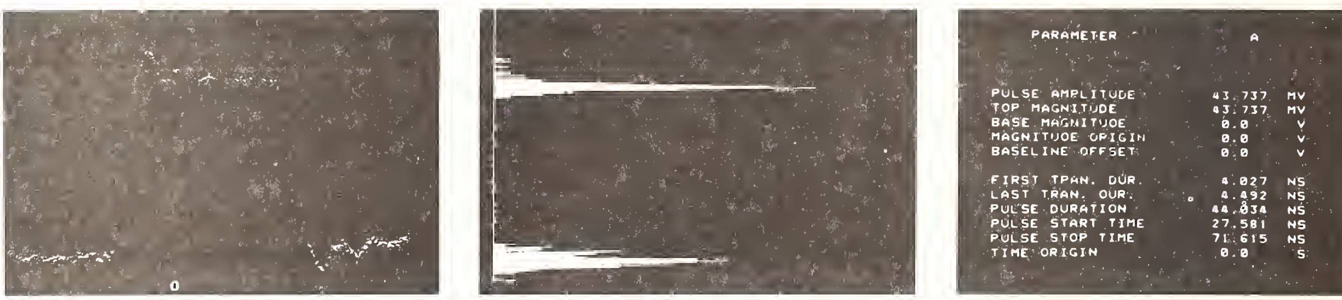

(a) (b) (c)

Figure 9 (a) Noisy pulse waveform (b) probability distribution histograms, (c) calculated pulse parameters.

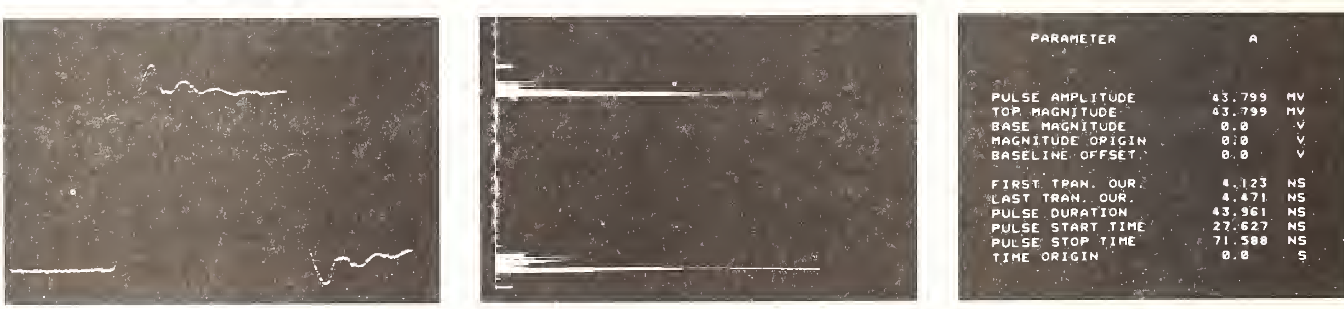

(a) (b) (c)

Figure 10 (a) Averaged noisy pulse waveform, (b) probability distribution histograms, (c) calculated pulse parameters.

- Figures 8(a), 9(a) and 10(a) show the pulse waveform data which were analyzed by the PPD program. Figures 8(a) and 9(a) show the waveform data from one digitization; sampling noise at the 10 mV/cm sensitivity is evident as in the latter. Figure 10(a) is the average of 10 digitized waveforms, each of which was similar to that shown in Fig. 9(a). Figures 8(b), 9(b) and 10(b) show the probability density histograms of the corresponding waveforms. For these figures the display routine adjusted the histogram data to provide a maximum horizontal deflection of 8 cm. The histograms, while exhibiting similar characteristics, are distinctly different, Fig. 9(b) begin markedly different from the other two.
- Figures 8(c), 9(c) and 10(c) show the calculated pulse parameter displays provided by PPD using the techniques, options, and algorithms described in previous sections. Note that, despite the differences between the waveform data and the significant differences between their histograms, the numerical results are in relatively close agreement.

Table 2 lists the salient results from Figs. 8(c), 9(c) and 10(c) and shows the variations (in percent of full scale) for all 9 executions of the three types of test described in Table 1. In Table 2 the extreme variations for each of the four major parameters are set in bold-face type. Long-term precisions of the order of ±0.5% of full scale, or better, are achieved throughout. As was expected, the Type B tests contribute a majority (6) of the extreme variations. Further, all nine runs, with the exception of run 7, were made after all equipment had been on for one-half to one hour. Run 7, which contributes 4 of the 8 extreme values in Table 2, was made after all equipment had been on for approximately six hours.

Table 2 Long term variations in indicated pulse parameters. Type A test arbitrarily taken as reference. Vertical full scale—800 mV; Horizontal full scale—100 nsec. Extreme variations for parameters are set in bold-face type.

Data for Run No. 1		*Variations in percent of full scale*								
		Run numbers								
		1	*2*	*3*	*4*	*5*	*6*	*7*	*8*	*9*
Pulse amplitude										
Type A	439.722 mV	···	+0.187	+0.250	+0.324	+0.450	+0.444	**+0.570**	+0.286	+0.273
Type B	437.370 mV*	**−0.294**	−0.123	−0.055	+0.105	+0.011	−0.134	+0.106	−0.178	−0.193
Type C	437.990 mV*	−0.217	+0.107	+0.121	+0.332	+0.160	+0.160	+0.366	+0.008	+0.241
First transition duration										
Type A	4.083 nsec	···	+0.063	−0.016	+0.049	+0.083	+0.048	+0.147	+0.038	+0.006
Type B	4.027 nsec	−0.056	+0.056	**−0.155**	+0.135	+0.043	−0.018	**+0.157**	+0.045	−0.088
Type C	4.123 nsec	+0.040	+0.062	−0.042	+0.038	+0.092	+0.006	+0.035	+0.121	+0.081
Last transition duration										
Type A	4.388 nsec	···	+0.038	+0.077	+0.013	+0.016	+0.141	+0.069	+0.046	+0.070
Type B	4.492 nsec	+0.104	**−0.099**	−0.062	+0.069	+0.003	+0.171	**+0.176**	+0.032	−0.090
Type C	4.471 nsec	+0.083	+0.077	+0.058	+0.059	+0.023	+0.157	+0.056	+0.085	+0.110
Pulse duration										
Type A	44.058 nsec	···	+0.182	+0.009	+0.036	−0.128	+0.045	−0.358	**+0.308**	+0.136
Type B	44.034 nsec	−0.024	+0.027	−0.170	+0.159	−0.272	+0.034	**−0.762**	−0.302	+0.078
Type C	43.961 nsec	−0.097	+0.063	−0.086	+0.021	−0.109	−0.064	−0.315	−0.251	+0.155

*Indicated data multiplied by 10.

The results summarized in Table 2 indicated that the operation of CAOS (and all other hardware) under the PPD program was approaching a state of statistical control, insofar as precision was concerned. The sample sizes are of course, too small to warrant any firm conclusions.

Hence, an additional program was written which executed the Type A test 100 times and computed the mean values and standard deviations for the four major pulse parameters. The results are tabulated in Table 3.

Table 3 Short term variations in indicated pulse parameters. Statistics on 100 Type A tests. Vertical full scale—800 mV; horizontal full-scale—100 nsec.

Pulse parameter	*Mean (in units shown)*	*Standard deviation (in units shown)*	*Standard deviation (in % of full scale)*
Pulse amplitude	445.974 mV	0.593 mV	0.0741
First transition duration	4.16860 nsec	0.03252 nsec	0.03252
Last transition duration	4.52299 nsec	0.03199 nsec	0.03199
Pulse duration	44.4658 nsec	0.0826 nsec	0.0826

The data in Tables 2 and 3, unfortunately, are only indicative of the precision that CAOS, or similar instruments, can bring to the pulse waveform measurement art. In all of the data presented variations from a variety of sources are combined. These sources of variation, in an estimated order of their contributions are:

1) the vertical and horizontal circuits of the sampling oscilloscope,
2) the pulse generator,
3) the A/D converter in the CAOS terminal,
4) the 20 dB attenuator,
5) the pulse distorting circuit, and
6) the interconnecting cables and connectors.

Variations due to items 3 through 6, above, are amenable to evaluation and control, but variations due to item 2, the pulse generator, are a formidable obstacle to find all conclusions relative to the precision provided by CAOS.

Precision and Accuracy

The discussion in the previous section considered precision only; some final comments on accuracy are in order. As Eisenhart concisely puts it, "...accuracy requires precision, but precision does not necessarily imply accuracy" [5]. The data presented in this paper demonstrate that CAOS and the PPD program provide precision pulse parameter determinations. But precision, valuable as it is as a prerequisite to accuracy, is only the first step. The second step from precision to accuracy is far from trivial, since it requires the development of a) pulse (or transition) generators and b) time mark generators whose characteristics are known to accuracies consistent with the precision CAOS provides.

As described elsewhere [1], the CAOS vertical calibration hardware provides dc calibration in the voltage (or vertical) axis of the oscilloscope. Useful as this feature is, it does not provide for determination of the transient response of the sampling channels. Sampling oscilloscopes with bandwidths in the 20 GHz region are currently available. Consequently, a pulse generator with a transition duration in the 5 to 10 psec range is required before an algorithm that compensates for oscilloscope frequency response can be included in CAOS software. Horizontal (i.e., sweep linearity) calibration of CAOS is, of course, possible with external oscillators or time mark generators of suitable accuracy.

Conclusions

The data presented in this paper -- using pulse parameter determination as a vehicle -- demonstrate the precision which can be realized by augmenting the sampling oscilloscope with appropriate digital processing. Since the CAOS hardware and procedures for acquiring waveform data are invariant, other digital processing algorithms that preserve and exploit the inherent system precision in other types of waveform analysis ensue. In addition to the program for pulse parameter determination, programs for spectrum analysis, convolution and deconvolution, digital filtering, and time jitter correction are available to the CAOS user. Programs for distortion analysis, circuit delay analysis, integration and others are envisioned and will be added as the need develops.

Digital systems for data acquisition, control, analysis and display are commonplace in industry and in laboratories. The oscilloscope, very probably, is the one instrument most used in the development of such systems. It is ironic that this versatile instrument itself is only now being given a degree of precision and greater versatility through automation of the type that CAOS provides.

It is a pleasure to acknowledge the encouragement and support of J. S. Birnbaum and the technical assistance of R. J. Arculeo and W. L. Keller.

References and Notes

[1] P. E. Stuckert, "Computer Augmented Oscilloscope System," *IEEE Trans. Inst. Meas.* **IM-18**, *299 (1969).*

[2] B. J. Elliott, "A System for Precise Observations on Repetitive Picosecond Pulse Waveforms," *IEEE Trans. Inst. Meas.* **IM-19**, 391 (1970).

[3] K. Maling is now located at the Systems Development Division Laboratory Poughkeepsie, New York.

[4] J. T. Boatwright, "Random Sampling - A Statistical Measurement Approach," *IEEE WESCON Technical Papers,* Vol. 10, paper 23/4, 1966.

[5] C. Eisenhart, "Realistic Evaluation of the Precision and Accuracy of Instrument Calibration Systems," *J. Res. Nat. Bureau Stand. Eng. Inst.* **67C**, *172 (1963).*

Status of Reference Waveform Standards Development at NBS

J. R. Andrews*
Picosecond Pulse Laboratory
Lafayette, Colorado 80026

N. S. Nahman and Barry A. Bell**
National Bureau of Standards
Boulder, Colorado 80303

ABSTRACT

NBS has developed a (step-like) pulse generator for use as a transfer standard for transition duration (10% - 90%), t_d. The generator consists of a tunnel diode step-like generator (t_d = 20 ps) driving a low pass filter. Three filters are available for t_d = 50, 100, and 200 ps. The low-pass filters, of NBS design, are 30 cm long, 7 mm diameter, coaxial lines filled with a lossy Debye-type liquid dielectric. The mathematical model describing these low pass filters is quite accurate. The necessary parameters for the model can be obtained from independent measurements. The complete available output waveform into a matched load (50 ohms) can be predicted to within less than 1.5%. A companion step-like generator is presently under development to provide well-known top and baselines with a transition duration of less than one nanosecond.

Key Words: Calibration; reference waveform generators; rise time; time domain measurements; transfer standards; transition duration; waveform generation; waveform measurements.

INTRODUCTION

The two objectives of the reference waveform standards development projects have been to develop two independent pulse generators for use as transfer standards for the pulse parameters: (1) transition duration and (2) base and topline, respectively. The status of these projects are discussed below in Sections 1 and 2.

---

* J. R. Andrews formerly with the Electromagnetic Technology Division, National Bureau of Standards, Boulder, Colorado.

** Barry A. Bell on detail from the Electrosystems Division, National Bureau of Standards, Washington, D.C.

I. TRANSITION DURATION TRANSFER STANDARD

1.1 Objective and Concept

The objective of NBS in this project was to develop a pulse generator suitable for use as a transfer standard for transition duration. The specific requirements were: (1) step-like pulse, (2) transition duration of the order of 100 ps, (3) smooth, gaussian-like transition, and (4) clean baseline and topline. The concept chosen for the implementation was to use a tunnel diode to generate a fast (∿ 25 ps), but not necessarily well known, step waveform. The fast transition is then slowed down using a known low-pass filter. If the step response of the filter is 10 times slower than the driving pulse, then the transition duration of the output pulse from the composite generator is approximately within 0.5% by the step response of the filter alone. This follows from a gaussian filter model excited by a step-like gaussian input signal. The output signal would be step-like and have a transition duration, TD_3, given by

$$TD_3 = \sqrt{TD_1^2 + TD_2^2}$$

where TD_1 and TD_2 are the transition duration of the input signal and the step-response of the filter, respectively. For TD_1 equal to one-tenth of TD_2, TD_3 is approximately equal to 1.005 TD_2.

1.2 Selection of Filter

Some pulse equipment manufacturers in the past have made low-pass filters which were designed for a clean time domain response. Some of these commercial filters were found to have a serious defect. The leading edge of their step response was distorted with many small glitches, figure 1. These glitches were readily observable using a 20 ps tunnel diode pulse generator and a 20 ps sampling oscilloscope. They were caused by multiple paths and reflections from the various elements used to construct the filter.

Another filter that has been proposed [1] is a long length of coaxial cable. The skin effect gives a loss proportional to $\sqrt{f}$. The pulse response of a cable is usually quite clean, but it is also unsuitable due to the extremely slow approach to its final value (commonly referred to as dribble-up), figure 2. Furthermore, low pass filters with a sharp cut-off frequency are also unsuitable due to ringing and overshoot in their time domain responses, figure 3, [2]. NBS has found that a suitable time domain filter for transition durations from 50 ps to 500 ps can be obtained from a coaxial line with a lossy dielectric [3].

1.3 Filter Model

A lossy, distributed filter was chosen by NBS for use as a transfer standard [3]. It consists of a coaxial line filled with a lossy liquid dielectric.

The dielectric is a dilute solution of 2-Heptanone in Heptane. The Heptane solvent is non-polar and essentially loss-less. The 2-Heptanone solute has a polar molecular structure and obeys the Debye dielectric equations [4]. The behavior versus frequency of the real (ε') and

imaginary (ε'') parts of the dielectric function (ε) are shown in figure 4. ε'_∞ is the dielectric constant of the non-polar Heptane. ε'_o, ε'' and the time constant τ are functions of the molal concentration of the 2-Heptanone in the Heptane.

Figure 5 shows the per unit length equivalent circuit of a coaxial line with a Debye-type dielectric. s is the complex frequency. L is the normal series inductance. k is the skin effect constant for the metal conductors. $C_1 + C_2$ is the normal low frequency shunt capacitance (proportional to ε'_o), τ is the relaxation time constant of the polar solution.

The transfer function, H(s), of a transmission line of length ℓ terminated in its characteristic impedance, $Z_o(s)$, is given by

$$H(s) = V_{out}(s)/V_{in}(s) = e^{-\gamma(s)\cdot\ell} \tag{1}$$

where $\gamma(s)$ is the propagation function. γ and Z_o are defined in terms of the series impedance per unit length, Z(s), and the shunt admittance per unit length, Y(s).

$$\gamma(s) = \sqrt{Z(s)Y(s)} \tag{2}$$

$$Z_o(s) = \sqrt{Z(s)/Y(s)} \tag{3}$$

$$Z(s) = sL + k\sqrt{s} \tag{4}$$

$$Y(s) = sC(s) \tag{5}$$

$$C(s) = A\,\varepsilon(s) \tag{6}$$

$$\varepsilon\,(j\omega) = \varepsilon'(\omega) - j\varepsilon''(\omega) = \varepsilon'_\infty + \frac{\varepsilon'_o - \varepsilon'_\infty}{1 + j\omega\tau} \tag{7}$$

By varying the molar concentrations, ε'_o and τ are varied and as a result, Z_o and γ can be adjusted. The effect of varying concentration on the step response transition duration is vividly demonstrated in figure 6.

Using eq. (1), and equivalent circuits for the connectors the complete step response waveform, figure 7, of a Debye line filter can be predicted. Note the clean, gaussian-like transition. The various filter parameters can be determined from independent measurements. k is a function of the line diameters and the metal conductivity. ε'_o is determined by 1 kHz capacitance bridge measurements. ε'_∞ is determined by the index of refraction of Heptane. L and A are determined by

the line diameters. With ε'_o and ε'_∞ known, by analyzing experimental time domain data [5] and/or frequency domain data [6] in terms of eq. (7), the value of τ can be determined.

1.4 Hardware

Figure 8 is a photograph of an NBS Debye line low-pass filter with a tunnel diode step generator attached. Three different filters have been designed and developed for transition durations of 50 ps, 100 ps and 200 ps. A 30 cm, 7 mm diameter coaxial air line is used. Different molal solutions are used in each of the three models. The center conductor diameter is varied to maintain a 50 ohm impedance in each model. Modified APC-7 connectors are used. The center conductor support bead was modified to provide a leak-proof seal.

The dielectric characteristics of the fluids used are quite temperature sensitive. The temperature coefficient of the transition duration is approximately $1\%/^{o}C$. Thus, it was necessary to provide temperature regulation to better than $0.1^{o}C$. The filters are operated at $30^{o}C$ and are only intended to be operated in a standard laboratory environment. Heaters and temperature sensors are installed in the filter box.

Also enclosed in the box is the necessary plumbing and valve for filling the line and an expansion bellows to compensate for fluid expansion and contraction due to temperature extremes encountered during shipping.

The tunnel diode (TD) used to drive the filter is of commercial manufacture. The TD bias supply and trigger pulse generator is an NBS design which is superior to commercially available units, figure 9. The NBS bias supply has the advantage that it automatically compensates the TD bias current for changing TD conditions such as temperature, various electrical loads ranging from a short to an open circuit and even using a different TD. The trigger pulse circuits were designed so that they introduced negligible distortion to the TD step-like pulse as shown in figure 10a. This was a considerable improvement over the commercial bias supply which added a 5%, 1/2 ns linear ramp distortion prior to the abrupt transition of the TD.

1.5 Waveforms

Deconvolved, measured output waveforms from the tunnel diode and the 50 ps, 100 ps, and 200 ps filters are shown in figure 10. Figure 11 is the predicted, available, reference waveform, $e_a(t)$, into a 50Ω load from the TD/100 ps low-pass filter combination. It was obtained by convolving the tunnel diode waveform with the filter impulse response function. The tunnel diode waveform, figure 10a, was first obtained by deconvolution of the measured TD waveform and a model of the sampling oscilloscope used to make the measurement. The deconvolution technique [8,9] and sampler model [10] were developed at NBS.

Figure 12 is included to demonstrate the agreement between theory and experiment. The solid curve, $e_a(t)$, is the mathematically predicted waveform (TD/100 ps filter), while the dotted one, $e_m(t)$, is the actual measured waveform. It is meaningful to compare two similar waveforms to

determine the difference between them [11]. The difference between these two waveforms, d(t), is shown for a 2 ns time window. The RMS difference was 0.4% while the maximum difference was 1.4%.

II. TOP AND BASELINE TRANSFER STANDARD

2.1 Objective and Concept

The objective for this NBS project is to develop a step-like pulse generator suitable for use as a transfer standard for both baseline and topline. The generator is to provide known baseline and topline magnitudes and to possess a predictable transition duration of less than one nanosecond. A laboratory experimental model or prototype has been built and is presently being modeled and evaluated using computer simulation. The information presented below describes the prototype generator and preliminary waveform data.

The basic concept of the generator, hereafter called the flat-pulse generator, is illustrated in figure 13. A known DC current, I, drives a terminated transmission line having the HF parameters: Characteristic impedance, R_o, and a velocity of propagation, v. The DC current produces a topline magnitude of IR_o volts. At t=0, the current generator is switched-off, and the transmission line output voltage, e(t) decreases to the baseline magnitude of zero. The step-like waveform, e(t), then provides known top and baseline magnitudes.

2.2 Pulse Generator

The flat-pulse generator block diagram is shown in figure 14. A crystal clock (10 MHz) drives logic countdown and delay circuits to produce a trigger output pulse and a delayed main pulse. The repetition rate is variable from 1 KHz to 1 MHz while the delay circuit produces selectable delays of 100 ns from zero to 300 ns. Oscillograms of the main output pulse are shown in figure 15 while figure 16 shows the output pulse as measured by the NBS Automatic Pulse Measurement System [12,13]. The pulse parameter magnitudes and amplitude values given in figure 16 should be multiplied by a factor of 2, e.g., the pulse amplitude is 511.486 millivolts. The magnitude histogram is given in the left hand side of figure 16 and attests to the flatness of the pulse. The prototype generator is shown in figure 17.

SUMMARY

The status of NBS reference waveform generator development has been presented. Two generators have been described, one being a transfer standard for pulse transition duration (50, 100, and 200 ps), and the other is a transfer standard for topline and baseline (nominally 0.5 and zero volts, respectively) having a predictable transition duration of less than one nanosecond. The development of the transition duration transfer standard has been completed while the top/baseline generator is in the prototype evaluation stage of development.

REFERENCES

1. McCaa, Jr., W. D.; Nahman, N.S. Generation of reference waveforms by uniform lossy transmission lines. IEEE Trans. Instrum. & Meas. IM-19(4) 382-390; 1970 Nov.

2. Blinchikoff, H. J.; Zverev, A. I. Filtering in the time and frequency domains. New York: J. Wiley and Sons; 1976.

3. Nahman, N.S.; Jickling, R.; Holt, D. Reference waveform generation using Debye dielectric dispersion. Nat. Bur. Stand. (U.S.) NBSIR 73-304; 1972.

4. Debye, P.: Polar molecules. Chemical Catalog Co.; 1929. (Also Dover Publications, New York).

5. Bagozzi, R. P.; Ives, W. R.; Nahman, N.S. Determination of the dielectric relaxation time in a Debye binary liquid by pulse measurements. Progress in Radio Science 1966-69, V.2, 257-265, URSI Brussels, 1971.

6. Von Hippel, A.; Dielectrics and waves. Wiley, New York, 1954.

7. Von Hippel, A.; Dielectric materials and applications, Wiley, 1954.

8. Nahman, N.S.; Guillaume, M.E. Deconvolution of time domain waveforms in the presence of noise. Nat. Bureau of Stand. (U.S.) Technical Note 1047; 1981 October.

9. Guillaume, Michel E.; Bizeul, Jean-Claude. "Mesure de la response impulsionelle d'um milieu de transmission: application aux fibres optiques" (Impulse response of a transmission medium: application to optical fibers), Annales des Telecommunications; 36(3-4), 1/8-8/8; 1981 March-April.

10. Riad, S. M.; Nahman, N.S. Modeling of the feed-through wideband sampling head. IEEE-MTT, Int. Microwave Symposium Conf. Digest, Ottawa, Canada, 1978, June 27-29.

11. Nahman, N. S. Error criteria and the use of reference waveforms. Proceedings of the ATE Seminar/Exhibit, Pasadena, CA. 1981, Jan. Benwill Publications Corp., Boston, MA. 02215; pp IV-21 to IV-28.

12. Gans, W. L. Present capabilities of the NBS automatic pulse measurement system. IEEE IM-25(4), 384-388; 1976 Dec.

13. Nahman, N.S.; et.al. Applications of time-domain methods to microwave measurements. IEE Proc. 127(Pt. H, No.2); 99-106; 1980 April.

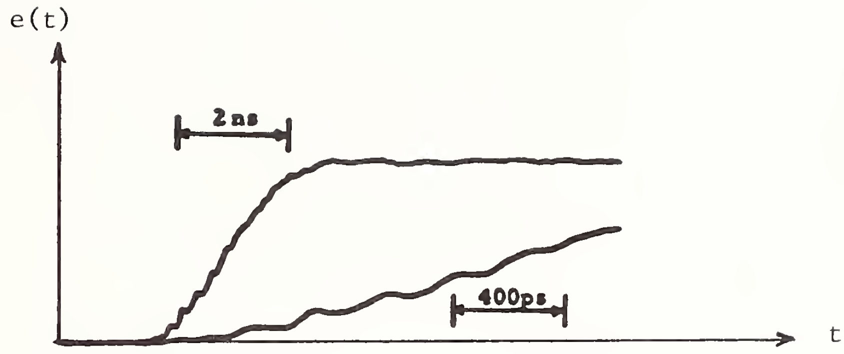

Figure 1. Commercial 2ns transition duration standard. Note small steps on the leading edge. The lower curve shows the leading edge on a faster time scale.

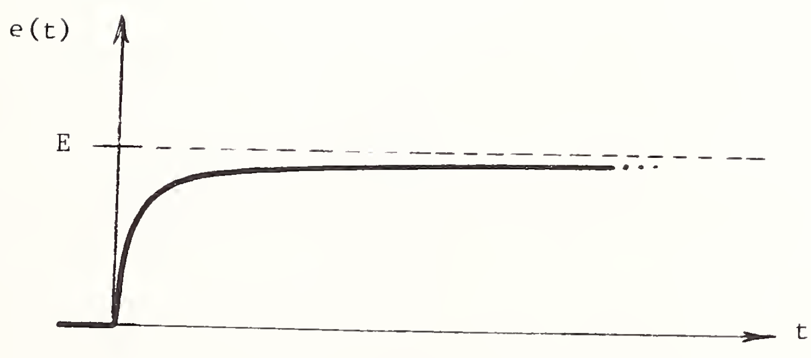

Figure 2. Step response of a typical coaxial cable with skin effect loss. Note the long dribble-up, i.e., the slow approach to the final value, E.

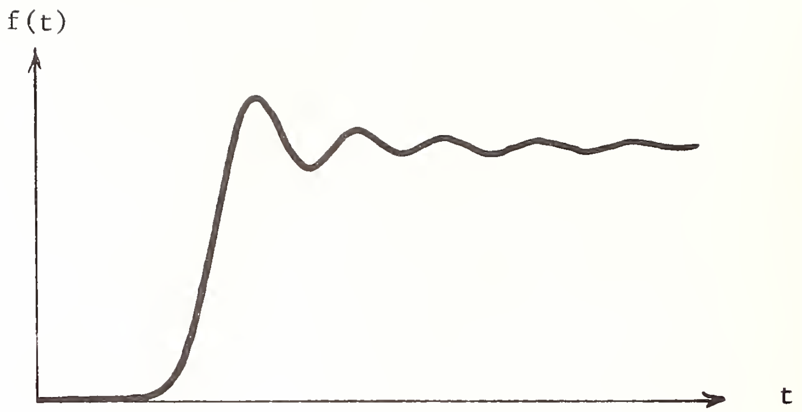

Figure 3. Typical step response, f(t) of a low pass filter having a sharp cut-off frequency.

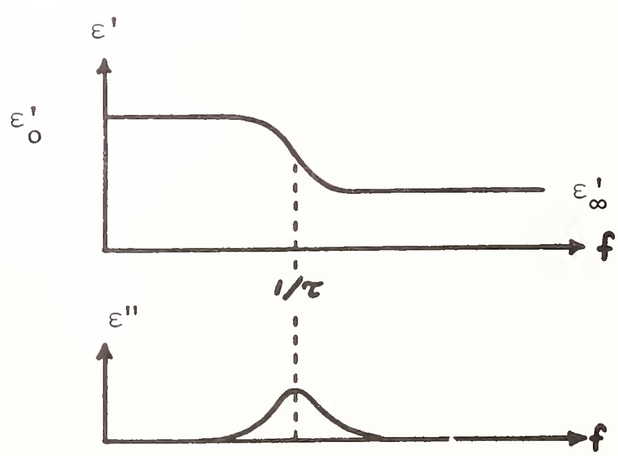

Figure 4. Debye type dielectric function.

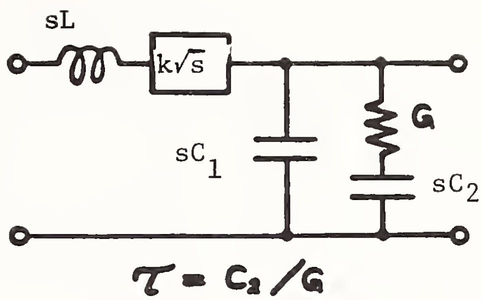

Figure 5. Per unit length equivalent circuit of a transmission line with Debye type dielectric.

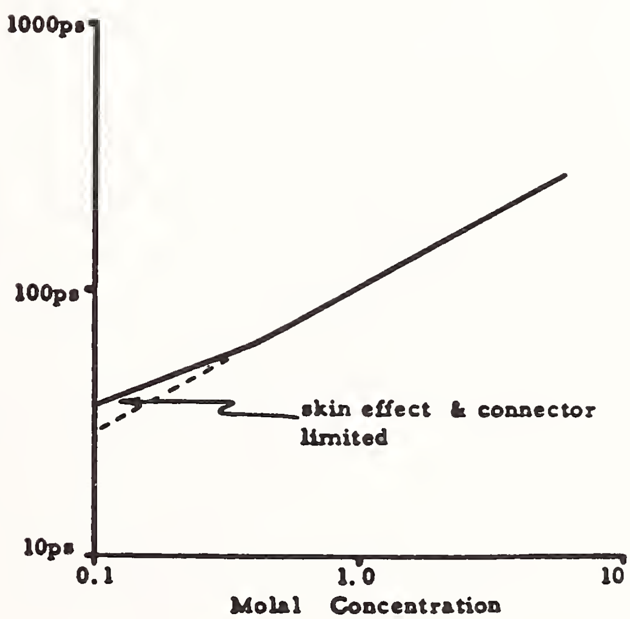

Figure 6. Step response transition duration versus Debye dielectric doping.

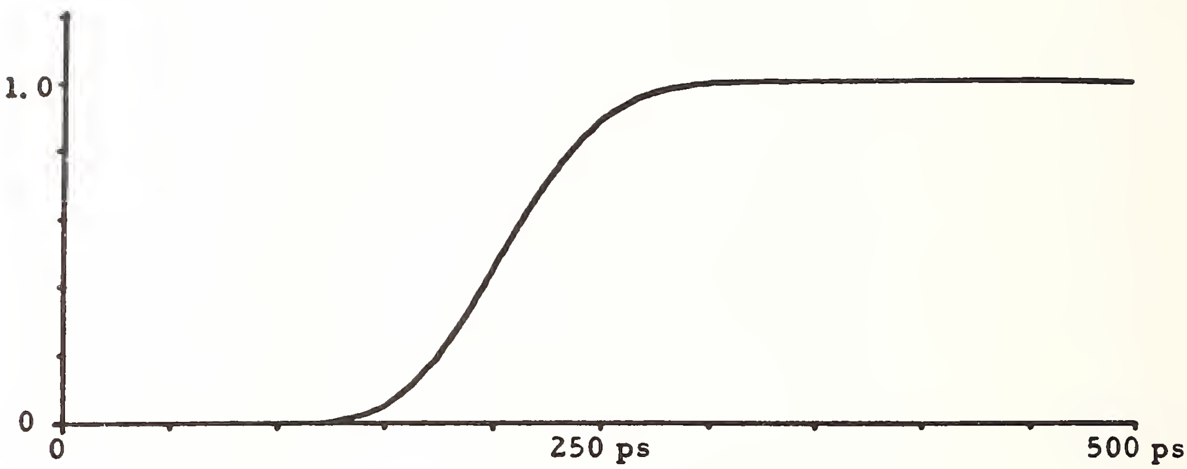

Figure 7. Step response of a Debye dielectric, coaxial low pass filter.

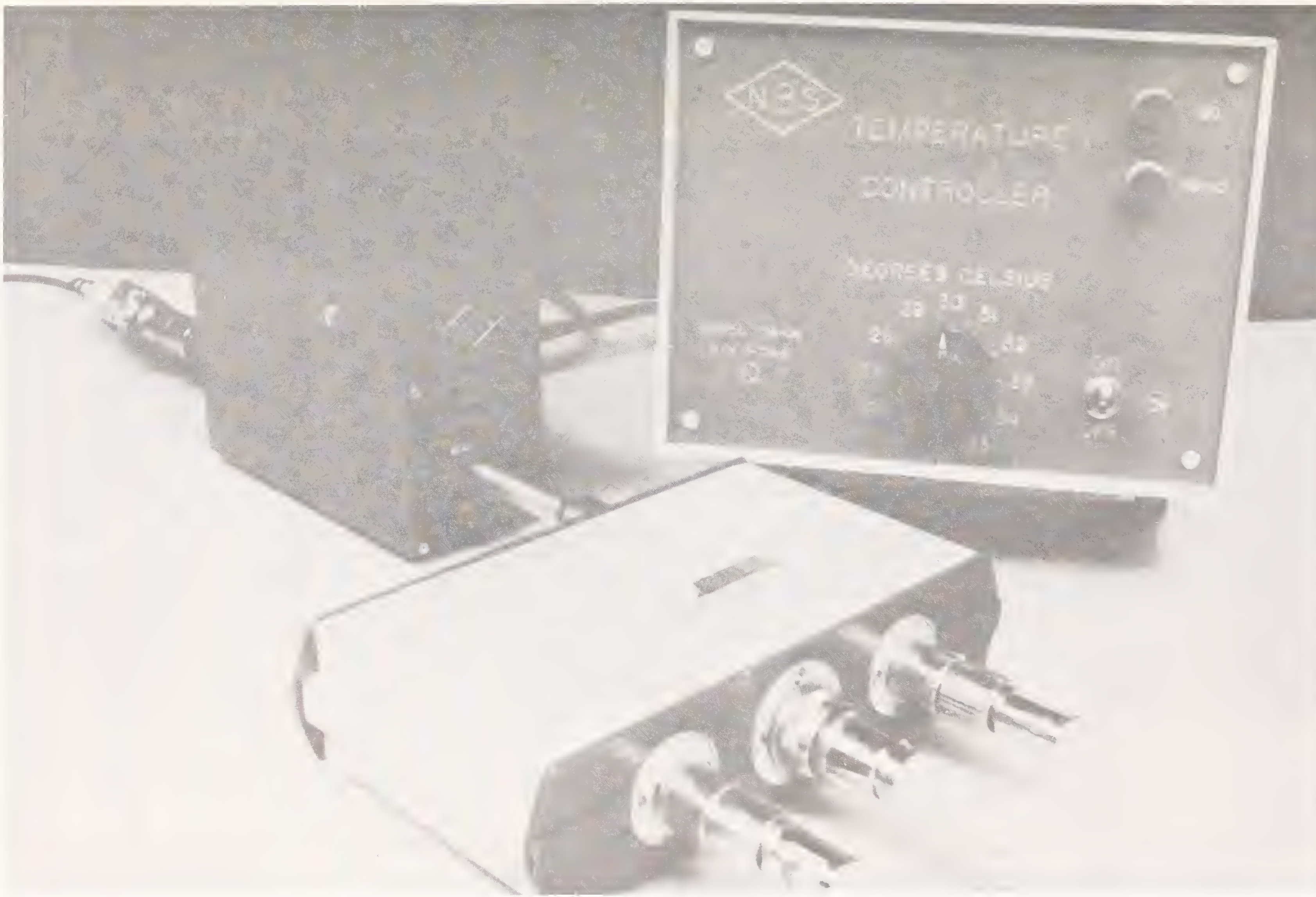

Figure 8. NBS Reference Waveform Pulse Generator

Figure 9. NBS Tunnel Diode Bias Supply.

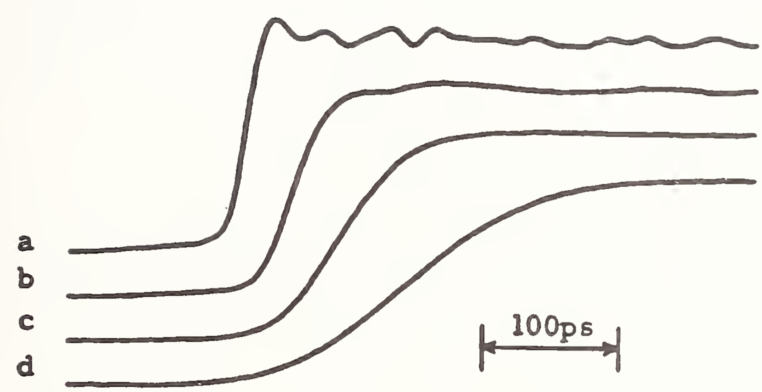

Figure 10. Measured and deconvolved waveforms from the (a) tunnel diode and the (b) 50 ps, (c) 100 ps, and (d) 200 ps low pass filters.

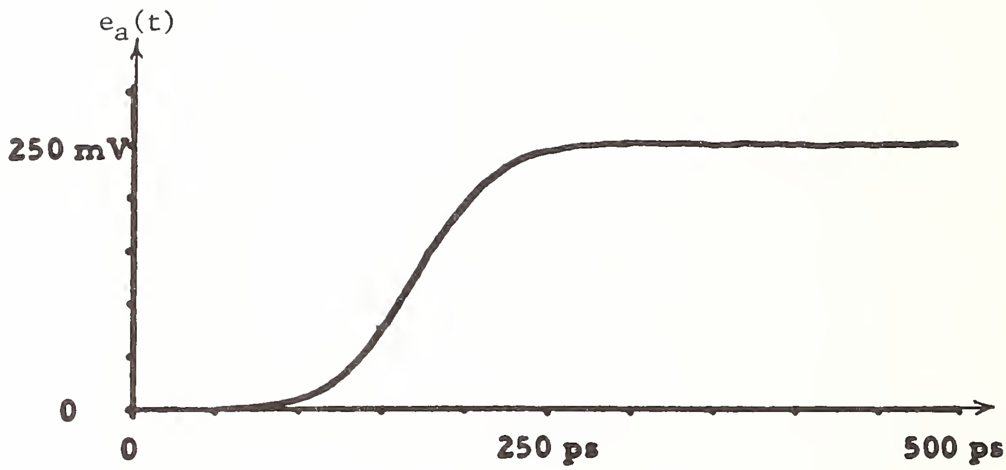

Figure 11. Available Reference Waveform into a 50 ohm load from the TD/100 ps filter combination, $e_a(t)$.

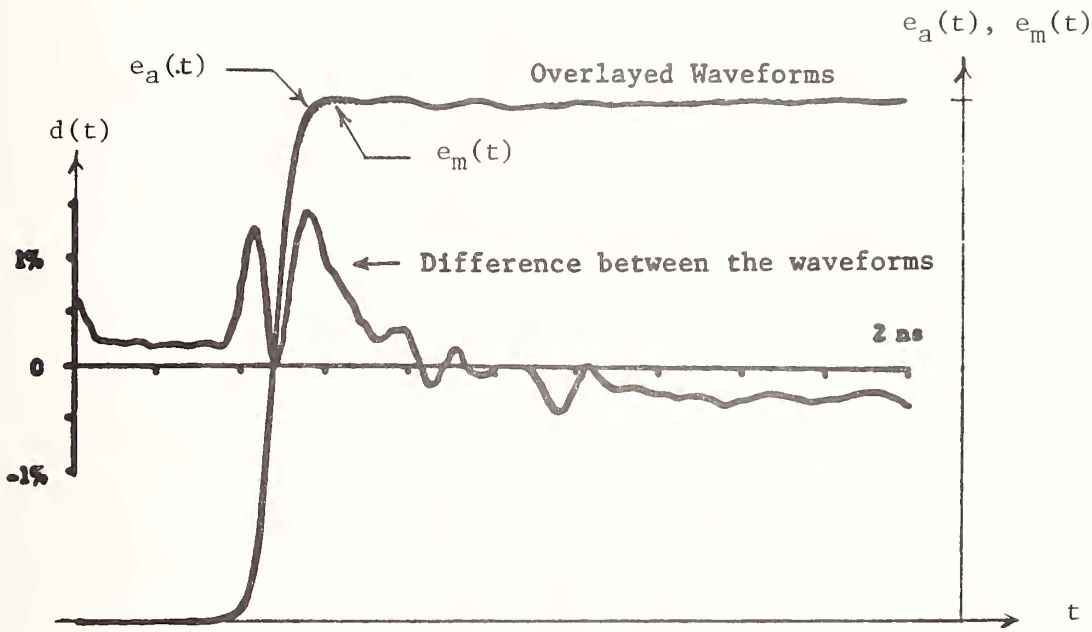

Figure 12. Overlay of a predicted 100 ps reference waveform, $e_a(t)$, and the actual measured waveform (dotted line), $e_m(t)$ and their resultant difference, d(t). The waveforms are aligned so that their 50% values coincide with each other.

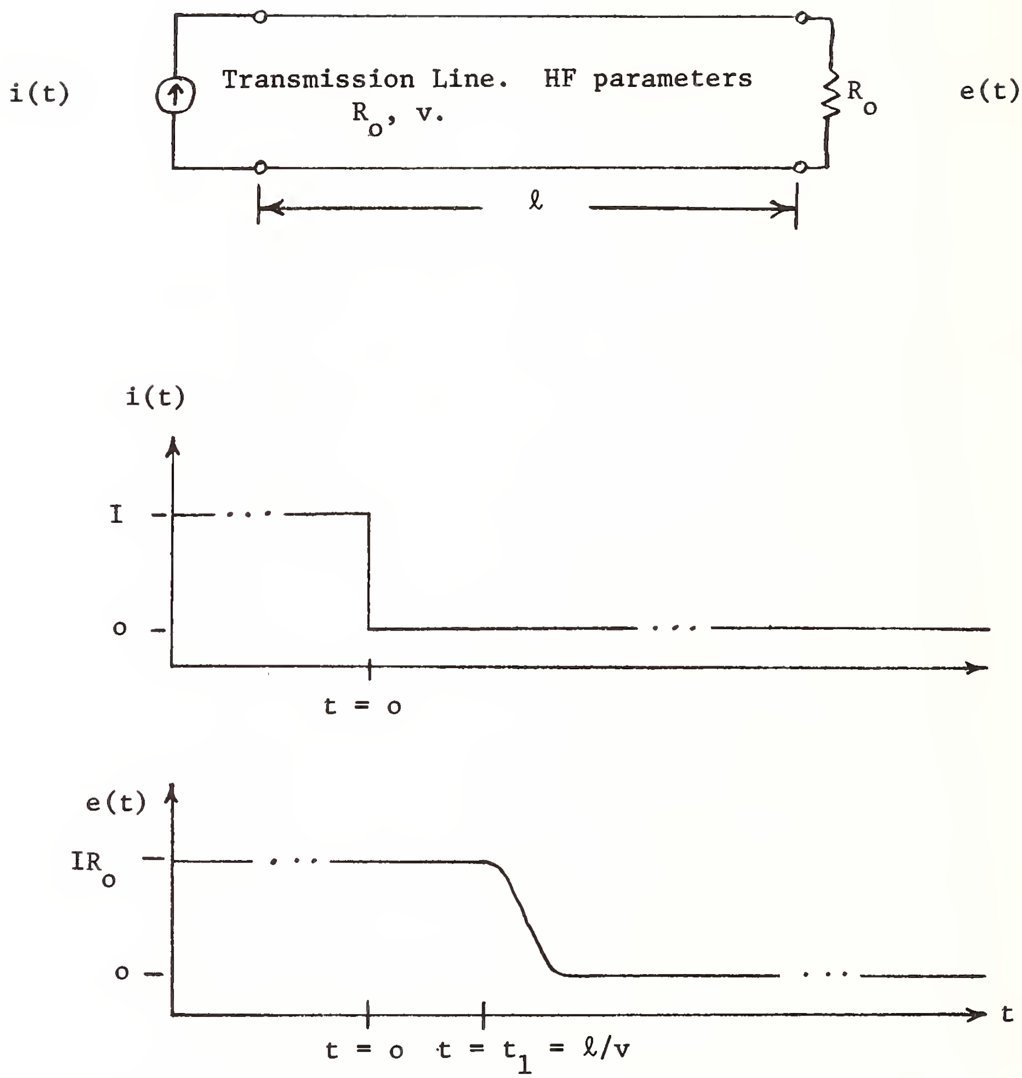

Figure 13. The basic concept of the flat-pulse generator. A known DC current, I, is applied to a transmission line load and then switched-off to establish a known step-like voltage, e(t).

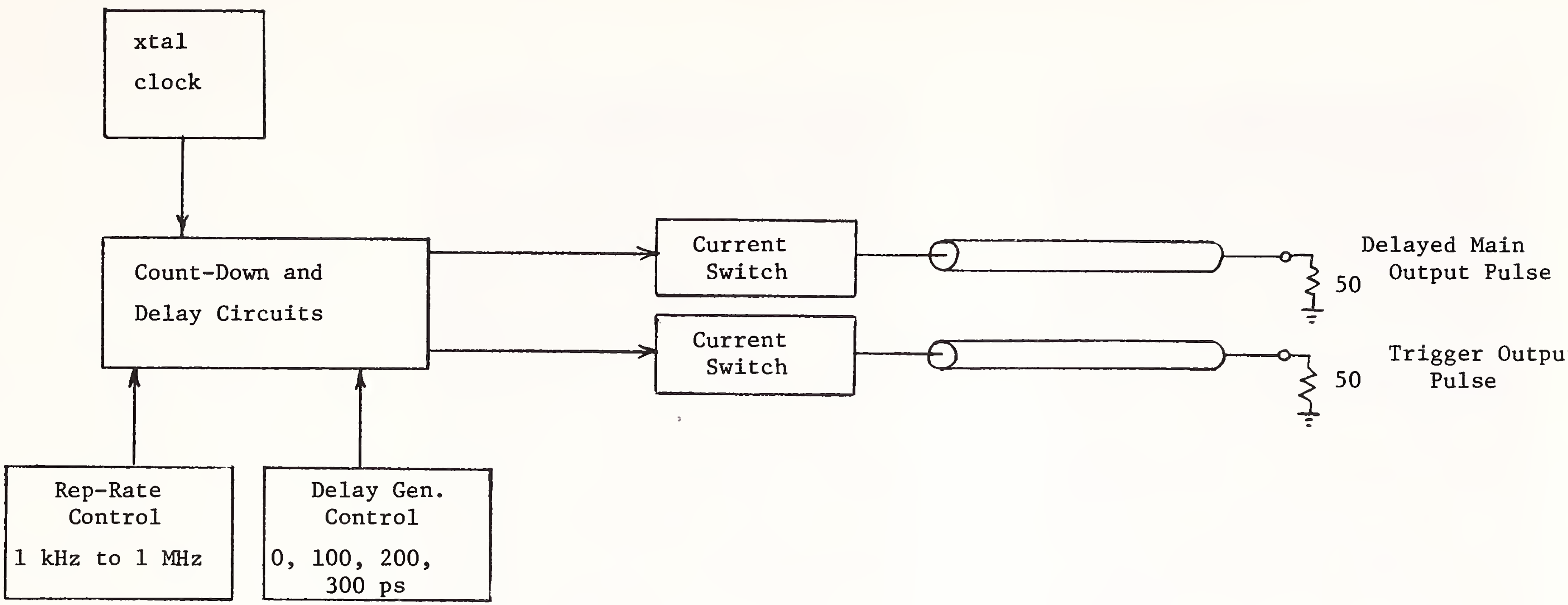

Figure 14. Block diagram of the flat-pulse generator.

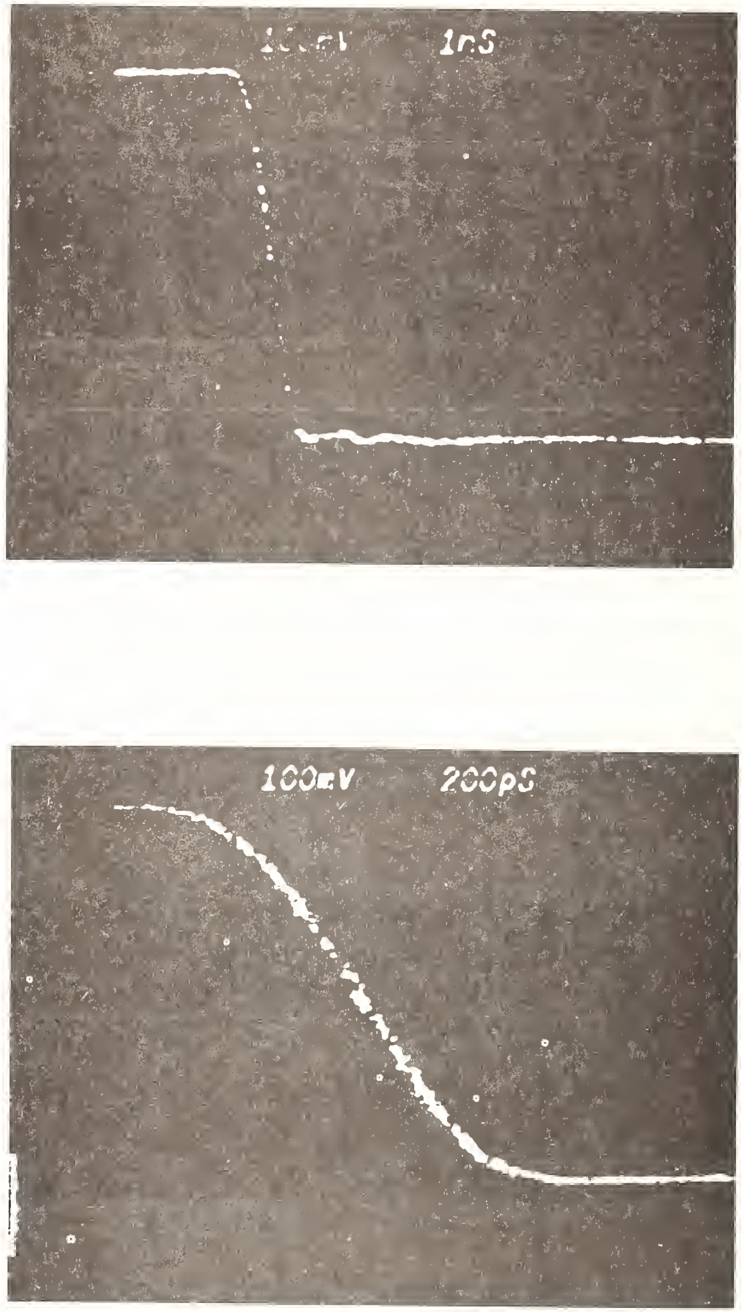

Figure 15. Main pulse output of the flat pulse generator. The lower oscillogram sweep rate is five times that of the upper one. See figure 16 for vertical/horizontal scales.

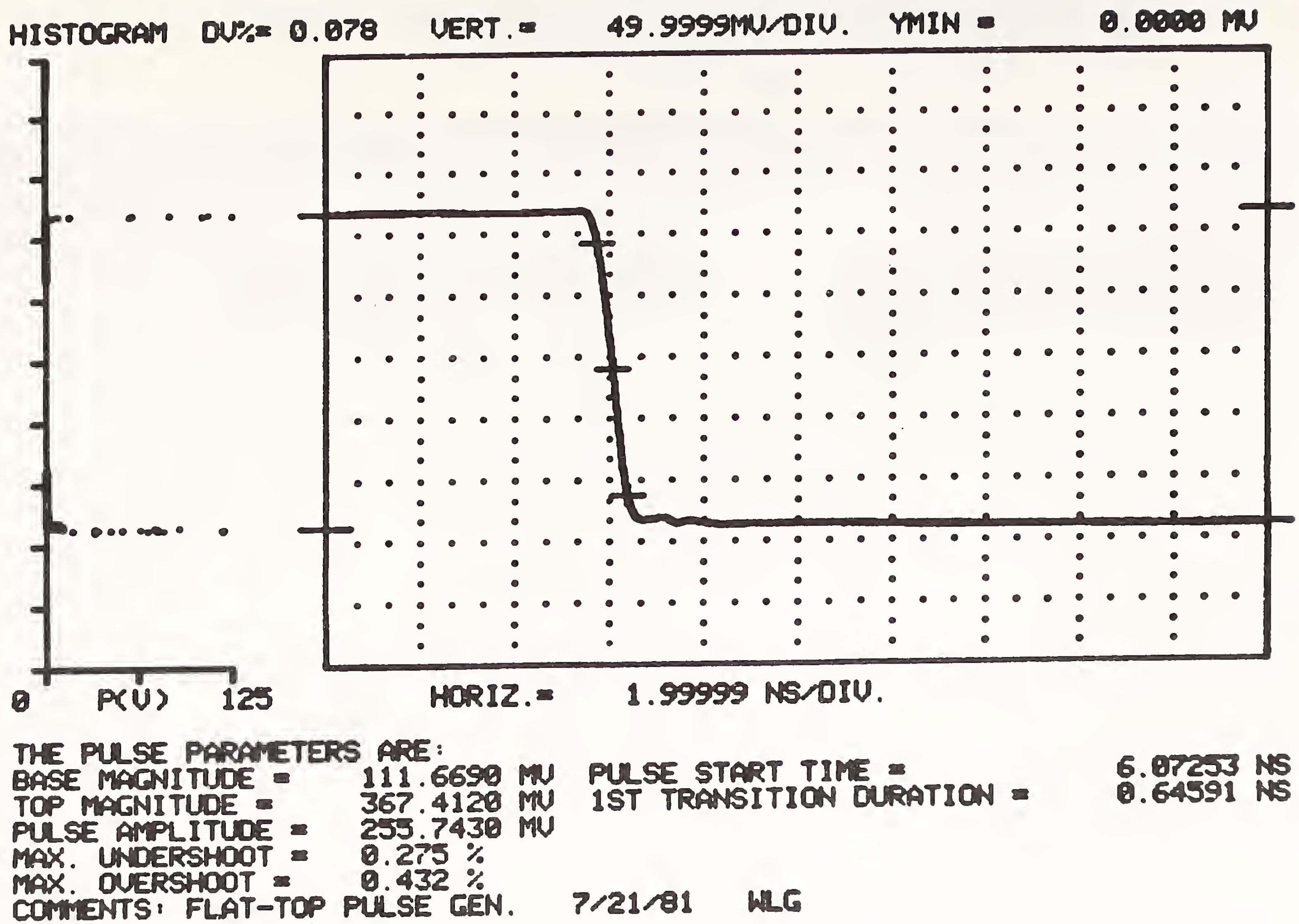

Figure 16. The flat-pulse of figure 15 as measured by the NBS APMS. The pulse amplitude and magnitude parameters listed are one-half the actual values. Note the magnitude histogram P(v) at the left.

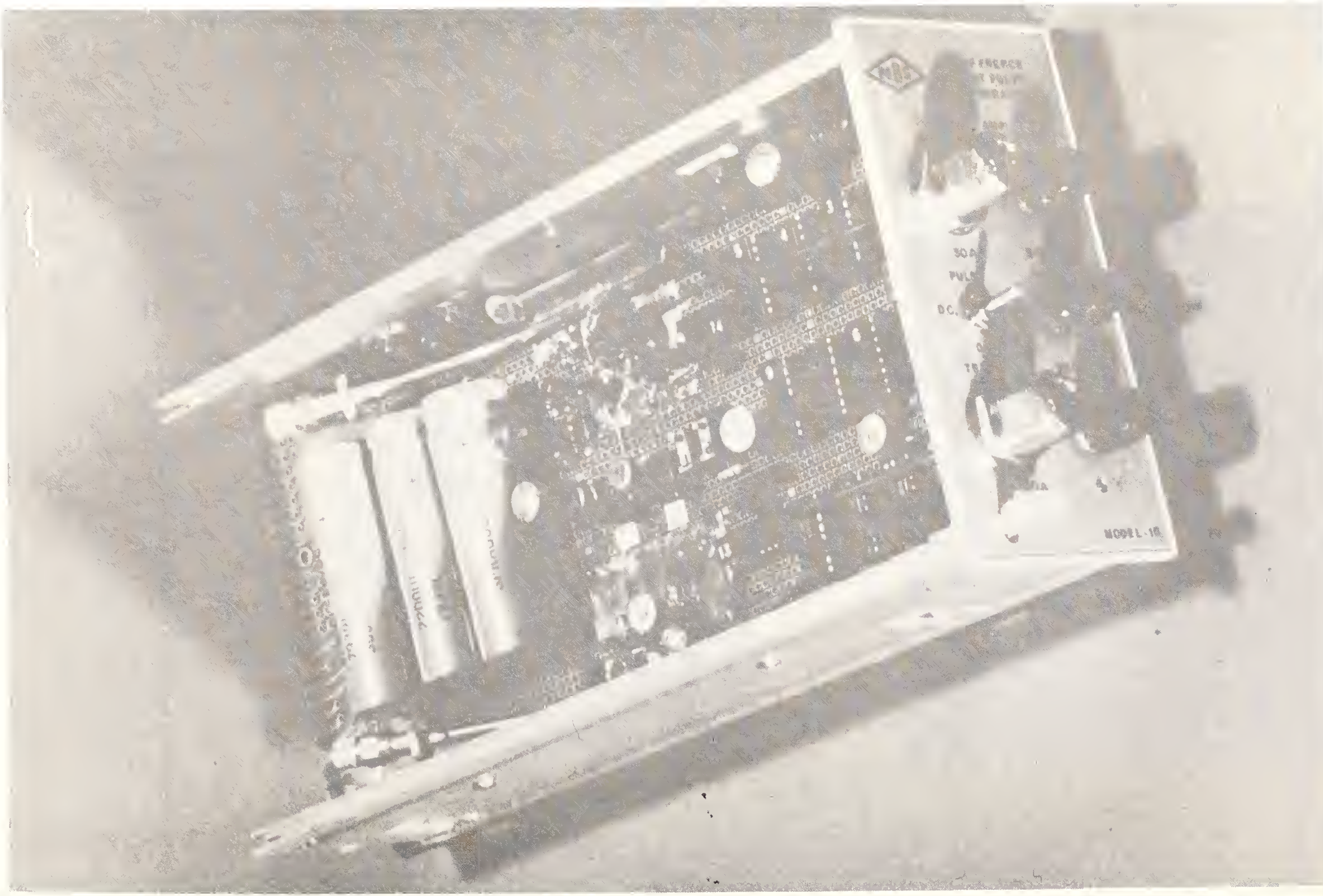

Figure 17. The prototype for the flat-pulse generator.

NBS-114A (REV. 9-78)

U.S. DEPT. OF COMM. BIBLIOGRAPHIC DATA SHEET	1. PUBLICATION OR REPORT NO. NBS SP 634	2. Gov't. Accession No.	3. Recipient's Accession No.

4. TITLE AND SUBTITLE

Proceedings of the Waveform Recorder Seminar

Proceedings of the Seminar on Waveform Recorder Measurement Needs and Techniques for Evaluation/Calibration, held in Boulder, CO, Oct. 15, 1981

5. Publication Date June 1982

6. Performing Organization Code

7. AUTHOR(S)

Robert A. Lawton, Editor

8. Performing Organ. Report No.

9. PERFORMING ORGANIZATION NAME AND ADDRESS

NATIONAL BUREAU OF STANDARDS
DEPARTMENT OF COMMERCE
WASHINGTON, DC 20234

10. Project/Task/Work Unit No.

11. Contract/Grant No.

12. SPONSORING ORGANIZATION NAME AND COMPLETE ADDRESS *(Street, City, State, ZIP)*

Same as Item 9.

13. Type of Report & Period Covered Final

14. Sponsoring Agency Code

15. SUPPLEMENTARY NOTES

Library of Congress Catalog Card Number: 82-600552

☐ Document describes a computer program; SF-185, FIPS Software Summary, is attached.

16. ABSTRACT *(A 200-word or less factual summary of most significant information. If document includes a significant bibliography or literature survey, mention it here.)*

In the past, for the most part, precision electromagnetic measurements were concerned with the measurement of parameters for sinusoidal (or steady state) excitation and response, e.g., magnitude, phase, and power. One reason for the popularity of frequency domain measurement was that in this domain only one complete data point need be recorded to constitute a useful measurement. Recording a thousand data points as required for precision time domain waveform measurements simply was not feasible. Today such frequency domain measurements are still important but now share their importance with transient pulse time domain measurements. With the emergence of integrated circuit components for (1) sampling or analog to digital conversion, (2) storage, and (3) control, real time digital waveform recording is now practical and widespread in usage. Furthermore, by coupling waveform recording components to minicomputers and microprocessors integrated circuitry it is now possible to record single events using compact systems (instruments) which acquire, record, process, and analyze transient signals. In fact, the incorporation of digital computation integrated circuitry appears to be a major driving force in expanding the role of waveform measurements in the academic, industrial and scientific communities.

We at the National Bureau of Standards are charged with the responsibility of encouraging the orderly development of consistent standards and measurement techniques. We have been actively engaged in waveform standards development for some time now and the papers in these proceedings will give a sample of what NBS and others in the waveform community have done already. The afternoon session consisted of a workshop which addressed the questions: Where do we go from here? and Why?, culminating in the selection of a steering committee for the development of standards for waveform recorders.

17. KEY WORDS *(six to twelve entries; alphabetical order; capitalize only the first letter of the first key word unless a proper name; separated by semicolons)*

converters; electromagnetics; encoders; pulse; waveform generation; waveform measurements; waveform recorder; standards.

18. AVAILABILITY ☒ Unlimited

☐ For Official Distribution. Do Not Release to NTIS

☐ Order From Sup. of Doc., U.S. Government Printing Office, Washington, DC 20402, SD Stock No. SN003-003-

☒ Order From National Technical Information Service (NTIS), Springfield, VA. 22161

19. SECURITY CLASS (THIS REPORT)	21. NO. OF PRINTED PAGES
UNCLASSIFIED	97
20. SECURITY CLASS (THIS PAGE)	**22. Price**
UNCLASSIFIED	

USCOMM-DC

NBS TECHNICAL PUBLICATIONS

PERIODICALS

JOURNAL OF RESEARCH—The Journal of Research of the National Bureau of Standards reports NBS research and development in those disciplines of the physical and engineering sciences in which the Bureau is active. These include physics, chemistry, engineering, mathematics, and computer sciences. Papers cover a broad range of subjects, with major emphasis on measurement methodology and the basic technology underlying standardization. Also included from time to time are survey articles on topics closely related to the Bureau's technical and scientific programs. As a special service to subscribers each issue contains complete citations to all recent Bureau publications in both NBS and non-NBS media. Issued six times a year. Annual subscription: domestic $18; foreign $22.50. Single copy, $4.25 domestic; $5.35 foreign.

NONPERIODICALS

Monographs—Major contributions to the technical literature on various subjects related to the Bureau's scientific and technical activities.

Handbooks—Recommended codes of engineering and industrial practice (including safety codes) developed in cooperation with interested industries, professional organizations, and regulatory bodies.

Special Publications—Include proceedings of conferences sponsored by NBS, NBS annual reports, and other special publications appropriate to this grouping such as wall charts, pocket cards, and bibliographies.

Applied Mathematics Series—Mathematical tables, manuals, and studies of special interest to physicists, engineers, chemists, biologists, mathematicians, computer programmers, and others engaged in scientific and technical work.

National Standard Reference Data Series—Provides quantitative data on the physical and chemical properties of materials, compiled from the world's literature and critically evaluated. Developed under a worldwide program coordinated by NBS under the authority of the National Standard Data Act (Public Law 90-396).

NOTE: The principal publication outlet for the foregoing data is the Journal of Physical and Chemical Reference Data (JPCRD) published quarterly for NBS by the American Chemical Society (ACS) and the American Institute of Physics (AIP). Subscriptions, reprints, and supplements available from ACS, 1155 Sixteenth St., NW, Washington, DC 20056.

Building Science Series—Disseminates technical information developed at the Bureau on building materials, components, systems, and whole structures. The series presents research results, test methods, and performance criteria related to the structural and environmental functions and the durability and safety characteristics of building elements and systems.

Technical Notes—Studies or reports which are complete in themselves but restrictive in their treatment of a subject. Analogous to monographs but not so comprehensive in scope or definitive in treatment of the subject area. Often serve as a vehicle for final reports of work performed at NBS under the sponsorship of other government agencies.

Voluntary Product Standards—Developed under procedures published by the Department of Commerce in Part 10, Title 15, of the Code of Federal Regulations. The standards establish nationally recognized requirements for products, and provide all concerned interests with a basis for common understanding of the characteristics of the products. NBS administers this program as a supplement to the activities of the private sector standardizing organizations.

Consumer Information Series—Practical information, based on NBS research and experience, covering areas of interest to the consumer. Easily understandable language and illustrations provide useful background knowledge for shopping in today's technological marketplace.

Order the **above** *NBS publications from: Superintendent of Documents, Government Printing Office, Washington, DC 20402.*

Order the **following** *NBS publications—FIPS and NBSIR's—from the National Technical Information Services, Springfield, VA 22161.*

Federal Information Processing Standards Publications (FIPS PUB)—Publications in this series collectively constitute the Federal Information Processing Standards Register. The Register serves as the official source of information in the Federal Government regarding standards issued by NBS pursuant to the Federal Property and Administrative Services Act of 1949 as amended, Public Law 89-306 (79 Stat. 1127), and as implemented by Executive Order 11717 (38 FR 12315, dated May 11, 1973) and Part 6 of Title 15 CFR (Code of Federal Regulations).

NBS Interagency Reports (NBSIR)—A special series of interim or final reports on work performed by NBS for outside sponsors (both government and non-government). In general, initial distribution is handled by the sponsor; public distribution is by the National Technical Information Services, Springfield, VA 22161, in paper copy or microfiche form.

U.S. DEPARTMENT OF COMMERCE
National Bureau of Standards
Washington, DC 20234

OFFICIAL BUSINESS

Penalty for Private Use, $300

POSTAGE AND FEES PAID
U.S. DEPARTMENT OF COMMERCE
COM-215

U.S.MAIL

THIRD CLASS